CRANFIELD UNIVERSITY

YAN ZHU

LONGITUDINAL CONTROL LAWS DESIGN FOR A FLYING WING AIRCRAFT

SCHOOL OF ENGINEERING

MSc by Research

MSc Thesis

Academic Year: 2011 - 2012

Supervisor: Dr. James Whidborne

February 2012

CRANFIELD UNIVERSITY

SCHOOL OF ENGINEERING
MSc by Research

MSc thesis

Academic Year 2011 – 2012

YAN ZHU

LONGITUDINAL CONTROL LAWS DESIGN FOR A FLYING WING AIRCRAFT

Supervisor: Dr.James Whidborne
February 2012

ABSTRACT

This research is concerned with the flight dynamic, pitch flight control and flying qualities assessment for the reference BWB aircraft. It aims to develop the longitudinal control laws which could satisfy the flying and handing qualities over the whole flight envelope with added consideration of centre of gravity (CG) variation.

In order to achieve this goal, both the longitudinal stability augmentation system (SAS) and autopilot control laws are studied in this thesis. Using the pole placement method, two sets of local Linear-Time-Invariant (LTI) SAS controllers are designed from the viewpoints of flying and handing qualities assessment and wind disturbance checking. The global gain schedule is developed with the scheduling variable of dynamic pressure to transfer gains smoothly between these two trim points. In addition, the poles movement of short period mode with the varying CG position are analysed, and some approaches of control system design to address the problem of reduced stability induced by CG variation are discussed as well. To achieve the command control for the aircraft, outer loop autopilot both pitch attitude hold and altitude hold are implemented by using the root locus method.

By the existing criteria in MIL-F-8785C specifications being employed to assess the augmented aircraft response, the SAS linear controller with automatic changing gains effectively improve the stability characteristic for the reference BWB aircraft over the whole envelope. Hence, the augmented aircraft equals to a good characteristic controlled object for the outer loop or command path design, which guarantee the satisfactory performance of command control for the BWB aircraft.

The flight control law for the longitudinal was completed with the SAS controller and autopilot design. In particular, the SAS was achieved with Level 1 flying and handing qualities, meanwhile the autopilot system was applied to obtain a satisfactory pitch attitude and altitude tracking performance.

Keywords:

SAS Control Law, Flying and Handing Qualities, Gain Scheduling, Pitch Attitude Hold, Altitude Hold, BWB Aircraft

ACKNOWLEDGEMENTS

It was unbelievable to have an opportunity of study abroad for my master degree until I was really in the campus of Cranfield Univerdity. From the 17th of February 2011, one year experience which is full of excitation, challenge, frustration and happiness will be impressive in my life. Fortunately, a great deal of help I have acquired from all of those who get me to the point where I am today.

My supervisor, Dr. James F. Whidborne, has done a wonderful job during my research and guided me to make this thesis possible. I have benefited from his enthusiasm for research and learning, moreover his concern and involvement with his students outside of school. Taking this opportunity, I would like to appreciate his patient help for me very much. In addition, my acknowledgments are expressed to Alastair K. Cooke who also guides me to seek solutions in flight dynamics and flying qualities problems. His strict and careful working attitude will influence me in the following study and working times.

I would like to dedicate this thesis to my parents who always make all efforts to support me. Though it is hard to pay them back for what they have done for me, I will express my great thanks to their love and would like to enjoy every success with them.

Particular thanks go to my husband Runzhao Guo who is also an aircraft designer in aerodynamics. Not only has he been a constant source of encouragement and love, but also provides me a lot of suggestion and support in my subject. My progress in every step both in life and academic study can not get without his help.

Further thanks to all my family and friends in china for their continuous support during the whole year.

I would like to appreciate China Scholarship Council (CCS), Aviation Industry Corporation of China (AVIC), and my company The First Aircraft Institute (FAI). I have been fortunate to take this opportunity and support provided by them to pursue the master degree in Cranfield University.

I am extremely lucky to make plenty of friends who made a wonderful environment in academic and language study. In particularly, I would like to thank Andrew Potter whom I bother many times to revise the grammar of this thesis.

The students from AVIC, especially my colleagues in FAI, who have experienced a wonderful, fantastic and very special year with me, I am grateful to their encouragement and considerate help.

Finally, I would like to save my deepest love and guilty to my grandmother who passed away when I could not accompany with her in May 2011. Nothing can I do except this thesis preserving a forever memory for her.

Yan Zhu

December, 2011

TABLE OF CONTENTS

LIST OF FIGURES

LIST OF TABLES

LIST OF EQUATIONS

NOMENCLATURES

$\bar{\bar{c}}$	Mean aerodynamic chord
C_L	Lift coefficient
C_l	Rolling moment coefficient
$C_{m\alpha}$	Pitching moment coefficient due to angle of attack
C_n	Yawing moment coefficient
$C_{z\alpha}$	Normal force coefficient due to angle of attack
F	Flight envelope
g	Acceleration due to gravity
h	Altitude
h_0	Aerodynamic centre position on reference chord
h_{CG}	Centre of gravity position on reference chord
I_y	Moment of inertia in pitch
K	Controller gain; Drag factor due to lift
m	Mass
M_q	Pitching moment due to pitch ratre
M_ω	Pitching moment due to downward velocity
N_α	Normal load factor per unit angle of attack
P	Equilibrium point
Q	Dynamic pressure
$Q_{aircraft}$	Present Dynamic Pressure of the Aircraft
S	Wing reference area
U_e	Axial component of steady equilibrium velocity
u	Axial velocity perturbation
v_0	Steady equilibrium velocity
w	Normal velocity perturbation
w_g	Normal wind velocity perturbation
Z_ω	Normal force due to downward velocity
Z_q	Normal force due to pitch rate

Greek letter

α	Angle of attack (deg)
β	Sideslip angle (deg)
q	Pitch rate (deg/s)
θ	Pitch angle (deg)
ϕ	Roll angel (deg)
δ_e	Elevator deflection (deg)
ζ	Damping ratio
w_n	Natural frequency (rad/s)
ρ	Air density (kg/m^3)

Abbreviations

AC	Aerodynamic Centre
CAP	Control Anticipation Parameter
CS	Certification Specifications for Large Aeroplanes
CG	Centre of Gravity
CSAS	Command and Stability Augmentation System
FBW	Fly-by-Wire
FAR	Federal Acquisition Regulation
JAR	Joint Aviation Requirements
LPV	Linear –Parameter–Varying
LTI	Linear–Time–Invariant
LTV	Linear–Time–Varying
SAS	Stability Augmentation System
SPO	Short Period Oscillation
PIO	Pilot-in-the-Loop Oscillatory
UAV	Unmanned Aerial Vehicle

Subscripts

c	Command
s	Short Period Mode
p	Phugoid Mode
dot	Differential

1 INTRODUCTION

For many years it has been very important aspect for aeronautic designers to realize aerodynamic efficiency improvement by suitable and realizable approaches. In recent years, it is achieved with the development of the flying wing concept [1].

It has been found that the flying wing is a special configuration with the advantages of better aerodynamic and economical efficiency. It can reduce the no-lift aerodynamic components, which is regarded as the more efficient aerodynamic configuration. Moreover, the Russian Central Aerodynamic Institute (TsAGI) demonstrates that this concept of the high capacity configuration can enhance the lift drag ratio by 20%~25% and decrease the direct operating cost by 7% ~ 8% compared with a conventional airplane at the same capacity. In addition, it is also feasible as the next generation of the advanced conventional aircraft [2].

In terms of civil transport airliners, one of the approaches for improving the efficiency is to increase the passenger capacity, which would reduce the direct operating cost per passenger and would provide relief for large airports by reducing the number of flights [2]. Additionally, the flying wing concept could increase the structure depth in the centre section of the aircraft which makes the wing span increase with less weight penalties and a high lift-to-drag ratio [3].

Currently, the advanced Very Efficient Large Aircraft (VELA) of a flying wing configuration, regarded as the future of very efficient airplanes, have not only been studied by TsAGI since the late 1980s, but also conducted by the collaboration between Airbus and Boeing under the International Scientific and Technical Centre grant No.548 [2]. In addition, China has paid more attention in this unconventional configuration and launched international collaboration projects and studies in recent years.

1.1 Background to the GDP Work

FW-11 (Blue Bird) is a new cooperative project from 2011 to 2013 between Cranfield University and Aviation Industry Corporation of China (AVIC) after the

previous cooperative project Flying Crane. It's the first year for the conceptual design as the 2011 Group Design Project (GDP). The 250 seat flying wing configuration airliner which is quite different from the conventional one was designed for the international market in 2020.

According to the requirement which was initially investigated, the main design aims are improved fuel consumption, comfort for passengers and environment friendliness. In order to achieve them, several techniques such as wing design, cabin layout, engine selection and structure design were adopted. Due to the high lift drag ratio, reduced weight and better specific fuel consumption (SFC), the FW-11 improves fuel consumption by about 29% compared to the A330-200. Nevertheless, the flying wing configuration also induces some large problems which require compromise on a variety of aspects: airfoil and interior capacity, seats, cargo and fuel tank location, CG position and stability, etc. Hence, it is a more challenging project than the previous one.

In terms of the GDP work (Appendix A), performance calculations including static stability analysis, drag estimation, trim and control have been calculated and studied for the design iteration and evaluation. The preceding work brings an insight into flying wing transport aircraft design is as follows:

- Due to the unconventional configuration, the longitudinal static stability margin was directly impacted by wing geometry parameters and interior layout. It was difficult to obtain as large a stability margin as conventional aircraft.
- According to the drag polar comparison with the flying wing and conventional baseline, it is clear that the flying wing is a more aerodynamic efficient concept with higher lift and lower drag. It is also needed to compromise with the drag reduction, lateral stability and control, and rudder design.
- Some differences were recognized in the longitudinal trim with stabilizer and elevator between conventional baseline and flying wing aircraft. For flying wing, the force arm and the area of longitudinal control surfaces influenced the tailplane volume ratio, namely the control surface effectiveness. Hence,

surfaces trimming deflection was used more than conventional aircraft, especially landing trimming deflection which increases due to the downwash influence.

- Control surfaces of the flying wing should provide sufficient control power and redundancy but not be excessively complicated for the control system design. The design process is a difficult, complex but significant task and so the systematical calculation and evaluation would be accomplished in the next design stage.

Hence, without a wealth of advanced multidisciplinary tools and prediction platforms, several difficulties and complexities are realised at the beginning of the flying wing design compared with the traditional configuration. It is supposed that this project might become much more challenging but interesting and attractive in the following design processes.

1.2 Background to the IRP Work

1.2.1 Proposition of IRP Study Content

It is believed that the application of the flying wing design technique brings challenges for the control system design due to a tailless profile such as:

- Insufficiency of stability margin.
- Larger or more surfaces are needed for pitch control due to smaller moment arms.
- Three axes coupling complex control laws design.

Therefore, in order to study further on the basis of the GDP work, the IRP work focuses on the control system design. Moreover, the longitudinal stability and pitch control are more significant aspects for the safety of the flying wing airplane than the lateral components. Hence, compared with the conventional configuration, it is crucial to improve the longitudinal characteristic for flying wing aircraft considering the occurrence of the weak stability or even instability [2]. Based on above considerations, the longitudinal control system design was proposed for study in this work.

1.2.2 Reference Aircraft Selection

Due to the insufficient information on the aerodynamic derivatives of the GDP aircraft FW-11 at the conceptual design stage, further study of control system design to that aircraft is not possible. Therefore, the Blended-Wing-Body (BWB) [4] which is one such flying wing variation aircraft, studied by Cranfield University was utilized as the reference aircraft model for this work.

Compared with the FW-11 and BWB aircraft, there are some similarities such as:

- In terms of the configuration, the FW-11 consists of the subsonic wing as conventional aircrafts and a large, apparent fuselage (Figure A-1). It is similar to the BWB reference aircraft in this study.
- All of the main control surfaces are designed on the trailing edge of the wing. Hence, the pitch control principles for both aircraft are almost the same.

Hence, the study of the BWB aircraft could provide a foundation for longitudinal control laws design for similar configuration aircraft such as the FW-11.

1.3 Aim and Objectives

Over the whole flight envelope, aircraft aerodynamics change with various altitudes and airspeeds. Moreover, it is a possible occurrence that the longitudinal control is weak static stable or unstable due directly to the tailless configuration in the flight. Therefore, the designed control laws need to satisfy the flying and handing qualities over the entire envelope with added consideration of centre of gravity (CG) variation.

For the reasons above, based on controller design at selected operating points, this project aims to create longitudinal control laws for improving aircraft flight qualities and implementation of control functions. It shall focus on the SAS design, flying and handing qualities assessment over the whole flight envelope, gain scheduling and outer loop autopilot control system design.

The objectives of this study are as follows:

- **Inner Loop SAS Design**

1. Aircraft model trim and linearization for the reference BWB aircraft based on the equilibrium points over the flight envelope.
2. According to the flying and handing qualities constraints, apply the linear model to design SAS to improve the system short period characteristics at selected equilibrium points via the state space pole placement method.

- **Assessment with the Entire Flight Envelope**
  1. Evaluate the dynamic response with the local controller gains in the flight envelope and assess the satisfactory flying and handing qualities.
  2. Design SAS controller for the unsatisfactory region of the flight envelope in order to obtain suitable system dynamics for the whole envelope.

- **Gain Scheduling with the local controllers**
  1. According to the current operating condition, develop a gain schedule with suitable variable parameters to vary the gains smoothly to obtain satisfactory flying and handing qualities.
  2. Reassess the scheduled gains at the interpolation area using the flying and handing qualities constraints.

- **Outer Loop Autopilot Design**

  Determine and design the pitch attitude hold control architecture and gains to achieve the pitch attitude and altitude command control and tracking function at the cruise point.

1.4 Methodology

The reference BWB aircraft platform used in this study is from the previous PhD research by Castro [5] and Rahman [6] at Cranfield University. Hence, this study is a continuation work with the aid of earlier efforts.

The main design principle is to search for one robust controller or a set of controllers which could be used to improve the flight control system characteristic with satisfactory flight qualities and performance over the whole envelope. The methodology for the longitudinal control laws design can be stated as follows.

1. Choose the flight qualities assessment constraints of the SAS from MIL-F-8785C specifications.
2. Select design points for the aircraft model, trim and linearize by the small perturbation principle.
3. Using pole placement design procedures, design SAS controller gains at the selected equilibrium point which meet the flight qualities constraints and has an acceptable wind disturbance response
4. Assess the whole flight envelope with these local gains. If it is satisfactory, the outer loop control laws can be developed, otherwise design a controller based on the linear aircraft model at an equilibrium point in the unsatisfactory region in the entire flight envelope. (It is necessary to schedule the gains scheme to smooth the gains variation at the operating condition.)
5. Determine the outer loop control function and apply the control architecture and gains to achieve the command control.

The study flow used in this thesis can be illustrated as Figure1-1 shows.

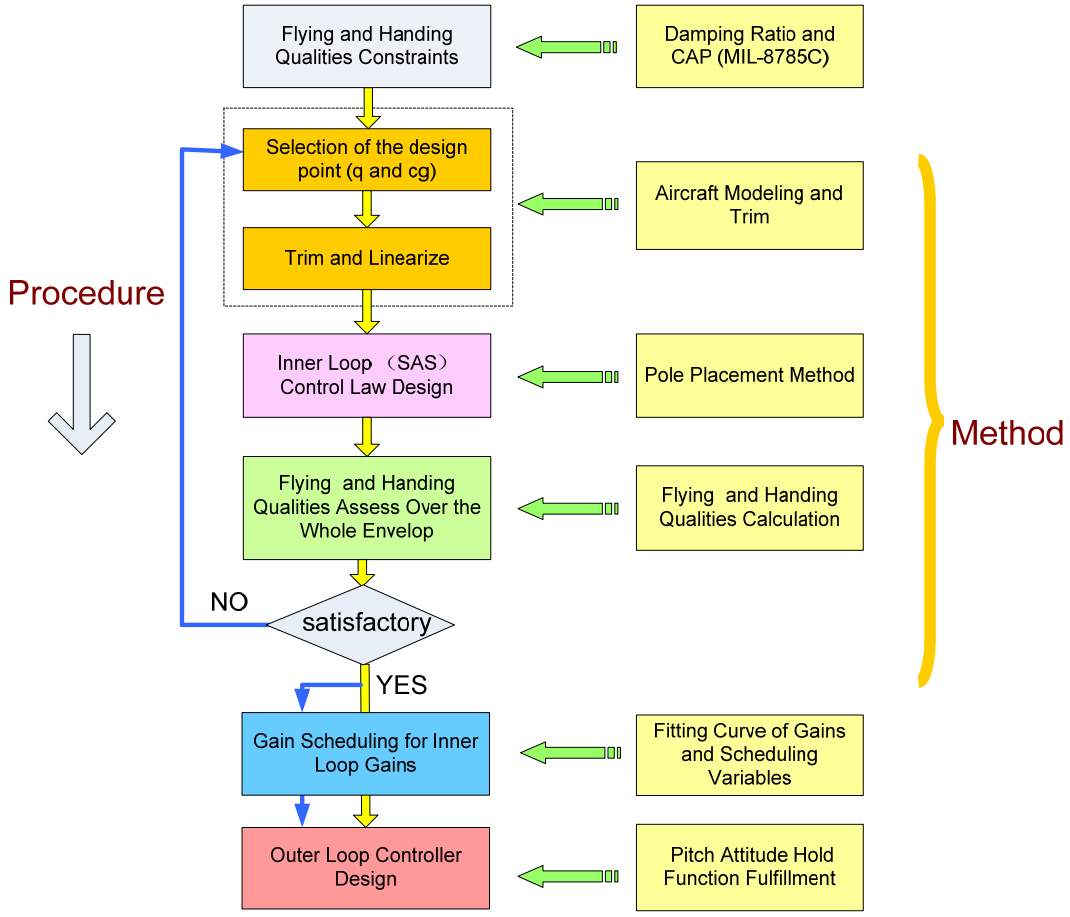

Figure 1-1 Study Flow Chart

1.5 Thesis Organization

Following the introduction in chapter 1, this thesis is organized in subsequent chapters as follows:

Chapter 2: A literature review is stated in this chapter. This describes the development of flying wing aircraft and details their advantages and drawbacks. Meanwhile, it includes stability and control analysis of airplanes, flying and handing qualities, and gain scheduling method development and application.

Chapter 3: The reference aircraft and the detailed criteria from MIL-F-8785C specifications for SAS design in this study are presented. Further more, this chapter covers the procedure of the BWB aircraft linearized mathematical model derivation and initial controller checking.

Chapter 4: The SAS controller is assessed over the whole envelope with flying and handing qualities constraints in Chapter 3, also with the second specific SAS design by pole placement method, procedures and design results.

Chapter 5: Derivation of the gain schedule with variables of dynamic pressure is achieved in order to ensure that the local controller gains are scheduled smoothly and serially for the whole envelope with satisfactory flying and handing qualities.

Chapter 6: The influence of short period dynamic response with respect to the CG position variation is discussed in this chapter.

Chapter 7: On the basis of SAS, outer loop control laws of both pitch attitude hold and altitude hold are implemented at the static stable cruise case.

Chapter 8: The last section concludes this research, summarises findings and makes recommendations for further work on this subject.

2 LITERATURE REVIEW

2.1 Background of Flying Wing Configuration

2.1.1 Definition and Concept Development

In terms of the fixed wing aircrafts, Lippisc in 1930 defined the four different types of aircraft shown in Figure2-1 based on their wing configurations: tailed, tandem wing, canard and tailless aircraft or flying wings.

It is clear that the distinguishing feature between the left and right side is the quantity of the main surface. The conventional configuration aircraft has two main surfaces, namely one behind the other compared to the tailless/flying wings which have one surface only [7].

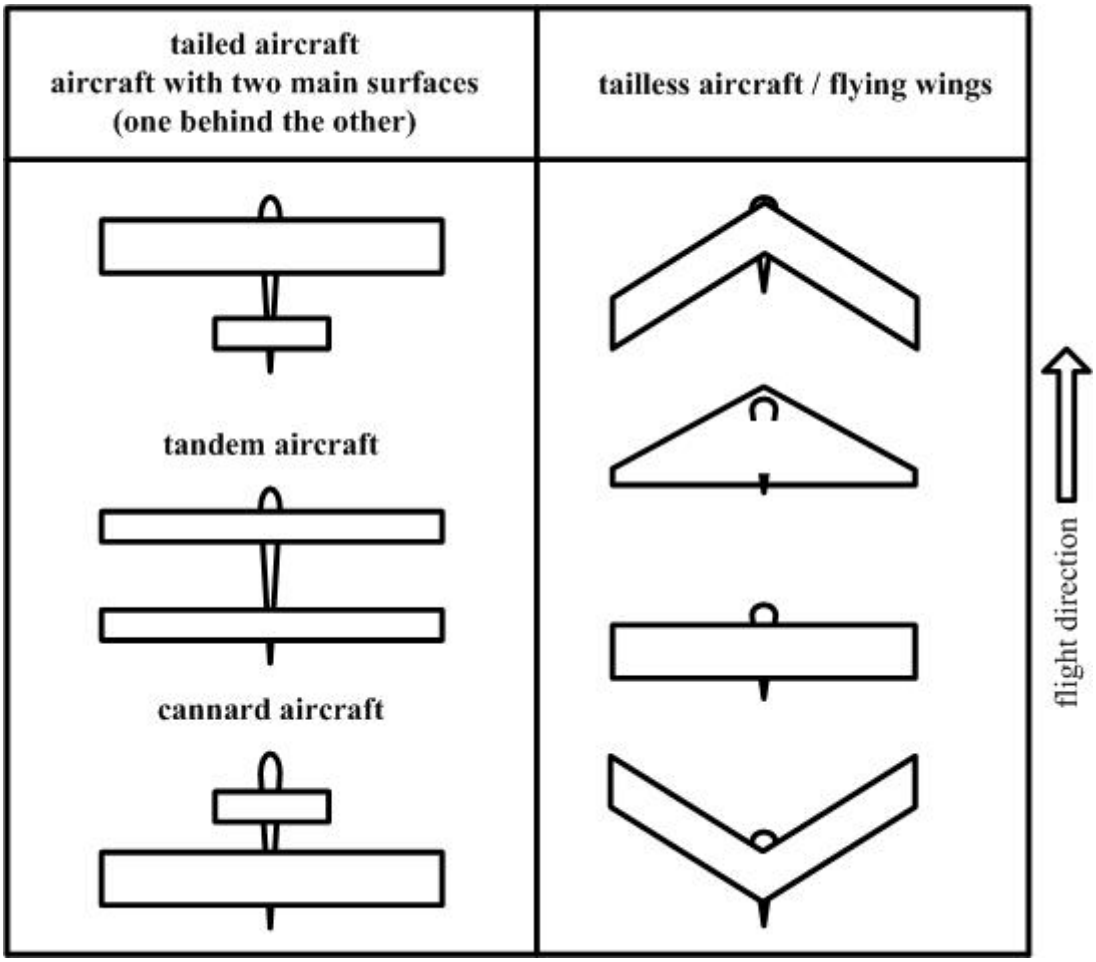

Figure 2-1 Schematic Diagram of Conventional and Fly-Wing Aircraft

Through recognizing the improved aerodynamic characteristic by only one lift surface, the flying wing has been continuously developed from the beginning of manned flight in the UK, US and Europe. In 1912, John Dunne of the UK flew the first swept flying wing successfully in the world (Figure2-2.a). Not only did he realize the advantage of wing sweep for increasing effective tail length (counteract the premature tip stall), but also he incorporated wash out or twist at the wing tip [8].

In Germany, the Hortern brothers of Reimar and Walter designed the first pure jet-powered flying wing bomber named Go-229(Figure2-2.b) for the German Air Force in World War II. The test flight was accomplished in 1945. This configuration is more or less similar to the Northrop's for certain aspects during the same period [8].

Certainly, in the US, it is believed that Northrop played a significant role in the contribution to the flying wings design. At its early design time, a flying wing YB-49 in Figure2-2.c was a prototype heavy jet bomber after World War II. This airplane was intended for service for the US Air Force, however, the YB-49 never entered into production.

With the development of FBW (Fly-by-Wire) control system, the B2 "stealth" (designed by Northrop Bomber in 1988 Figure2-2.d), which is a long-range, low-observable, heavy bomber capable of penetrating sophisticated and dense air-defence shields [9]. By virtue of the fly-by-wire control system which provides stability augmentation, trimming, computation data of CG position and weight, FSC warnings, etc., the B-2 is able to achieve Level 1 flying qualities over its whole flight envelope [10].

Nowadays, due to the excellent performance in the slow-to-medium speed range of the flying wing configuration, it is still a practical concept for aircraft designers and there has been continuous interest in applying it to a tactical transport aircraft design. Boeing has been continuing to engage in paper projects for a tailless transport aircraft, which is sized as the Lockheed C-130 Hercules but with better range and 1/3 more load [11]. Many companies, such as Boeing, McDonnell Douglas and de Havilland, have also studied the flying-

wing configuration airliner, but none have been entered into practical application [1].

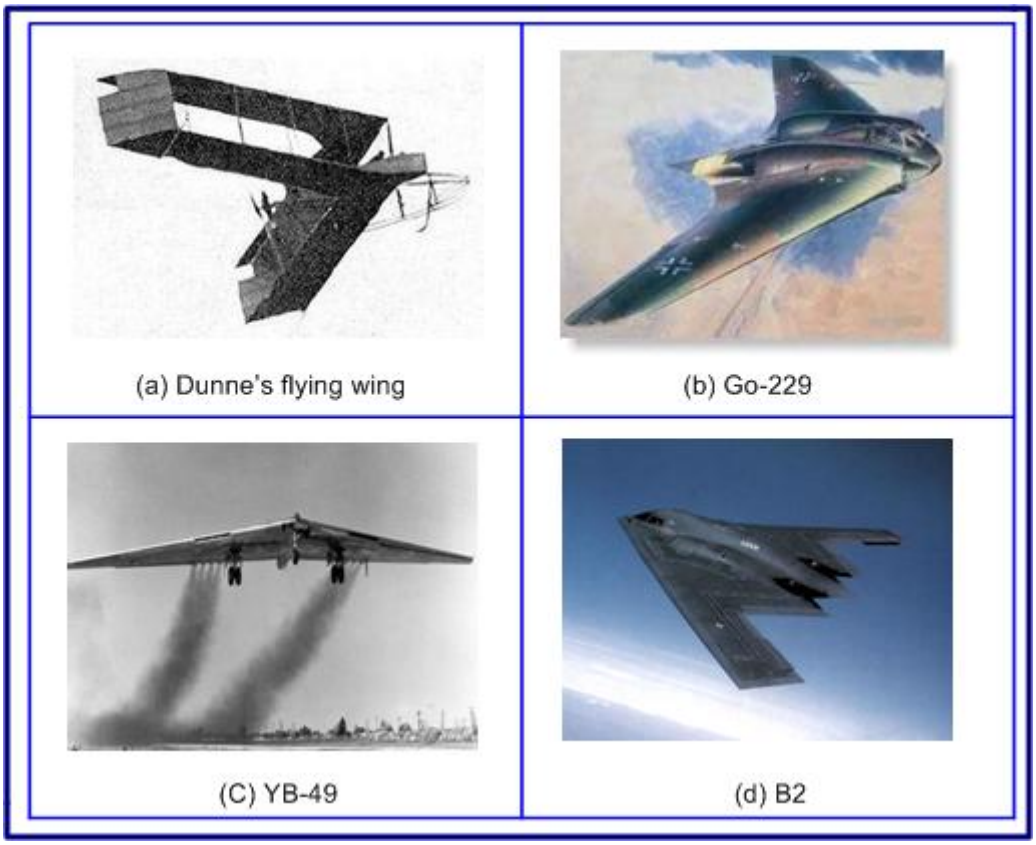

Figure 2-2 Dunne's Flying Wing, Go-229, YB-49 and B2 Bomber

2.1.2 Blended Wing Body Aircraft

The BWB is an alternative airplane configuration incorporating features from a futuristic fuselage and the flying wing. These are well integrated for improving the aerodynamic performance.

This hybrid design combines high-lift wings with a wide airfoil-shaped body, which results in increased lift and reduced drag of the whole aircraft. This shape not only provides the advantages in aerodynamic and fuel efficiencies of a pure flying wing design over a fuselage-and-wing configuration, but also creates larger interior space in the centre portion of the aircraft [3].

Figure 2-3(a) shows the X-48 BWB (developed by Boeing and NASA from the late 1990s), which is an experimental Unmanned Aerial Vehicle (UAV) for investigation of BWB aircrafts characteristics. In addition, in Figure2-3(b) (a

proposed transport airplane), the BWB is also recognised as the most promising aircraft configuration for the future civil transport market [10].

Figure 2-3 BWB Aircrafts

2.1.3 Problems of the Flying Wing

Due to its tailless configuration, the BWB is aerodynamically efficient with a higher lift to drag ratio among the fixed flying wing. Moreover, it contributes to structural weight which generates the better fuel efficiency and lower emissions.

However, inherent design challenges of control system design need to be dealt with .Firstly, owing to the lack of a horizontal stabilizer, the centre of gravity would be more likely to be situated behind the aerodynamic center, which generates a nose-up pitching moment leading to longitudinal instability. In addition, the lever arm between control surfaces and the aerodynamic centre (ac) is smaller in comparison with a tailed airplane. To compromise with these, more or bigger area elevators or other control surfaces offering effective pitch control to compensate for the nonexistent stabilizer are required [1][2].

Further difficulties come from the problem of balancing the thickness of the aerofoil with the inner space for the payload, fuel tank, flight systems, and even engines. Furthermore, because the wing is integrated with the fuselage, there is a lack of surfaces to design the emergency escape exit except the passenger boarding gate. Hence, the emergency egress is also another main problem for the commercial flying wing transport aircraft [1][3].

2.2 Stability and Control

The stability of an aircraft is its ability to recover to the initial steady motion after a disturbance on the condition of no movement of the controls by the pilot [12]. There are three axes concepts of longitudinal, lateral and directional stability. This thesis only focuses on the longitudinal stability.

In the flight dynamics analysis, there are two kinds of stability that will be present as follows.

2.2.1 Static Stability

Static stability defines the aircraft initial tendency to return to equilibrium following some disturbance from equilibrium. An aircraft would display three different types tendency [13] as Figure 2-4 shows respectively.

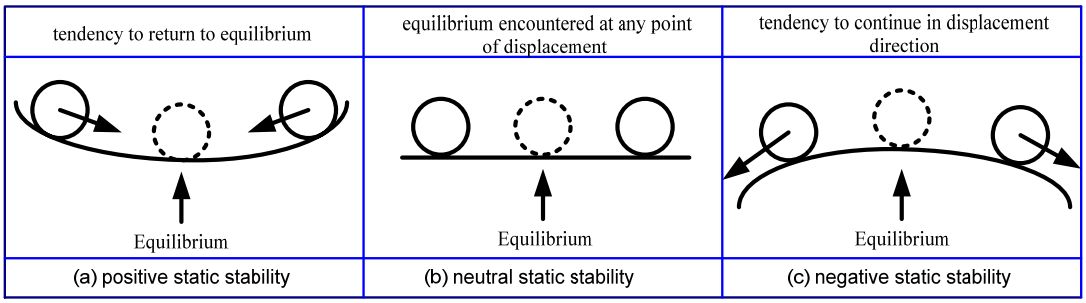

Figure 2-4 Positive, Neutral and Negative Static Stability

In terms of the aircraft longitudinal static stability, it is described that the aircraft can produce a restoring nose down pitching moment (C_m) as the increasing nose up angle of attack α, namely the coefficient of pitch moment due to angle of attack need to be negative for static stability. Because longitudinal stability depends on the angle of attack which has a linear correlation with the overall lift coefficient (C_L), it could be defined with respect to the negative value dC_m/dC_L. This phenomenon is due to the position relationship between the aircraft centre of gravity (CG) and aerodynamic centre (AC). The airplane is statically stable if the CG position lies in front of the ac. Furthermore, in terms of control fixed static stability, the distance between AC and CG is called the control fixed static margin as K_n, the slope of the C_m and C_L. If the K_n is positive, the greater its

value the greater the degree of stability processed by the statically stable aircraft [14].

It is clear that a stable aircraft could benefit pilots as the aircrafts would possess the tendency to recover to straight and level flight. Nevertheless, the manoeuvrability (trade-off for stability) should be simultaneously taken into account. Much stability margin means the pilot conquer a greater return tendency to change the attitude. Therefore, in the design process, both of them should be balanced to design the various levels of stability, which enables to obtain a satisfactory level for keeping normal flight without strenuous effort for pilot [10].

2.2.2 Dynamic Stability

While static stability is defined as the original tendency when disturbed from equilibrium, dynamic stability is explained by the resulting motion with time which is more complex than the static stability. Figure 2-5 illustrates positive, neutral and negative dynamic tendency with the amplitude of the system oscillation decreasing, constant and increasing.

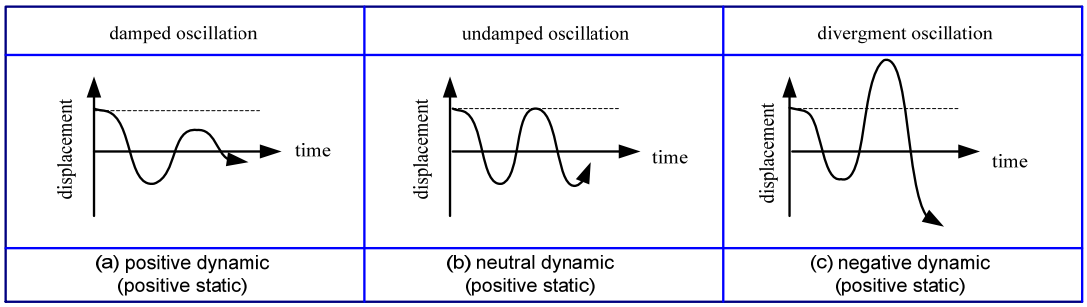

Figure 2-5 Positive, Neutral and Negative Dynamic Stability

In any system, positive static stability is a necessary but not sufficient condition for the positive dynamic stability. If static stability is positive, however, dynamic stability could be positive, neutral or negative. If static stability is neutral or negative, dynamic stability will be the same as the static stability.

Damping is the definitive parameter to effect the disturbance reduction. According to the different value of the damping ratio ζ, the system responses, shown in Figure 2-6, are divided into three cases as follows:

1) under-damping ($0 < \zeta < 1$)
2) critically damping ($\zeta = 1$)
3) over-damping ($\zeta > 1$)

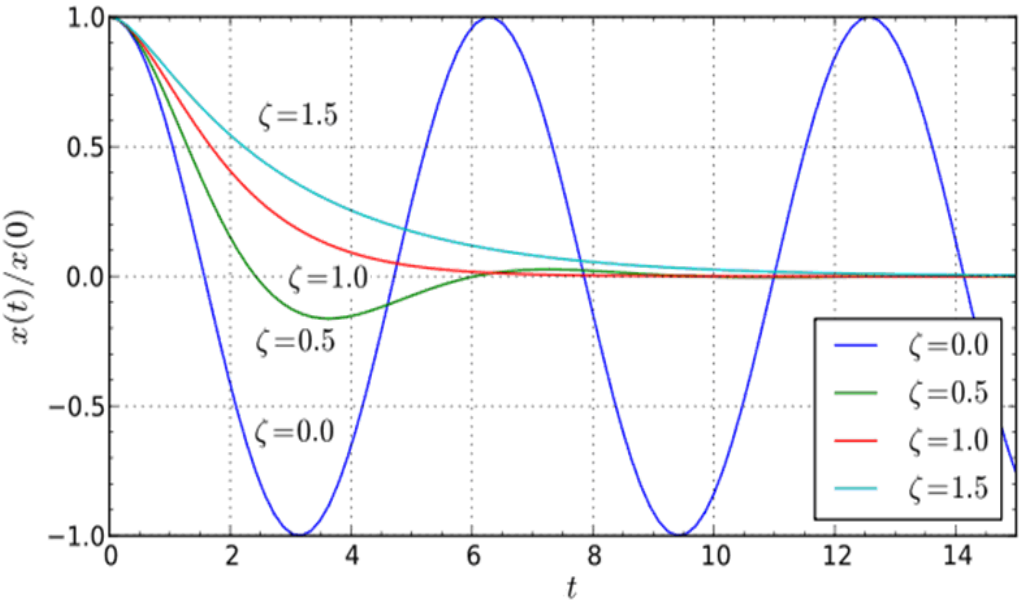

Figure 2-6 Dependence of System Responses on the Value of ζ

A short period mode damping ratio of 0.7 is the ideal value for traditional second order control system as Cook stated [15]. This gives a satisfactory stability margin and results in the shortest mode settling time following a disturbance.

In aircraft control laws design, the dynamic response stability of attitude, velocity and acceleration, in both short period and phugoid mode, are all important criteria for flying and handing qualities [5]. Hence, dynamic response analysis and evaluation should be understood on the basis of static stability assessment.

2.3 Flying and Handing Qualities

2.3.1 Overview

Due to the increasing frequency of aircraft crashes in the early 1900s, aeronautical engineers became aware of the importance of certain principals of aircraft design [16]. These could construct the relationship between flying qualities and stability theory. Thus, the further step, employs mathematical theory to engineering practice, would not be difficult [7].

Nowadays, flying and handing qualities play a significant and necessary role in control system design for manned aircraft [17]. Cook describes: "*The flying and handing qualities are properties that govern the ease and precision with which it responds to pilot commands in the execution of the flight task*" [15]. In order to ensure the accomplishment of desired mission safely and successfully with the minimum amount of workload for the pilot, the control system needs to satisfy the corresponding specification and standards.

2.3.1.1 Civil Requirements

At present, civil requirements, for both FARs-25 (JARs-25 is similar) and CS-25, are relevant to conventional aircraft. A comprehensive suite of safety and performance requirement is a series of necessary documents with which any commercial transport aircraft must comply for the grant of airworthiness certificate. It is much more appropriate that these specifications apply to civil transport aircrafts as Boeing and Airbus series. However, there are few items to quantify the flying and handing qualities in both documents and so more quantitative criteria have been developed in military requirements [18].

2.3.1.2 Military Requirements

MIL-F-8785C is the best know specification and was first produced in 1954. The latest issue is the MIL-F-8785C which was released in 1980. This is the beginning of modern flying and handing qualities specification in that the desired aircraft dynamic responses were specified for the first time [5]. Moreover, all military services agreed upon a unifying standard. In this

document, the airplane dynamic responses of longitudinal and lateral mode were quantified with frequency and damping ratio requirements [19].

With the development of control technology such as the Active Control Technology (ACT) and Fly-by-Wire (FBW) control system, the MIL-STD-1797 was issued in 1987. It considers the high gain use, high authority augmentation, and reflection of intended mission into the document. In 1997, an updated issue of MIL-STD-1787B was published to completely deal with the flying qualities problems of new generation aircraft [5].

2.3.2 Longitudinal Short Term Small Amplitude Criteria

There are plenty of criteria the have been applied to assist control system designers for ensuring the satisfying dynamic response, including mainly CAP criterion, bandwidth criterion, the Neal-Smith criterion and Gibson's drop-back criterion [20].

2.3.2.1 Control Anticipation Parameter (CAP) Criterion

The CAP criterion was developed to predict the precision that a pilot could expect in controlling an aircraft's flight path. Nevertheless, it is required to obtain a lower order equivalent system to apply this criterion for highly augmented aircraft. Although the normal acceleration response is determined by the aerodynamic property, the CAP criterion aims to assess the transient peak magnitude of angular pitching acceleration which is mainly decided by the short period dynamics after the pitch control input. Therefore, it is significant and universally used to evaluate acceptability of the short period mode feature according to aerodynamic properties and the different operating conditions [21].

2.3.2.2 Bandwidth Criterion

Bandwidth criterion is one of the pilot-in-loop methods for which the pilot model is just a gain. This criterion requests the bandwidth frequency where the phase margin is 45^{o} or where the gain margin is 6db when operated in a closed pilot-in-loop compensatory pitch attitude tracking task [17].

2.3.2.3 Neal-Smith Criterion

The Neal-Smith criterion is a frequency domain criterion that attempts to rectify the short comings of time domain criteria, particularly for the pitch tracking task which has emerged as an essential measure of pilot handing opinion [8]. Three definitions of handling parameters used in the closed loop tracking performance assessment are minimum bandwidth (3.5rad/s), -3db droop and closed loop resonance [22]. This method presents as a two-dimensional plot lead and lag compensation versus pilot-in-loop resonance, which illustrates the tendency of resonance, even PIO.

2.3.2.4 Gibson's Dropback Criterion

The Gibson's dropback criterion aims to design a command and stability augmentation system (CSAS) which could endow an aircraft with satisfactory handing qualities [22]. This criterion is described as limiting values with pitch rate overshoot ratio versus the ratio of attitude dropback to steady pitch rate. It is an acceptable value when it lies in the range between 1.0 and 3.0 [23]. Unfortunately, since the flight path or attitude system have zero steady-state pitch rate response to a step control input, Mitchell [5] demonstrates that the restriction of this criterion is that the measure of pitch rate overshoot is not suitable in the assessment of these systems.

2.3.2.5 Summary

Table 2-1 summaries the comparison between the criteria stated above.

Table 2-1 Comparison of Criteria

Criterion	Analysis method	Evaluation objectives	Model
CAP Criterion	Time Domain	Short period dynamics	Short term response transfer function
Bandwidth Criterion	Frequency domain	Adequate stability margin and attitude tracking	Closed pilot-in-loop compensatory (gain) equivalent CSAS
Neal-Smith Criterion	Frequency domain	Tracking performance handing qualities	Closed pilot-in-loop compensatory (lead and lag) equivalent CSAC
Gibson's Dropback Criterion	Time domain	Precision tracking	Short term response transfer function

2.3.3 The Cooper-Harper Rating Scale

With the purpose of aircraft flying and handing qualities assessment, plenty of methods are available for the control system designers. Cooper and Harper developed the pilot opinion rating scale in 1969 which is called the Cooper-Harper rating scale, Figure 2-7 [24]. The aviation industry has long relied on this evaluation tool for the assessment of flying and handling qualities during flight or simulation tests. It defines the flight task that the pilot needs to perform. The significant contribution of this measurement tool is that it provides a standardized scale that can be used to compare the handing qualities across aircraft [19]. In addition, it also helps test pilots articulate specific types of aircraft handling problems. Hence, this tool could help pilots assess the qualities more clearly rather than express them in terms of their opinions.

In order to obtain a meaningful and simple interpretation between piloting and analytical domains, the MIL-F-8785C definitions of three flying quality levels are equivalent to the different Cooper-Harper rating scale as Table 2-2 shows [15].

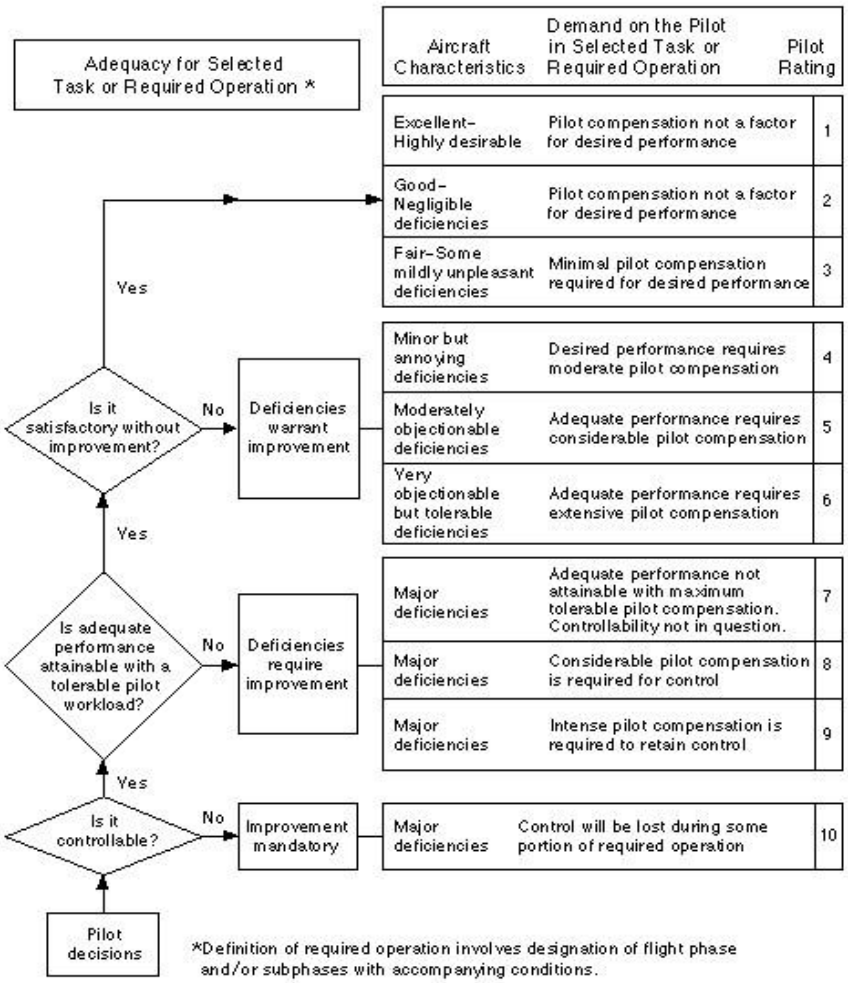

Figure 2-7 Cooper-Harper Rating Scale

Table 2-2 Equivalence of Cooper-Harper Rating Scale with Flying Quality Levels

level / Flying qualities	Level 1			Level 2			Level 3		Below level 3
Cooper-Harper rating scale	1	2	3	4	5	6	7	8	9	10

2.4 Gain Scheduling

2.4.1 Introduction

When developing controllers for aircraft by using a linear mathematical model at different trim flight conditions, the gains would be demanded to implement the controller's function as some form of scheduling over the wide flight envelope. Nowadays, gain scheduling is a popular and important technique that can be used in the flight control system design [25].

The idea of the gain scheduling approach is to control nonlinear systems by using a series of linear controllers which offers satisfactory control performance at each selected design point. In comparison to the classical control method, gain scheduling control can provide control over the whole envelope rather than only being valid around the neighbourhood of a design point [26].

Figure 2-8 shows the basic control structure by gain schedule. On the basis of a linearized aircraft model and corresponding controllers at the different design cases, the scheduling variables are input measured parameters to change the appropriate linear controller for the aircraft control system. The Mach number and altitude could be the various combinations with different linear controller parameters.

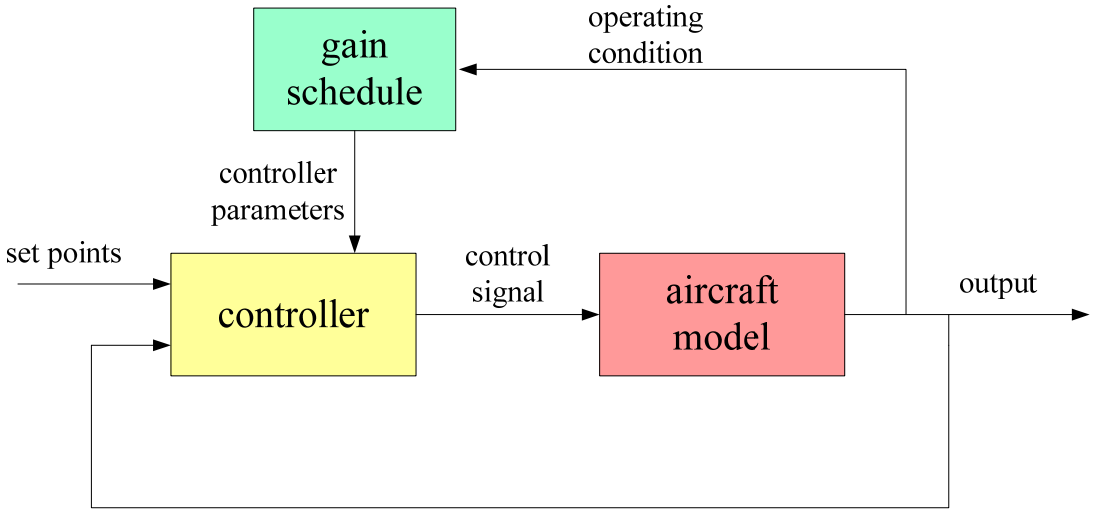

Figure 2-8 Basic Control Structure by Gain Schedule

This method has wide and successful engineering application. In the aerospace field, gain scheduling is regarded as a most common systematic method to address the nonlinearity of aircraft dynamics during the entire flight envelope.

In order to tackle difficulties of controlling the new generation jet airplanes, the advent of the guided missile and expended flight envelope, gain scheduling started in earnest toward the end of World War II. In the mid 1950s, this approach was used mainly for military applications, including missile guidance and autopilots of the B-52. Due to extensive implementation costs, the widespread application of the gain scheduling did not start to arise until the advent of digital computation [25]. In resent years, mainly based on the following reasons, there have been an increasing number of published studies and references in this field [27]:

1. A suite of control design methods and tools on simple linear model could be used by designers.
2. Flight control clearance and certification procedures are usually on the basis of linear methods.
3. Even if the model information is limited to a few trim cases and corresponding linearization models, gain scheduling could still be used.
4. The controller gains can be quickly changed in response to changes in the aircraft dynamics.

2.4.2 Application in Flight Control

It is well known that the aircraft aerodynamics and control effectiveness of the control surfaces vary according to altitude, Mach number or dynamic pressure. Therefore, gain scheduling aims to eliminate these effects [28].

Taking the B-52 autopilot for example, the compensation for the changing control surface effectiveness incorporates an airspeed-based mechanism which is used to vary the gains of the position feedback transducer of the servo actuator. The scheduled loop gain can maintain the appropriate closed-loop system bandwidth, which avoids the more complicated approach of scheduling many different gains. Later, the mechanism for scheduling by airspeed replaced

by dynamic pressure which was introduced to maintain reasonably constant gains [28].

In recent years, the approach of gain scheduling has been considered as a standard approach to develop Linear-Time-Invariant (LTI) controllers for Linear-Time-Varying (LTV) or nonlinear systems (approximated by LPV system) in control theory [18].

With varying levels of success, LPV control synthesis techniques not only have already been used in high-performance airplanes as representative as the F14, F16, F18, and the VAAV Harrier, but also as turbofan engines, air/fuel regulation, missiles and recent reconfigurable controllers respectively [29].

2.4.3 Design Procedure

According to reference [26], the procedure for designing a gain scheduled controller for a nonlinear model can be defined as follows:

1. The most common method is to linearize the aircraft model at a set of equilibrium cases over the whole flight envelope.
2. Design a series of linear controllers and gains to be used to stabilize the system at each operating points by the corresponding linear model.
3. Choose suitable scheduling variable parameters and schedule each controller gains to create a global controller with the parameter changing according to the current value of the scheduling variables.
4. Evaluate the flying and handing qualities by linear and non-linear analysis and extensive simulation.

2.4.4 Summary

Gain scheduling has been described as the process of designing controllers to suit each design condition and reconstructing the resultant set of gains into a single continuous controller. It is one such control technology that is particularly suitable for overcoming nonlinearities in aircraft flight control system design.

In spite of a great deal of effort and the contributions which have been made to gain scheduling studies in the last decades, some restrictions still remain. These include constraints on the maximum changing rates of scheduling

parameters, the guarantee of the stability and performance, etc. Hence, a number of methods have been proposed recently including Dynamic State-Feedback Gain Scheduling (DGS) [25], linear matrix inequality based constructions of H_∞ optimal controllers [28], etc.

The gain scheduling method has universal applications in practical engineering areas and researches. Moreover, it still brings practical advantages such as simplicity, generality, low computational complexity and ease of implementation. Therefore, this conventional technology contains a significant practical meaning in several areas of engineering.

2.5 Conclusion

From the preceding comments in the literature review, a great deal has been studied in the background of tailless configuration aircraft and content which is related to control system design.

Firstly, it is required to learn the historical background and characteristics of the flying wing concept, particularly the advantages and drawbacks, which may also occur for BWB aircraft. In spite of the challenges that exist today, the BWB is still considered as the most promising configuration for the future of advanced transport aircraft. Consequently, with the development of modern airplane design concepts and flight control systems, research in flying and handing qualities drives numerous studies to improve aircraft performance based on stability and control analysis. Nowadays, tailless aircraft such as the B2 and some tailless Unmanned Aerial Vehicles (UAV) demonstrate that this configuration of airplane can be flown and controlled adequately. In specific control methods, the conventional gain scheduling gives an insight to one of the practical engineering approaches which could be used to solve nonlinear control problems.

Finally, it is not until the tools and hardware of control system design for the BWB transport aircraft are constructed and the substantial problems are successfully eliminated, that this kind of efficient aircraft can be realised for future transport market.

3 SAS CONTROL LAWS DESIGN

Most high performance commercial and military aircrafts require some form of stability augmentation. Some of present military aircrafts are actually static unstable so that these airplanes would be impossible to fly without the control system. In terms of the control system design, the SAS feeds back certain signals of aircraft response to servomechanisms which drive the aerodynamic control surfaces. In this way the aerodynamic derivatives which are used to produce a damping and frequency effect on the motion could be changed [30].

In this chapter, the background and general data of the reference aircraft will be introduced initially. It is followed by the flying and handing quality constraints to this SAS design. On the basis of the model trim and linearization, the initial SAS controller C_1 will be described with the flying and handing qualities assessment and wind disturbance simulation.

3.1 Introduction of the Reference BWB Aircraft

The reference BWB aircraft is based on the EU's VELA project which is the first step to develop the large transport aircraft in a long term strategy. It aims to deal with the demand of large and efficient airliner, furthermore, to take advantage of this strategy to contribute to strength of the European aerospace industry in the international market for the next 30 to 50 years [3].

The technical objective of the VELA is to establish methods, design procedures mainly including aerodynamic, structures, stability and control and multidisciplinary tools for the unconventional configuration as BWB. In addition, it creates a technological reserve that could be utilized for the future advanced aircraft research as well [3] [10].

Based on the previous research results, a series of BWB configurations have been developed for validation [3]. In this thesis, all the geometry and aerodynamic data used for longitudinal control laws design study are obtained from the Canfield University PhD work [5] [6] of Castro and Rahman.

The layout of the BWB aircraft is shown in Figure 3-1. For longitudinal control, all flaps (elevators and ailerons) are deflected as a whole elevator without the consideration of control surfaces allocation. The maximum flap deflection range $\pm 30^{\circ}$ is assumed for all flaps [6].

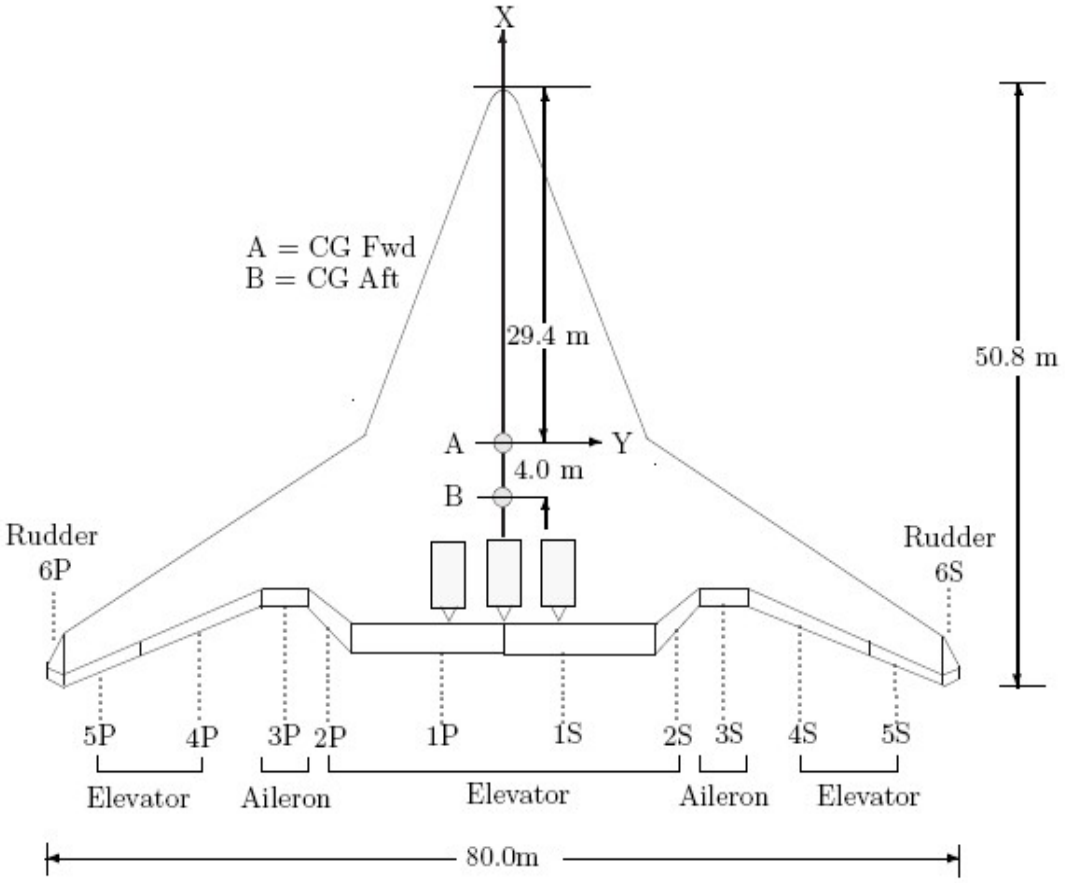

Figure 3-1 Layout of the Reference BWB Aircraft

The general parameters of the BWB aircraft are demonstrated in Table 3-1 [6]. More specific aircraft data including geometric properties, mass, aerodynamic derivatives are referred to the Appendix A in reference 6.

Table 3-1 Basic Parameters of the Reference Aircraft

	Approach case	Cruise case
Mach number	0.23	0.85
Altitude (m)	Sea level	10059
Mass (kg)	322,599	371,280
Reference area (m^2)	841.70	
Mean aerodynamic chord (m)	12.31	
CG range(m)	29.4~34.4	
Aerodynamic centre (m)	31.6	

3.2 Flying and Handing Quality Constraints

It is essential to ensure the flying and handing qualities limitation as the requirements for the control laws design exploration according to the aircrafts classification, flight phase categories and qualities levels in MIL_F_8785C specifications [31]. In Table 3-2, these basic parameters of the reference BWB aircraft are defined.

Table 3-2 Basic Parameters of the Reference Aircraft

Specification Requirements	Reference BWB Aircraft	Description
Classification	Class Ⅲ	Heavy transport
Flying Qualities Levels	Level 1	Flying qualities clearly adequate for the mission flight phase
Flight Phase Category	Category B/C	Cruise / Taking-off and Landing phase

Many existing criteria could be applied for assessment of the longitudinal flying and handing qualities. The purpose of a pitch SAS is to provide satisfactory damping and natural frequency for the short period oscillation (SPO) mode [30]. Hence, in this study, the criteria in MIL-F-8785C specifications applied in the SAS controller design are as follows:

- Damping ratio limitation
- Control Anticipation Parameter (CAP) criteria

3.2.1 Damping Ratio limits

In terms of longitudinal dynamic response time, the SPO and phugoid mode could be considered separately. In MIL-F-8785C specifications, acceptable limits on the stability of SPO are quantified by the range of damping ratio with respect to flight phase categories and qualities levels as Table 3-3 shows. For the phugoid mode damping ratio limits, these are quantified in Table 3-4 [31].

Table 3-3 MIL-8785c Short Period Mode Requirements

Category A(rapid manoeuvring) Category C(take-off and landing)		**Category B (gradual manoeuvring)**	
Level 1	0.35-1.3	**Level 1**	0.3-2.0
Level 2	0.25-2.0	**Level 2**	0.2-2.0
Level 3	0.15	**Level 3**	0.1

Table 3-4 MIL-8785c Phugoid Mode Requirements

Flight Qualities Levels	**Minimum Damping Ratio**
1	0.04
2	0
3	Unstable, period $T_p > 55s$
Ideal frequency $\omega_{np} < 0.1\omega_{ns}$	

It is explicit that the limits of short period damping ratio are a range constraints which provide relatively large regions for designers. Cook demonstrated that the ideal damping ratio of SPO mode is 0.7, which could provide a satisfactory margin of stability and results in the shortest settling time after a disturbance [15]. Moreover, if this value is more than 1.0, the system will enter into the over-damping state and the settling time will tend to be longer. Hence, the ideal damping ratio range is considered as $0.7 \le \zeta \le 1$ in this study. For phugoid mode, damping ratio limits are relaxed due directly to the long period which provides a long time to pilots to control the aircraft.

3.2.2 CAP Criteria

Clearly, a good longitudinal short term second order system, particularly the damping and frequency of the SPO mode, could provide the good satisfactory handing cues.

CAP quantifies suitable SPO mode characteristics appropriate to the aerodynamic properties and operating condition. It could be clarified according to natural frequency (ω_{ns}) and the value of normal load factor per unit angle of attack (N_α) by equation (3-1) [15].

$$CAP = \frac{\dot{q}(0)}{N_z(\infty)} = \frac{\omega^2{}_{ns}}{N_\alpha} \tag{3-1}$$

where:

$$\omega^2{}_{ns} = \sqrt{M_q Z_\omega - M_\omega (Z_q + U_e)} \tag{3-2}$$

$$N_\alpha = -Z_\omega U_e / g \tag{3-3}$$

CAP is evaluated graphically by parameters ω_{ns} and N_α using reduced second order aircraft model for the step response of SPO mode. Taking flight phase A for example, the level 1 to level 3 limits in the CAP criteria of MIL-F-8785C specifications are described in Figure 3-2 [31].

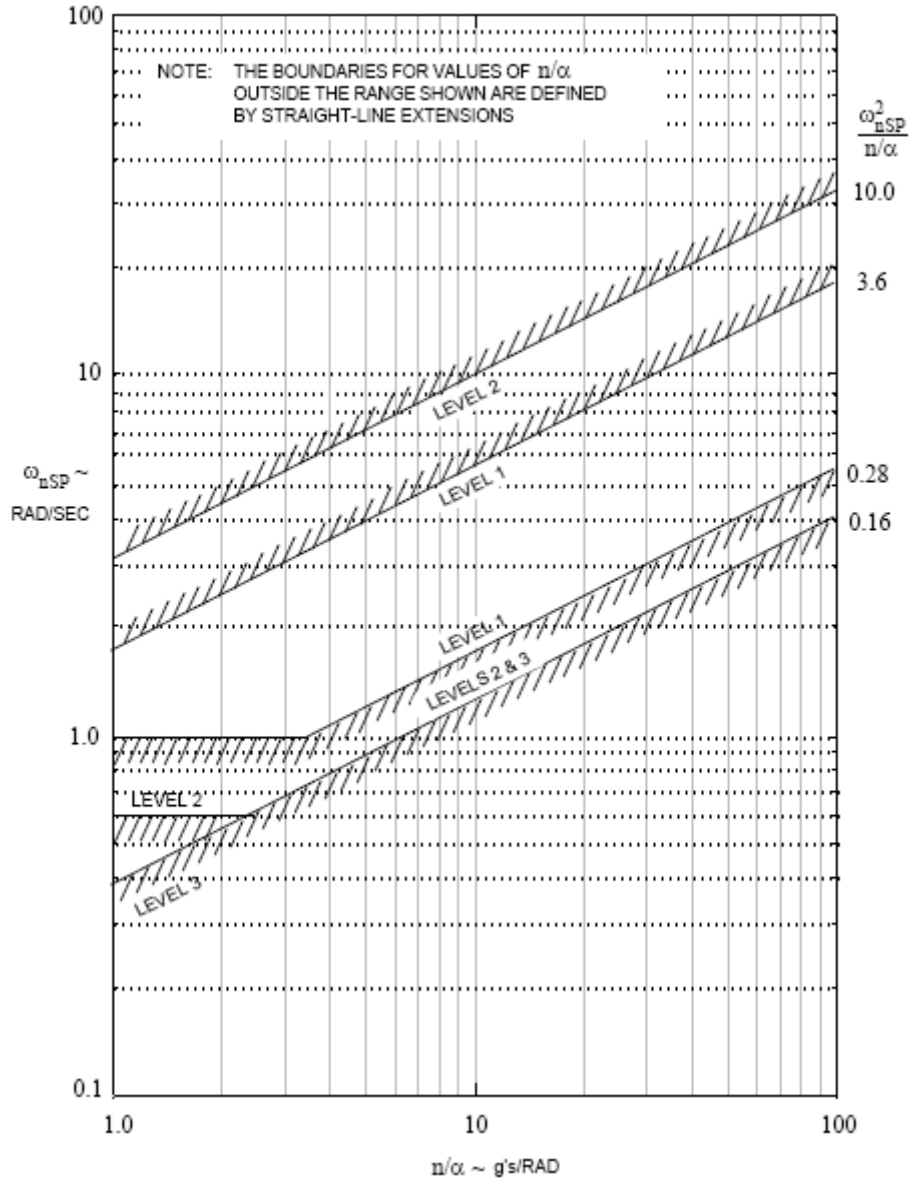

Figure 3-2 CAP Requirements – Category A Flight Phase

3.3 Aircraft Model Trim and Linearization

3.3.1 Aircraft Model Trim

A trim state defines the initial condition which the dynamics of interest may be studied. Trimming aims to bring the forces and moments acting on the aircraft into equilibrium so that the three axes forces and moments are all zero. It is convenient to use the MATLAB trim utility for solving the equation of motion for a steady level flight. At this condition, all the state derivatives are assumed zero

excluding position derivatives. Consequently, the longitudinal equation of motion at above constraints is expressed by equation (3-4) [4].

$$\begin{bmatrix} \dot{u} \\ \dot{w} \\ \dot{q} \\ \dot{\theta} \\ \dot{h} \end{bmatrix} = \begin{bmatrix} (X+T_x)/m + (rV - qW)/m - g\sin\theta \\ (Z+T_z)/m + (qU - pV)/m + g\cos\theta \\ M/I_y - pr(I_x - I_z)/I_y - (p^2 - r^2)I_{xz}/I_y \\ q\cos\phi - r\sin\phi \\ U\sin\theta - V\cos\theta\sin\phi - W\cos\theta\cos\phi \end{bmatrix} \tag{3-4}$$

In this study, the aircraft trimming is realised by the MATLAB program < TRIM_LINMOD_HQUALITY_BWB .m> which is presented in Rahman's PhD thesis [6]. The reference aircraft can be trimmed over the whole envelope (Chapter 4.1) at the required equilibrium conditions including true airspeed, altitude, CG position and flight path angle.

3.3.2 Aircraft Model Linearization

For a rigid symmetric aircraft, the general equations of motion are constructed based on Newton's second motion law. The principle and procedures can be found in plenty of textbooks. By using small perturbation method and further decoupling the equation into longitudinal and later motion at a trim condition, an aircraft could be described as a classical example of a linear dynamic system [15].

In order to use matrix method for equations of motions solving, state equations of the Linear-Time-Invariant (LTI) multi-variable system form is written in equation (3-5).

$$\begin{aligned} \dot{x}(t) &= Ax(t) + Bu(t) \\ y(t) &= Cx(t) + Du(t) \end{aligned} \tag{3-5}$$

where: A —State matrix ($n \times n$)

B —Input matrix ($n \times m$)

C —Output matrix ($r \times n$)

D —Direct matrix ($r \times m$)

$x(t)$—column vector of n state variables

$u(t)$—column vector of m input variables

$y(t)$—column vector of n output variables

In terms of longitudinal state space equation (without the engine control) with variables of u, α, q, θ in body axes system, the coefficients of state matrix A (aerodynamic stability derivatives) and B (control derivatives) can be written as the concise form in equation (3-6) [15]; moreover, the output equation is shown as equation (3-7) [15]. The calculation for all the coefficients can be found in reference 15 Appendix 2. The following work will be developed on the basis of these state space equations.

$$\begin{bmatrix} \dot{u} \\ \dot{w} \\ \dot{q} \\ \dot{\theta} \end{bmatrix} = \begin{bmatrix} x_u & x_w & x_q & x_\theta \\ z_u & z_w & z_q & z_\theta \\ m_u & m_w & m_q & m_\theta \\ 0 & 0 & 0 & 1 \end{bmatrix} \begin{bmatrix} u \\ w \\ q \\ \theta \end{bmatrix} + \begin{bmatrix} x_{\delta_e} \\ z_{\delta_e} \\ m_{\delta_e} \\ 0 \end{bmatrix} \delta_e \tag{3-6}$$

$$\begin{bmatrix} u \\ w \\ q \\ \theta \end{bmatrix} = \begin{bmatrix} 1 & 0 & 0 & 0 \\ 0 & 1 & 0 & 0 \\ 0 & 0 & 1 & 0 \\ 0 & 0 & 0 & 1 \end{bmatrix} \begin{bmatrix} u \\ w \\ q \\ \theta \end{bmatrix} + \begin{bmatrix} 0 \\ 0 \\ 0 \\ 0 \end{bmatrix} \delta_e \tag{3-7}$$

According to the relation between α and w in equation (3-8), equation (3-7) is given by equation (3-9) to deal with the inclusion of α (feedback signal in SAS) in longitudinal decoupled state matrix [15].

$$\alpha \cong \tan\alpha = \frac{w}{v_0} \tag{3-8}$$

$$\begin{bmatrix} \dot{u} \\ \dot{\alpha} \\ \dot{q} \\ \dot{\theta} \end{bmatrix} = \begin{bmatrix} x_u & x_w v_0 & x_q & x_\theta \\ z_u / v_0 & z_w & z_q / v_0 & z_\theta / v_0 \\ m_u & m_w v_0 & m_q & m_\theta \\ 0 & 0 & 0 & 1 \end{bmatrix} \begin{bmatrix} u \\ \alpha \\ q \\ \theta \end{bmatrix} + \begin{bmatrix} x_{\delta_e} \\ z_{\delta_e} / v_0 \\ m_{\delta_e} \\ 0 \end{bmatrix} \delta_e \tag{3-9}$$

3.4 SAS controller C_1 at initial Point P_1

Assuming the state vector $x(t)$ is used for negative feedback to achieve the stability augmentation and $v_C(t)$ is the input demand variable vector, the control law could be written as:

$$u(t) = v_C(t) - Kx(t) \tag{3-10}$$

K is the feedback gain matrix.

Thus, by substituting equation (3-10) into equation (3-5) the closed loop of augmented aircraft is

$$\begin{aligned} \dot{x}(t) &= [A - BK]x(t) + Bv_C(t) \\ y(t) &= [C - DK]x(t) + Dv_C(t) \end{aligned} \tag{3-11}$$

Obviously, a new state matrix $A_{aug} = A - BK$ is the augmented aircraft matrix with improved flying qualities.

In terms of signal feedback influence to the system dynamic response, the SAS feedbacks are angle of attack and pitch rate in order to improve the natural frequency and damping respectively. The basic SAS architecture is shown in Figure 3-3 [15].

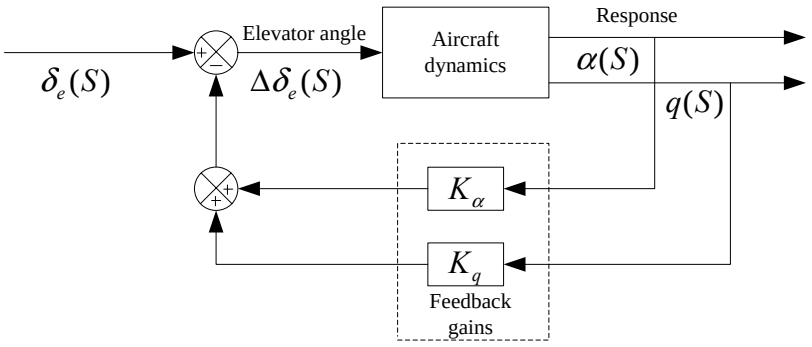

Figure 3-3 Basic SAS Architecture

3.4.1 Controller Gains of C_1

Based on the Rahman's work [6], the control law of stability augmentation system (SAS) at trim point P_1 in Table 3-5 was designed. Consequently, it is supposed that this controller C_1 as the initial controller for checking the flying and handing quality requirements at P_1 and the whole envelope.

Table 3-5 Trim Point P_1 Condition

Aircraft / Flight Configuration	Value/Status	Units
CG Position	30.4	m
Altitude	1500	m
Airspeed	100	m/s
Flight Condition	Straight and level flight	
Flight Phase Category	Category C	

The reduced short period dynamics at this design point is [6]

$$\begin{bmatrix} \dot{\alpha} \\ \dot{q} \end{bmatrix} = \begin{bmatrix} -0.5960 & 0.9874 \\ -1.1816 & -0.2007 \end{bmatrix} \begin{bmatrix} \alpha \\ q \end{bmatrix} + \begin{bmatrix} -0.1304 \\ -1.7745 \end{bmatrix} \delta_e \tag{3-12}$$

The feedback gains K_{C_1} are [6]

$$K_{C_1} = [K_{\alpha\_C_1} \; K_{\mathrm{q\_C_1}}] = [-0.55 \; -1.41] \tag{3-13}$$

Based on equation (3-11), (3-12) and (3-13), the transfer function could be given as follows:

$$\frac{\alpha(s)}{\delta_e(s)} = \frac{-0.1365\,(s+12.47)}{(s^2 + 3.295s + 3.519)} \quad \text{(deg/deg)} \tag{3-14}$$

$$\frac{q(s)}{\delta_e(s)} = \frac{-1.6757\,(s+0.5724)}{(s^2 + 3.295s + 3.519)} \quad \text{(deg/s/deg)} \tag{3-15}$$

3.4.2 Flying and Handing Qualities Assessment

As the SAS controller C_1 engaged in, the SPO reduced second order system variables α and q was considerably improved with a small settling time (2.5s for α and 3s for q) in Figure 3-4. The specific damping and CAP of the SPO mode are improved as Table 3-6 and Figure 3-5 shows. It can be seen that both the damping and CAP are satisfactory with the MIL-F-8785C specifications constraints.

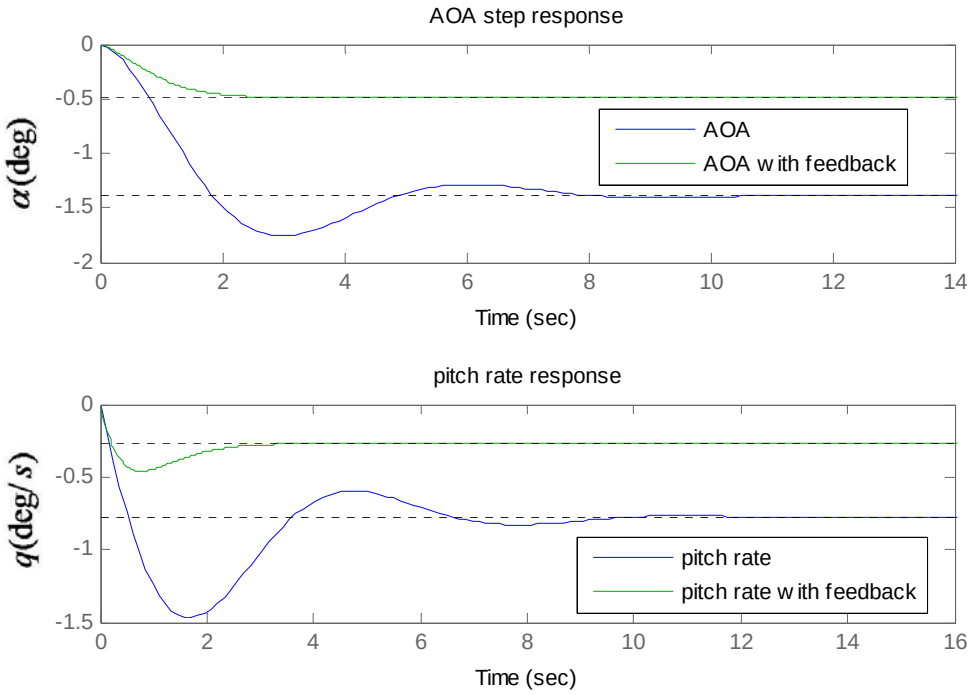

Figure 3-4 SPO Mode Responses on Reduced Second Order System

Table 3-6 Dynamic Response Comparison

Open loop without feedback			**Closed loop with feedback**		
ζ_s	ω_n	**CAP**	ζ_s	ω_n	**CAP**
0.38	1.11	0.18	0.88	1.87	0.53

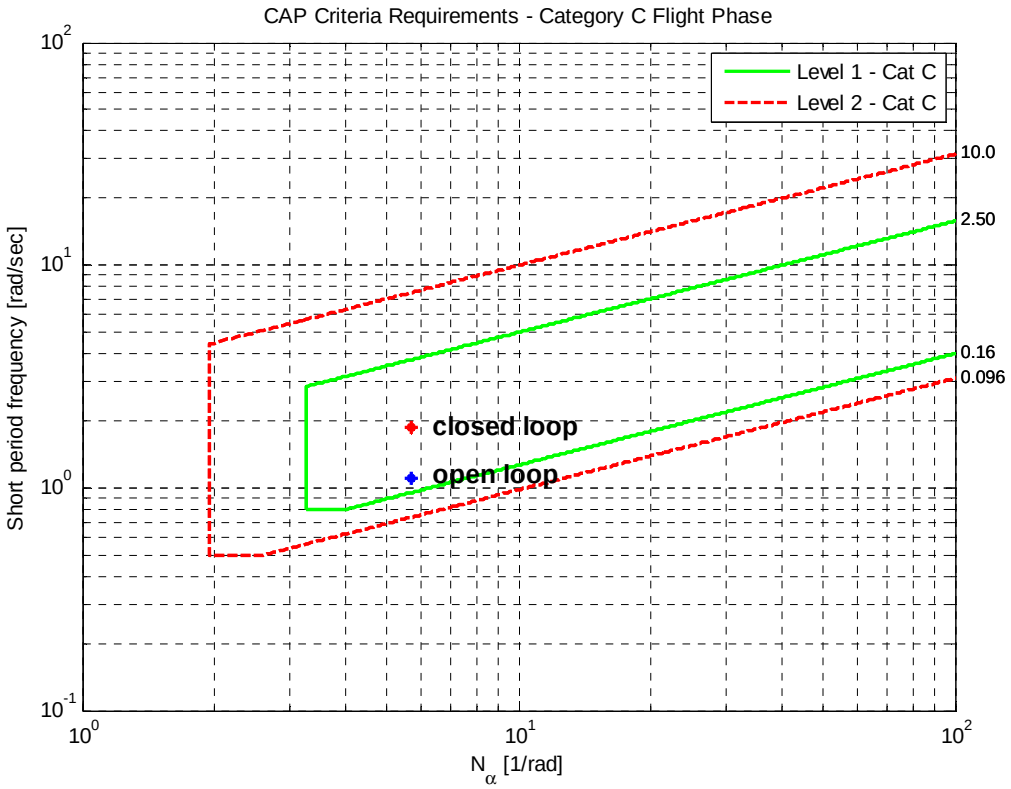

Figure 3-5 CAP of C_1 in Category C

3.4.3 Check C_1 with Full Order System Model

In terms of the open loop full order system with SPO mode and phugoid mode, namely the state space equation (3-6), the resulting state and control matrix coefficients can be calculated by aerodynamic derivatives in reference 6 Appendix A. Thus, the closed loop system is given in equation (3-16) according to equation (3-11).

$$\begin{bmatrix} \dot{u} \\ \dot{\alpha} \\ \dot{q} \\ \dot{\theta} \end{bmatrix} = \begin{bmatrix} 0.0045016 & -12.712 & -23.699 & -9.6055 \\ -0.00067807 & -0.71241 & 0.79399 & -0.019931 \\ 0.0022233 & -1.9931 & -2.558 & 0 \\ 0 & 0 & 1 & 0 \end{bmatrix} \begin{bmatrix} u \\ \alpha \\ q \\ \theta \end{bmatrix} + \begin{bmatrix} -2.5002 \\ -0.1365 \\ -1.6757 \\ 0 \end{bmatrix} \delta_e \qquad (3\text{-}16)$$

Thus, transfer functions of each output variables (u, α, q, θ) with respect to elevator deflection are presented as follows.

$$\frac{q(s)}{\delta_e(s)} = \frac{-1.6757\,s\,(s+0.5648)\,(s-0.01597)}{(s^2+0.002839s+0.00814)\,(s^2+3.263s+3.417)} \quad \text{(deg/s/deg)} \qquad (3\text{-}17)$$

$$\frac{\alpha(s)}{\delta_e(s)} = \frac{-0.1365(s+12.29)(s^2-0.004702s+0.008265)}{(s^2+0.002839s+0.00814)(s^2+3.263s+3.417)} \quad \text{(deg/deg)} \qquad (3\text{-}18)$$

$$\frac{u(s)}{\delta_e(s)} = \frac{-0.043634(s-14.7)(s+1.204)(s+0.1926)}{(s^2+0.002839s+0.00814)(s^2+3.263s+3.417)} \quad \text{(m/s/deg)} \qquad (3\text{-}19)$$

$$\frac{\theta(s)}{\delta_e(s)} = \frac{-1.6757(s+0.5648)(s-0.01597)}{(s^2+0.002839s+0.00814)(s^2+3.263s+3.417)} \quad \text{(deg/deg)} \qquad (3\text{-}20)$$

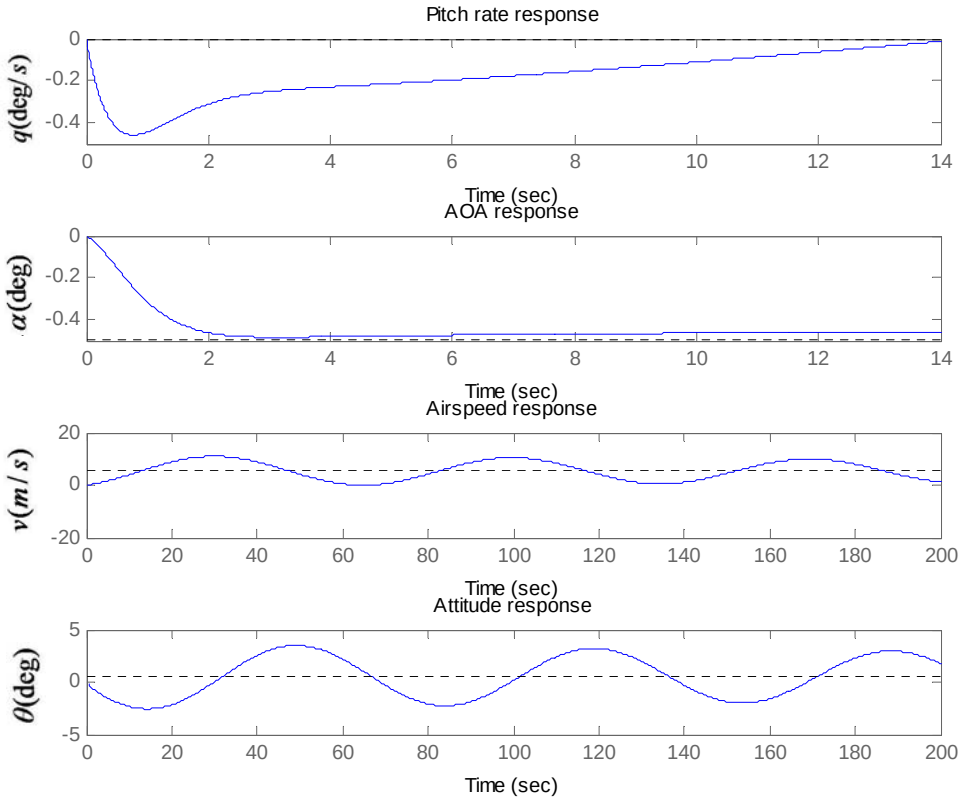

Figure 3-6 Output Variables Response for 1° Step Elevator Command

Thus, the short period damping and natural frequency are $\delta_s = 0.64$ and $\omega_{ns} = 1.33$ rad/s, while for phugoid, the above parameters are $\delta_p = 0.08$ and $\omega_{np} = 0.1$ rad/s. All of them meet the requirements in Section 3.2. Obviously, as Figure 3-6 shows, the short period mode response of angle of attack α and pitch rate q are faster than the aircraft without augmentation. Meanwhile, the phugoid dynamic response of airspeed is stable and slow but oscillatory.

Compared with the pitch rate response of the reduced second order system, the full order system response is influenced by the positive (right half plane) zero. Hence, in order to improve the phugoid dynamics, the other control law could be implemented. For example, in Chapter 7 the autopilot of pitch attitude hold will be designed to control the variables θ.

3.5 Wind Disturbance Simulation

In Chapter 3.4, the aircraft dynamics have been analyzed on the vehicle response to a deterministic pilot control input (step). Nevertheless, the atmosphere rarely is calm but usually is characterized by winds, gusts, and turbulence. Hence, it is also realistic to take the effects of external influence into account on the aircraft response dynamics [32]. In this section, both the discrete sharp-edged gust and the time-varying wind perturbation are considered.

3.5.1 Aircraft Model Modification

3.5.1.1 Assumptions

In this research, the aircraft is in steady level flight at the time that the gust is encountered with no action taken by the pilot. To simplify this analysis in body axes, the aircraft is considered as a point mass in order to neglect the gradient of turbulence. Moreover, it is also assumed that the forward speed and the altitude of the aircraft are unchanged during the passage into the turbulence.

3.5.1.2 Equations of Motion in Turbulence

In order to study the influence of atmospheric disturbances on aircraft motions, the equations of motion should be modified initially.

Generally, the effect to an aircraft when it enters the up-gust (positive) is the variation of relative airflow, which induces changes in direction of the resulting velocity and further impacts an upward acceleration. Therefore, the influenced forces and moments related to the relative equations of motions are shown in equation (3-21) [33].

$$\begin{bmatrix} \dot{u} \\ \dot{w} \\ \dot{q} \\ \dot{\theta} \end{bmatrix} = \begin{bmatrix} x_u & x_w & x_q & x_\theta \\ z_u & z_w & z_q & z_\theta \\ m_u & m_w & m_q & m_\theta \\ 0 & 0 & 0 & 1 \end{bmatrix} \begin{bmatrix} u \\ w \\ q \\ \theta \end{bmatrix} + \begin{bmatrix} x_{\delta_e} & 0 \\ z_{\delta_e} & -z_{w_g} \\ m_{\delta_e} & -m_{w_g} \\ 0 & 0 \end{bmatrix} \begin{bmatrix} \delta_e \\ w_g \end{bmatrix} \quad (3\text{-}21)$$

Compared with equation (3-6), there are two added coefficients in the control matrix which are calculated by equation (3-22) and (3-23).

$$z_{w_g} = C_L \alpha / m^{'}, \text{ where } m^{'} = \frac{m}{\frac{1}{2}\rho V_0 S} \quad (3\text{-}22)$$

$$m_{w_g} = C_L \alpha (h_{CG} - h_0) / I_y^{'}, \text{ where } I_y^{'} = \frac{I_y}{\frac{1}{2}\rho V_0 S \bar{\bar{c}}} \quad (3\text{-}23)$$

At this design point, the open loop equations of motion could be modified as equation (3-24) shows [6].

$$\begin{bmatrix} \dot{u} \\ \dot{w} \\ \dot{q} \\ \dot{\theta} \end{bmatrix} = \begin{bmatrix} 0.0045016 & -0.11568 & -20.174 & -9.6055 \\ -0.066448 & -0.63733 & 96.667 & -1.9531 \\ 0.0022233 & -0.01093 & -0.19526 & 0 \\ 0 & 0 & 1 & 0 \end{bmatrix} \begin{bmatrix} u \\ w \\ q \\ \theta \end{bmatrix} + \begin{bmatrix} -2.5002 & 0 \\ -13.376 & 0.58761 \\ -1.6757 & 0.12856 \\ 0 & 0 \end{bmatrix} \begin{bmatrix} \delta_e \\ w_g \end{bmatrix} \quad (3\text{-}24)$$

3.5.2 Vertical Wind Gust Perturbation

3.5.2.1 Turbulence Simulink Model

Matlab simulation approach is used to test the aircraft dynamic responses with the designed controllers when it encounters a turbulent vertical up-gust. This gust is represented using parameters $v_w = 6m/s$ and a scale of $L = 12.5\bar{\bar{c}} = 150m$ (acting time is $L/v_0 = 1.5s$) [34]. The simulink mathematical model is illustrated in Figure 3-7.

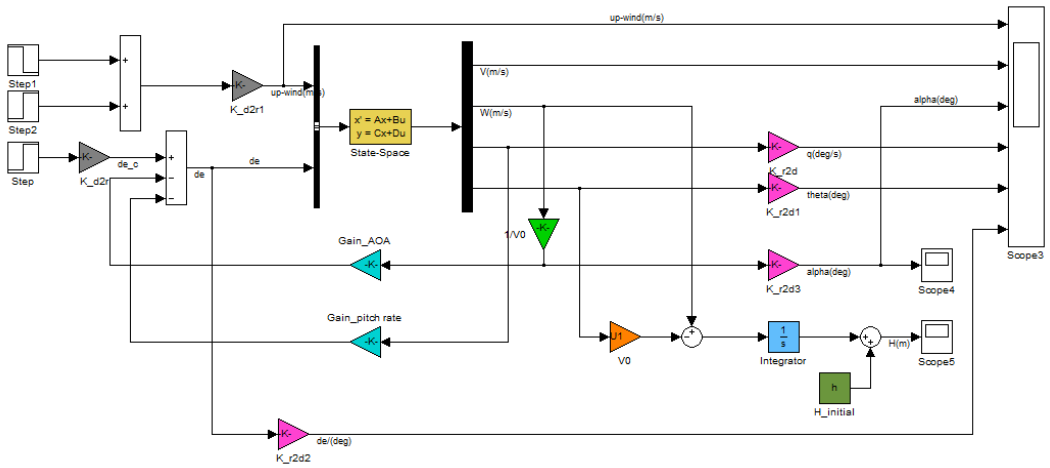

Figure 3-7 Matlab Simulink Model for Wind Disturbance Simulation (up-gust)

3.5.2.2 Aircraft Responses

In Figure 3-8, it is seen that an up-wind gust disturbs the aircraft by increasing its angle of attack. This increased angle of attack increases lift and drag which cause the aircraft to climb and decelerate. At this static stability point, the increased lift produces the aircraft pitch nose-down moment to decrease the angle of attack and to recover its original value [35]. By the aid of SAS, both α and q are recovered within 4s and the phugoid mode is convergent with a small elevator deflection.

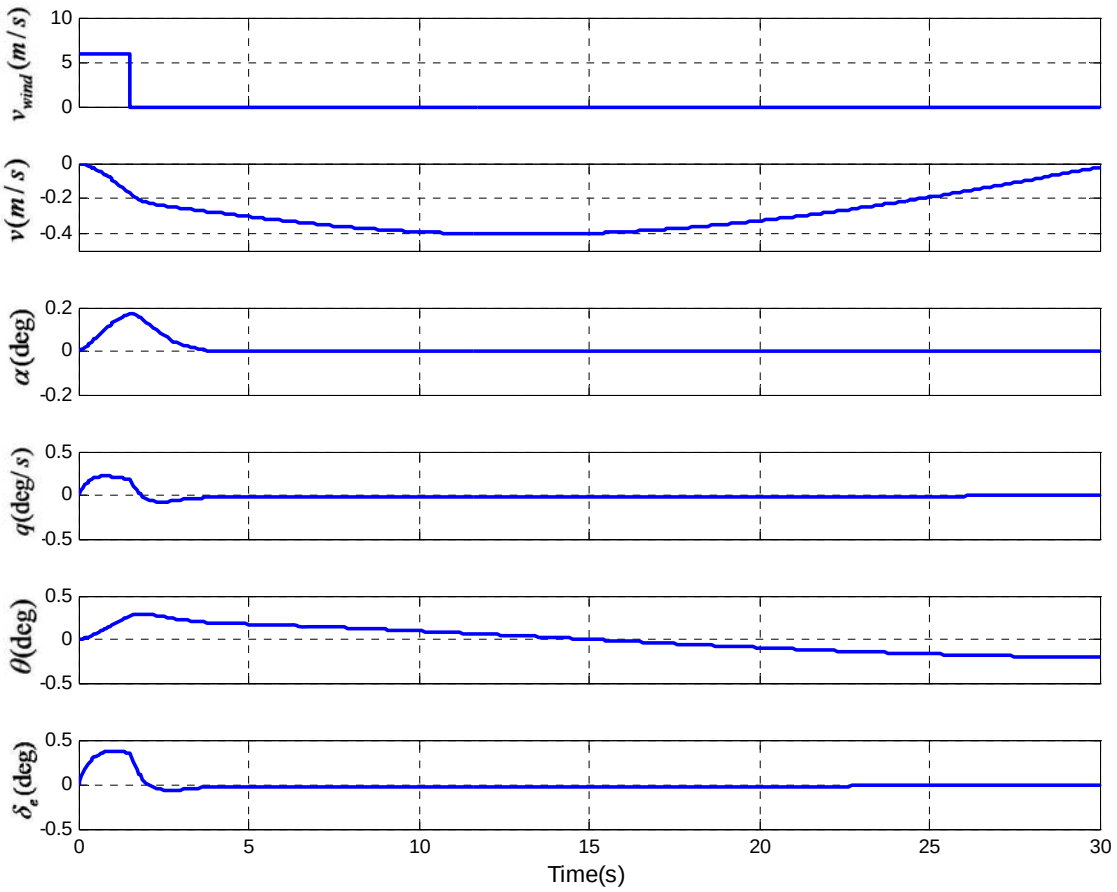

Figure 3-8 Response of Up-wind Gust

3.5.3 Vertical Time-Varying Wind Perturbation

3.5.3.1 Turbulence Model

In general, atmospheric turbulence consists of a random continuous variation in the condition of atmosphere. The Dryden turbulence model is considered valid for use in describing isotropic turbulence as found in natural phenomena, providing the scale of turbulence is appropriate. It is convenient to utilize the Dryden wind turbulence model block of MATLAB to generate an atmospheric turbulence.

Figure 3-9 shows the aircraft response at P_1 (100m/s, 1500m) with SAS when it encounters the turbulence which is the mathematical representation in the MIL-F-8785C specifications.

3.5.3.2 Aircraft Responses

Due to the continuous turbulence, the responses of aircraft fluctuate within small amplitudes. Moreover, during the 50s, this system is continuously stable with no divergence.

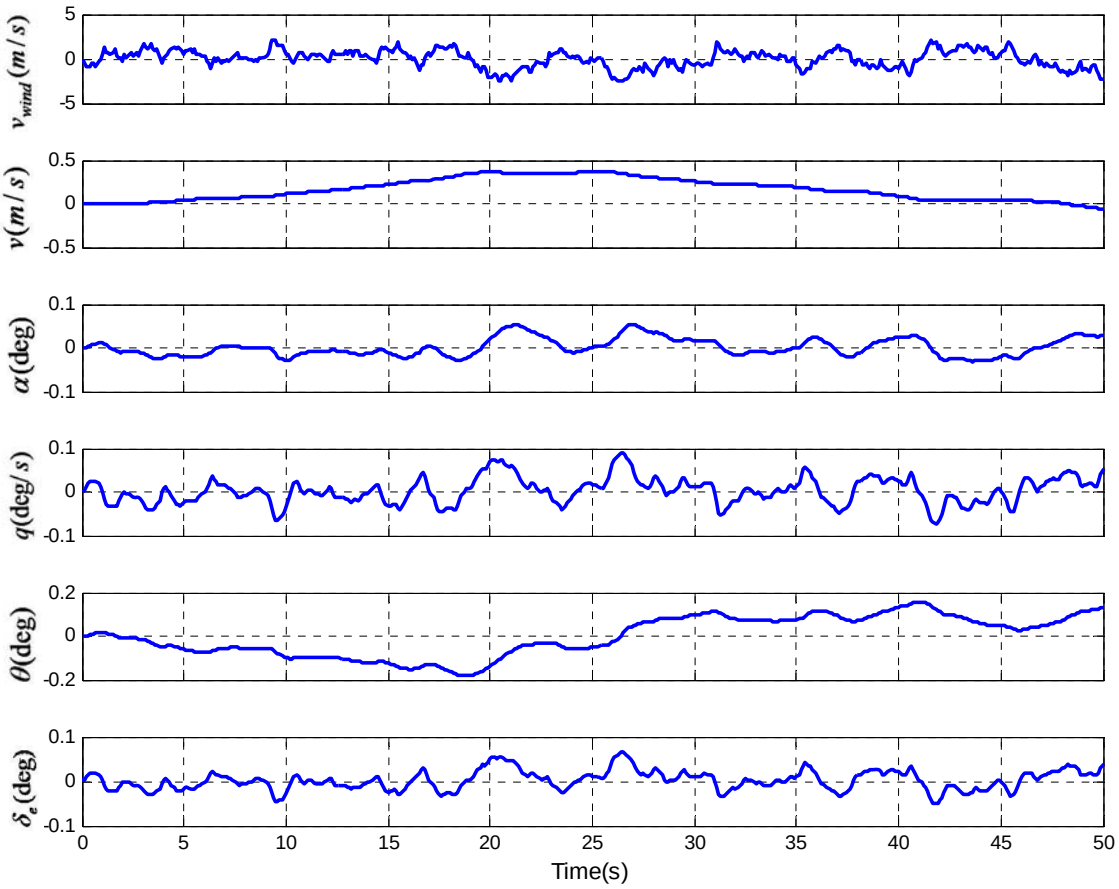

Figure 3-9 Response of Vertical Turbulence

3.6 Summary

The SAS controller C_1 has been presented and assessed with the damping and CAP criteria at P_1. On the basis of wind disturbance model of the discrete sharp-edged gust and the time-vary wind perturbation, C_1 is checked with the realistic atmosphere perturbation. It is found that SAS controller C_1 was applied to obtain the Level 1 flying and handing qualities and good performance after

wind disturbance. Then the controller C_1 is going to be assessed over the whole envelope in the following chapter.

4 ASSESSMENT OVER WHOLE FLIGHT ENVELOPE

The initial SAS controller C_1 has been evaluated in Chapter 3. Due to the responsive change in aircraft dynamics with the flight condition, it is necessary to check the controller over the flight envelope with the flying and handing qualities. Therefore, the satisfactory region F_1 ($F_1 \subset F$) of C_1 will be developed on the basis of flight envelope F exploration. Next, the second controller C_2 will be designed which could satisfy the region F_2. Thus, these two controllers C_1 and C_2 could provide the satisfactory flying and handing qualities over the entire envelope.

4.1 Flight Envelope Exploration

It is a complicated task to explore the accurate flight envelope accurately, because sufficient aircraft aerodynamic data and engine performance data should be provided in detail. Therefore, a simple method is applied for envelope exploration in order to acquire the operating points and flying qualities assessment in the following work.

The reference BWB aircraft installs three engines of the RR TRENT 500, static trust is 287KN each [6]. The engine performance data with respect to Mach number and altitude is simulated from the MATLAB engine modal established by Rahman [6] and especially estimated at the high altitude and Mach number condition. All the relative data and graphs are illustrated in Appendix B.

In Figure 4-1, there are three boundaries of the flight envelope being calculated [36].

- **Right boundary**(without structure load limitation)

Right boundary is limited by the maximum speed with respect to engine performance. The apparent approach used for this boundary is that graphing cross points of required trust and engine provided trust.

- **Left boundary**

In terms of left boundary, it is ensured by the stall airspeed according to the variation of aircraft altitude.

- **Ceiling**

11000m is selected which is referred to the cruise altitude of 10059m [4].

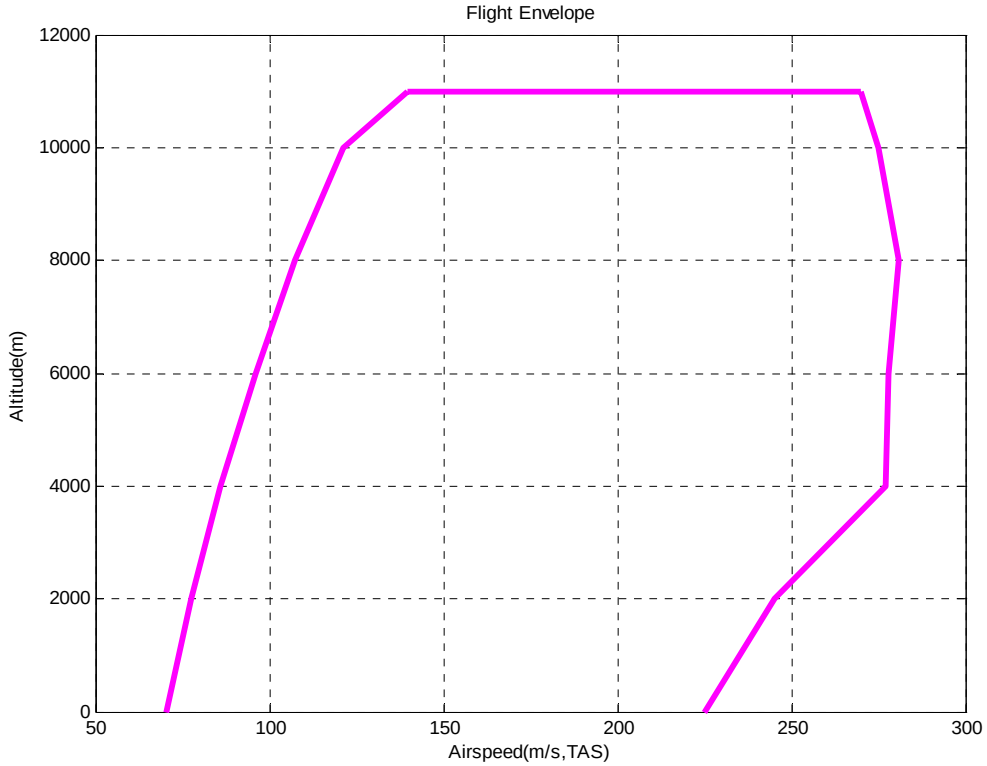

Figure 4-1 BWB Aircraft Flight Envelope

In order to assess the flying qualities over the entire flight envelope, a set of trim points are ensured which can cover the whole flight envelope by interval of altitude of 500m and airspeed of 20m/s as Figure 4-2 shows. The trimmed and reduced order linear aircraft dynamics models for the SAS design then can be derived at the corresponding points.

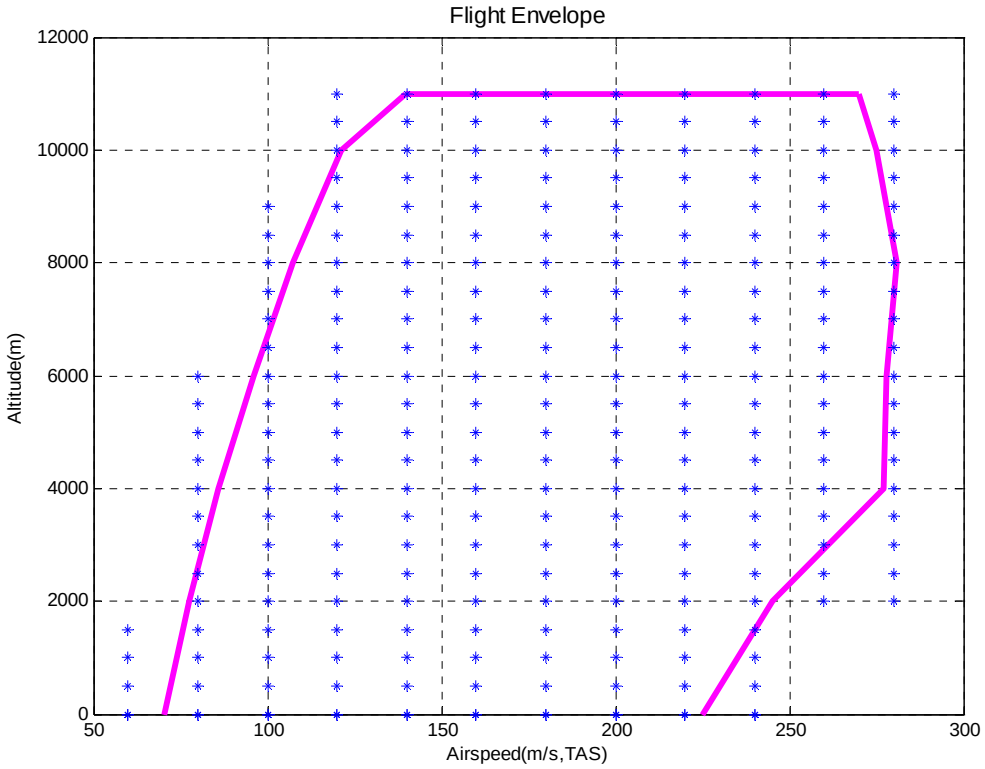

Figure 4-2 Operating Points in F

4.2 Flying and Handing Qualities Assessment with C_1

Using the damping ratio and CAP criterion mentioned in Section 3.2, the damping increases from left to right in F, while the CAP could satisfy the whole envelope with the level 1 quality in Category C flight phase. The satisfactory damping area is the hatched area in F_1 in Figure 4-3. Moreover, the open loop CAP of P_1 and closed loop CAP of P_1 and boundary points A, B, C, D in the flight envelope as examples are described in the Figure 4-4.

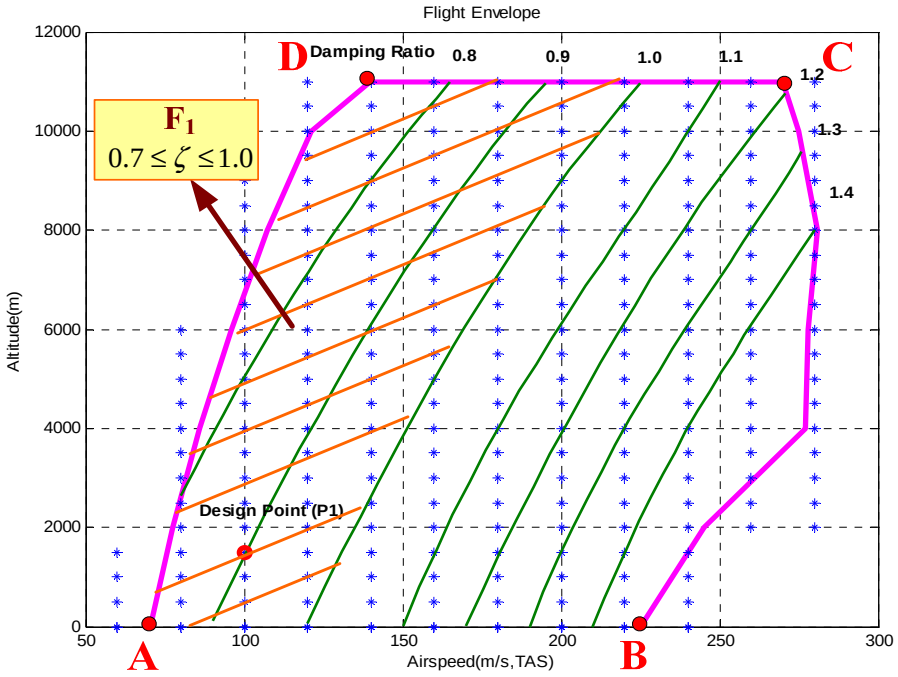

Figure 4-3 Damping Assessment for the Whole Envelope of C_1

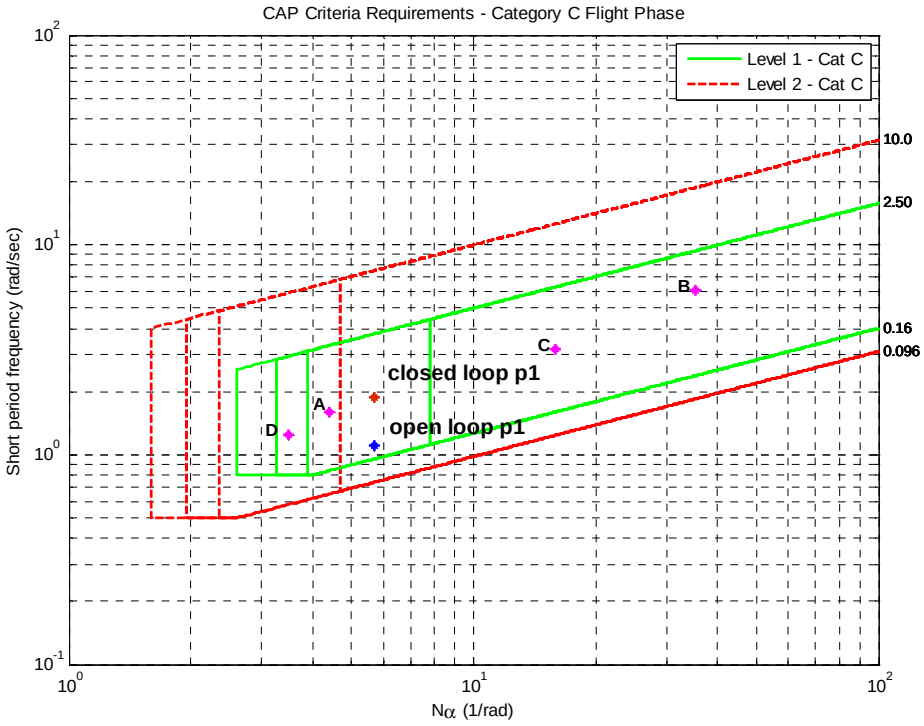

Figure 4-4 CAP Assessment for the Whole Envelope of C_1

4.3 SAS Control Laws Design C_2 at the Second Point P_2

4.3.1 Controller Gains of C_2

For the aim of obtaining the expected response to cover the whole flight envelope, the second design point P_2 in Table 3-7 is chosen for SAS design.

Table 3-7 Trim Point P_2 Condition

Aircraft / Flight Configuration	Value/Status	Units
CG Position	30.4	m
Altitude	6000	m
Airspeed	220	m/s
Flight Condition	Straight and level flight	
Flight Phase Category	Category B	

The reduced second order system is shown below [6].

$$\begin{bmatrix}\dot{\alpha}\\ \dot{q}\end{bmatrix}=\begin{bmatrix}-0.8938 & 1\\ -3.623 & -0.2827\end{bmatrix}\begin{bmatrix}\alpha\\ q\end{bmatrix}+\begin{bmatrix}-0.1941\\ -5.4877\end{bmatrix}\delta_e \tag{4-1}$$

The transfer functions are as follows:

$$\frac{\alpha}{\delta_e}=\frac{-0.19075(s+27.76)}{(s^2+1.156s+3.704)}\quad \text{(deg/deg)} \tag{4-2}$$

$$\frac{q}{\delta_e}=\frac{-5.2418(s+0.7526)}{(s^2+1.156s+3.704)}\quad \text{(deg/s/deg)} \tag{4-3}$$

Using the pole placement method (program in Appendix D.4) on the basis of the reduced second order system, the anticipation damping ratio and frequency are selected as 0.8 for cruise and 2.5 to increase CAP respectively.

Thus, feedback gains are derived as

$$K_{C_2} = [K_{\alpha\_C_2} \; K_{\mathrm{q\_C_2}}] = [-0.03 \; -0.50] \tag{4-4}$$

4.3.2 Flying and Handing Qualities Assessment with C_2

A comparison of the open loop damping ratio and CAP with the closed loop condition is shown in Table 4-1 and Figure 4-5. The AOA and pitch rate step response of reduced order system are illustrated in Figure 4-6.

Table 4-1 Damping and CAP Comparison with Open Loop and Close Loop

Open loop without feedback			**Closed loop with feedback**		
ζ_s	ω_n	**CAP**	ζ_s	ω_n	**CAP**
0.29	1.96	0.18	0.79	2.48	0.30

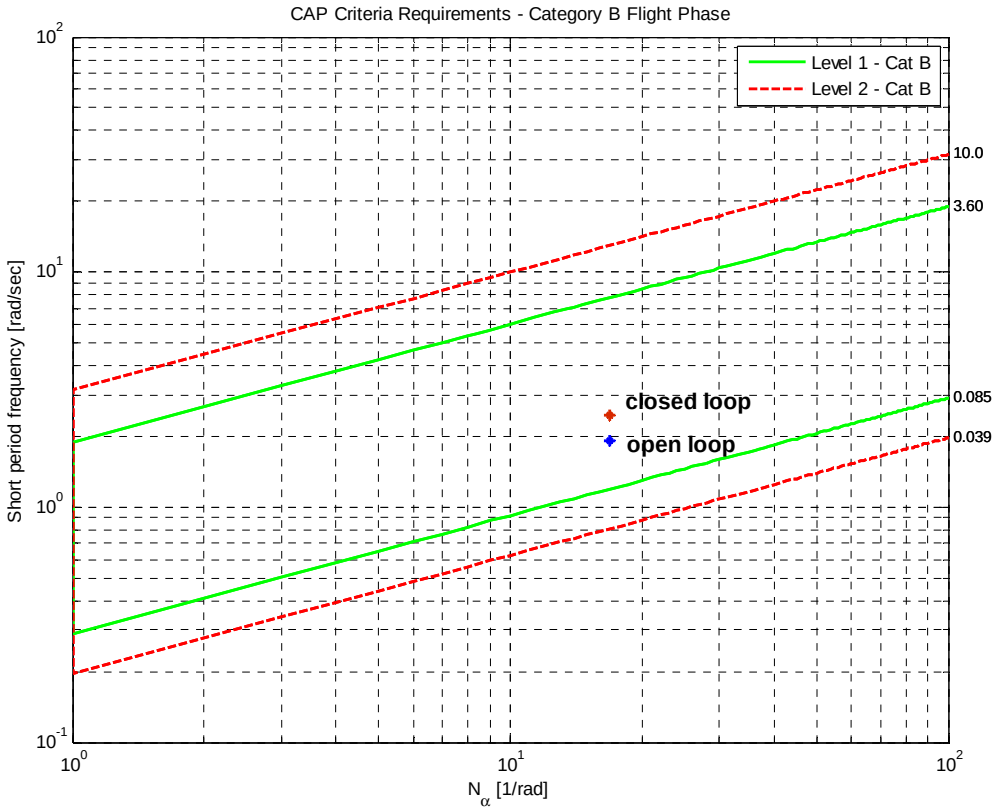

Figure 4-5 CAP of C_2 in Category B

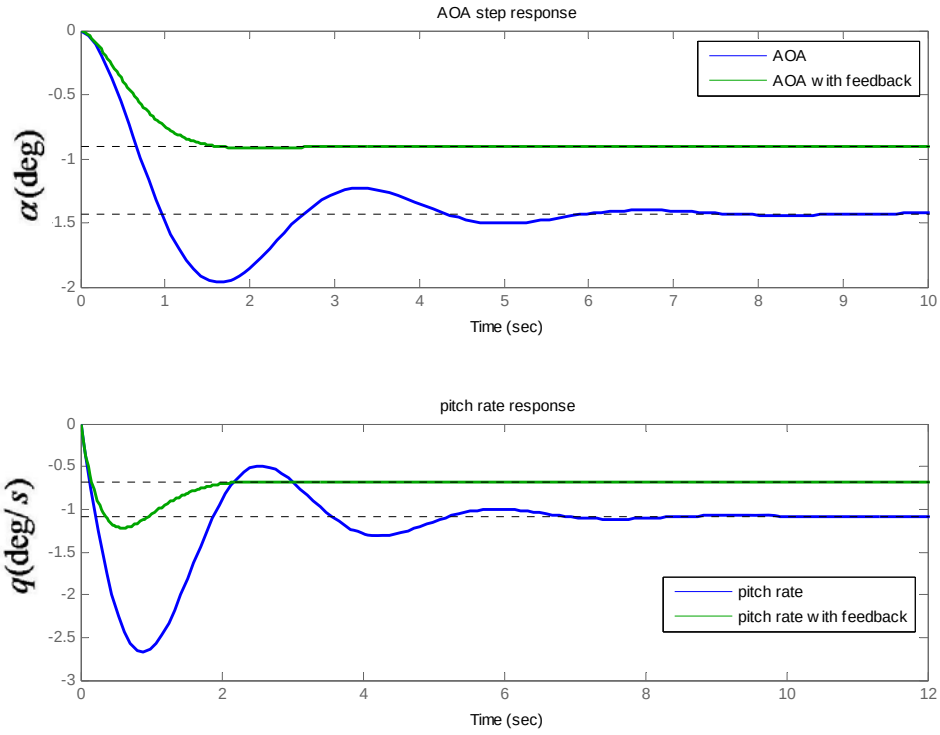

Figure 4-6 1^{o} Step Response of Open Loop and Closed Loop

It is clear that the damping and CAP has been improved whilst the response of α and q are stabilized faster than before.

4.3.3 Check with Full Order System Model

For this case, the closed control matrix and transfer functions for each output variables (u, α, q, θ) with respect to elevator deflection are shown below [6]. The system dynamic responses are demonstrated in Figure 4-7.

$$\begin{bmatrix} \dot{u} \\ \dot{\alpha} \\ \dot{q} \\ \dot{\theta} \end{bmatrix} = \begin{bmatrix} -0.0019232 & -8.8821 & -16.752 & -9.7613 \\ -9.247e-005 & -0.88898 & 0.99148 & -0.0031969 \\ 0.0011902 & -3.6342 & -0.28269 & 0 \\ 0 & 0 & 0 & 0 \end{bmatrix} \begin{bmatrix} u \\ \alpha \\ q \\ \theta \end{bmatrix} + \begin{bmatrix} -1.9365 \\ -0.19419 \\ -5.4877 \\ 0 \end{bmatrix} \delta_e \qquad (4\text{-}5)$$

$$\frac{q(s)}{\delta_e(s)} = \frac{-5.4877(s+0.7617)(s+0.0009963)}{(s^2+0.005647s+0.002254)(s^2+3.918s+6.109)} \quad \text{(deg/s/deg)} \qquad (4\text{-}6)$$

$$\frac{\alpha(s)}{\delta_e(s)} = \frac{-0.19419\,(s+28.3)\,(s^2+0.001343s+0.001304)}{(s^2+0.005647s+0.002254)\,(s^2+3.918s+6.109)} \quad \text{(deg/deg)} \qquad (4\text{-}7)$$

$$\frac{u(s)}{\delta_e(s)} = \frac{-0.033796\,(s-48.94)\,(s+1.453)\,(s+0.2948)}{(s^2+0.005647s+0.002254)\,(s^2+3.918s+6.109)} \quad \text{(m/s/deg)} \qquad (4\text{-}8)$$

$$\frac{\theta(s)}{\delta_e(s)} = \frac{-5.4877\,(s+0.7617)\,(s+0.0009963)}{(s^2+0.005647s+0.002254)\,(s^2+3.918s+6.109)} \quad \text{(deg/deg)} \qquad (4\text{-}9)$$

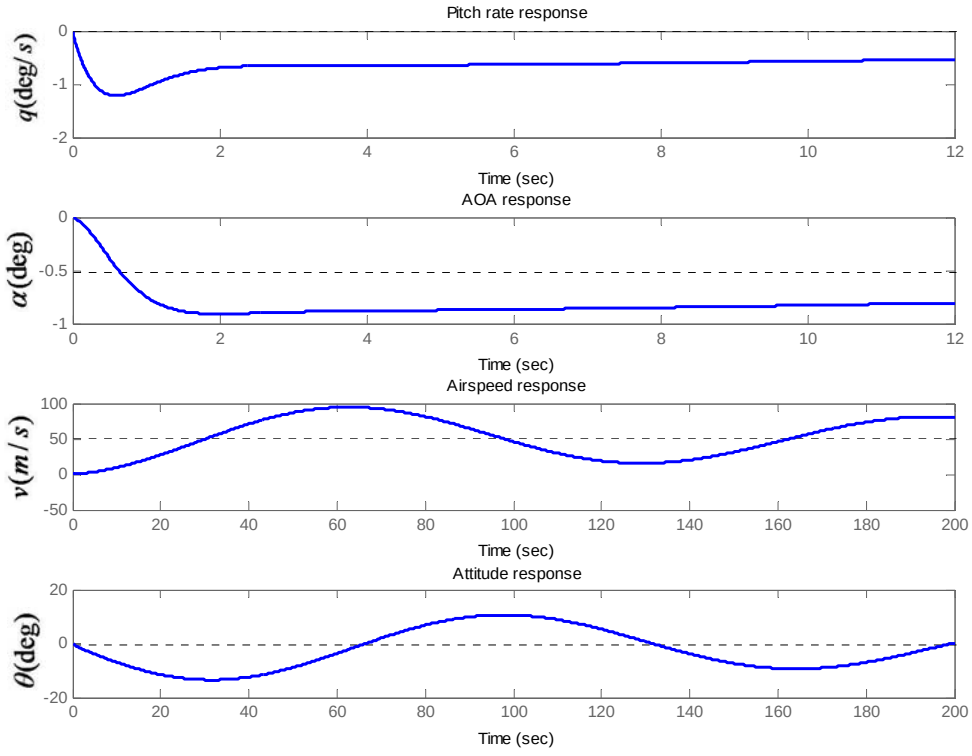

Figure 4-7 1^o Step Response of Augmented System

According to the above transfer functions, at this condition, the damping ratio and natural frequency of the SPO mode are $\delta_s = 0.79$ and $\omega_{ns} = 2.47 rad/s$, while for phugoid, these parameters are $\delta_p = 0.06$ and $\omega_{np} = 0.047 rad/s$. All of them meet the requirements in Section 3.2.

4.3.4 Wind Disturbance Simulation

In this section, the effect of external atmospheric influence is also to be taken into account on the aircraft response dynamics with C_2 employed. The wind models are the same as both the discrete sharp-edged gust and the time-vary wind perturbation in Section 3.5. The aircraft responses of both winds are illustrated in Figure 4-8 and Figure 4-9 respectively.

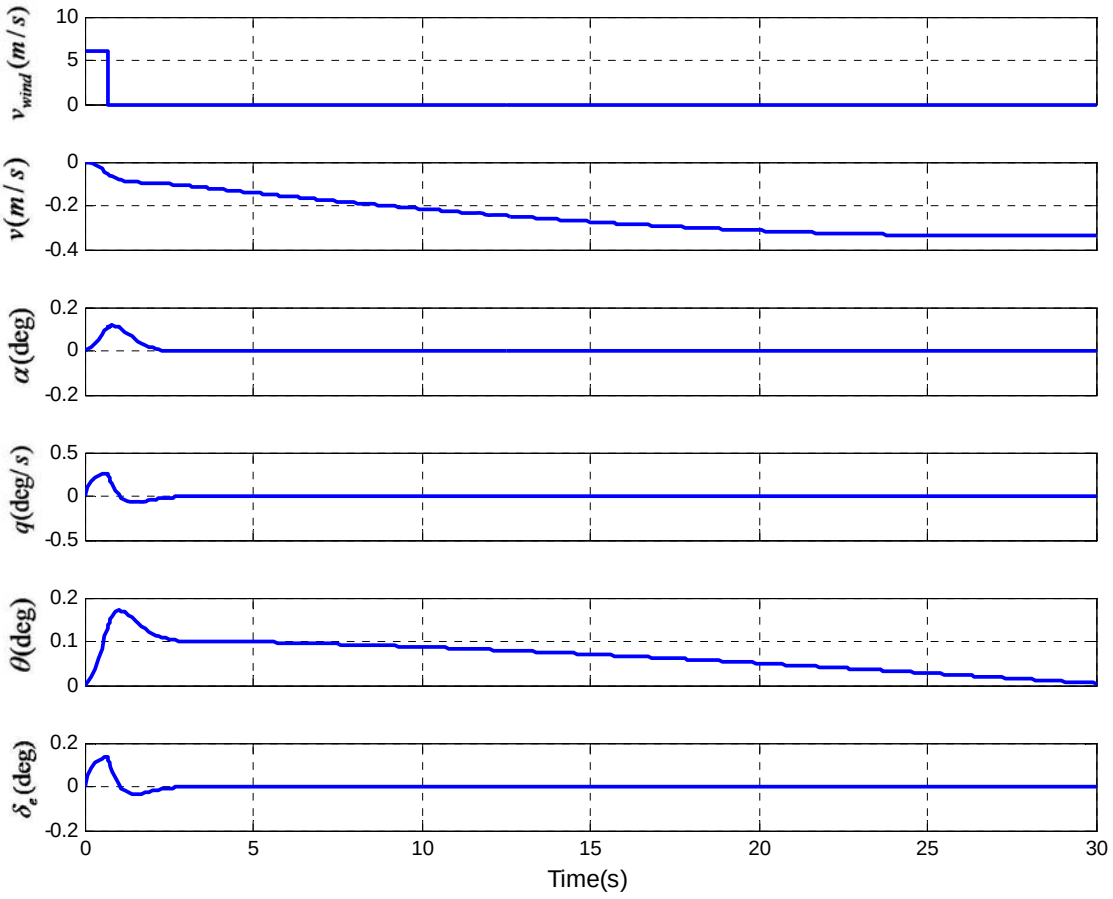

Figure 4-8 Response of Up-wind Gust

As good performance as the results in Subsection 3.5.3.1, by the aid of SAS C_2, both α and q are recovered within 4s and the phugoid mode is convergent with a small elevator deflection.

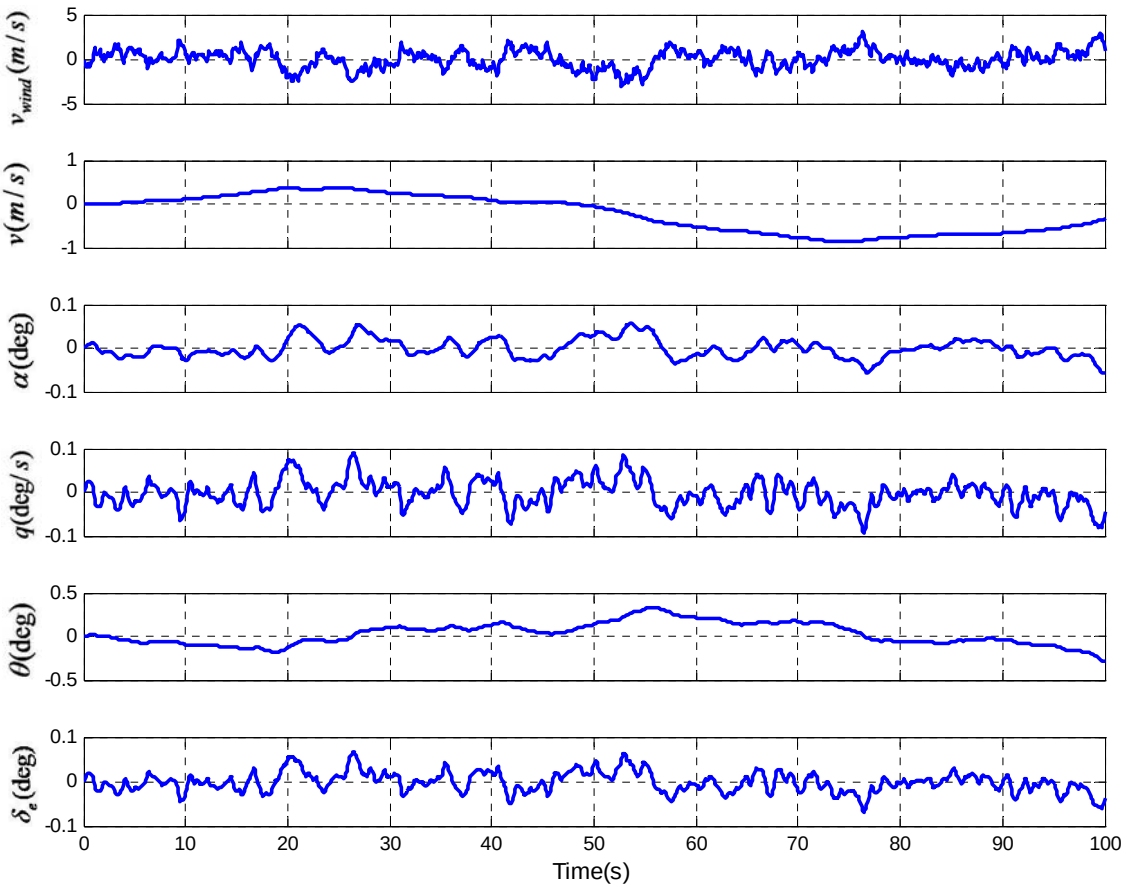

Figure 4-9 Response of Vertical Turbulence

Due to the continuous turbulence, the responses of aircraft fluctuate within small amplitudes. Moreover, during the 50s, this system is continuously stable with no divergence.

4.4 Flying and Handing Qualities Assessment with C_2

Following the method in Chapter 4.2, the satisfactory damping region is the dashed area F_2 in Figure 4-10. It is the same as the controller C_1 that the CAP could satisfy the whole envelope with the level 1 quality in Category B flight phase. The open loop CAP of P_2 and closed loop CAP of P_2 and boundary points A, B, C, D in the flight envelope as examples are described in the Figure 4-11.

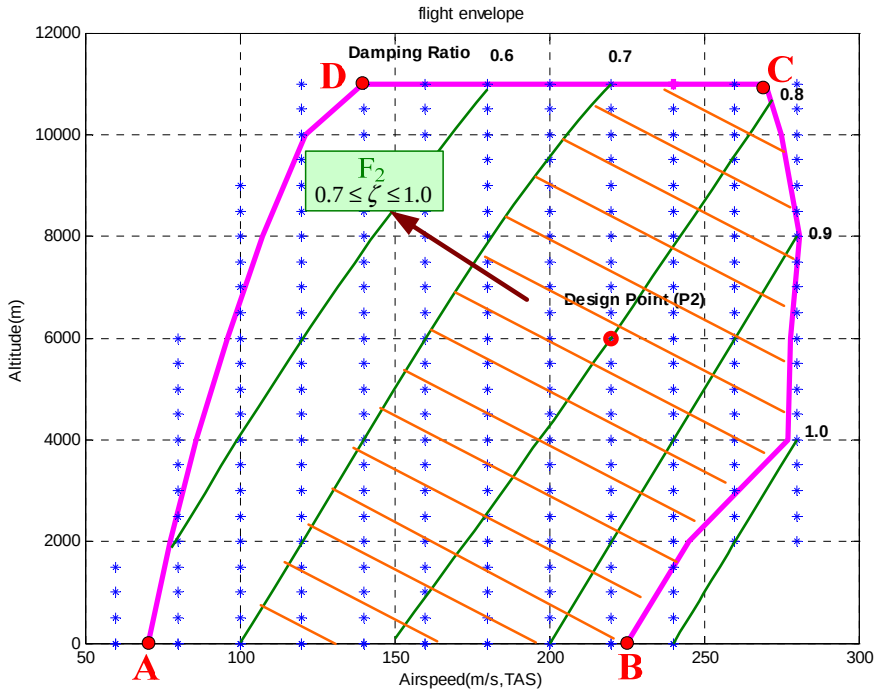

Figure 4-10 Damping Assessment for the Whole Envelope of C_2

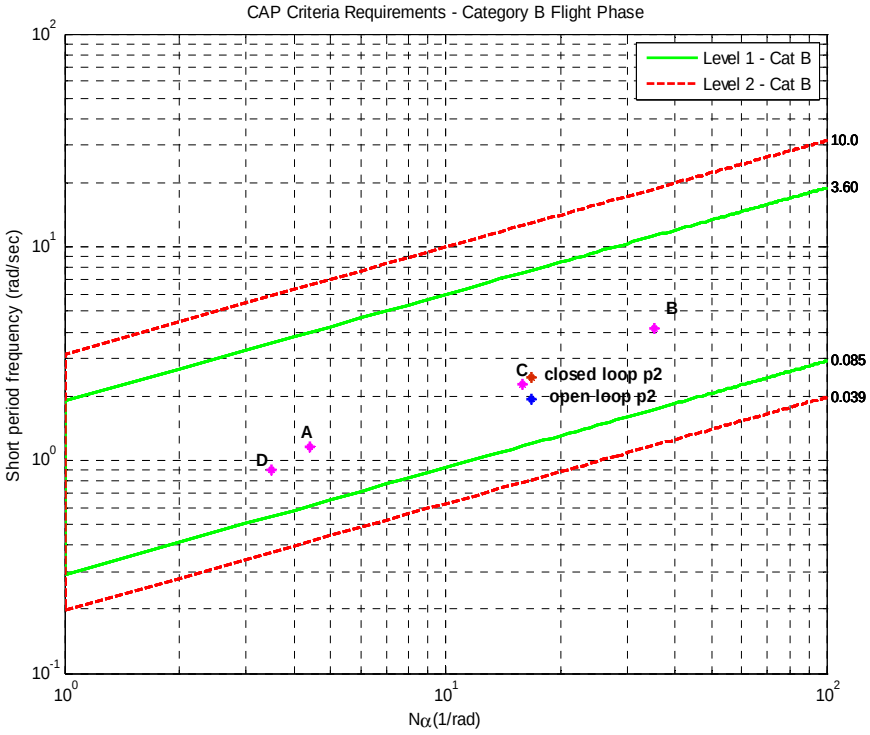

Figure 4-11 CAP Assessment for the Whole Envelope of C_2

4.5 Summary

In Chapter 3 and Chapter 4, two linear controllers have been developed at each design point. Then these are assessed over the set of operating points in the explored entire envelope F by the certain damping range and the level 1 CAP flying and handing qualities in MIL-F-8785C specifications.

The whole envelope F has been divided into two subsets $F_1(C_1)$ and $F_2(C_2)$ with overlapped area $F_{1,2}$(light blue area) in Figure 4-12. Hence, the linear SAS controllers could satisfy the entire envelope. Consequently, the gain scheduling will be applied to smoothly transfer gains from C_1 to C_2 in the following chapter.

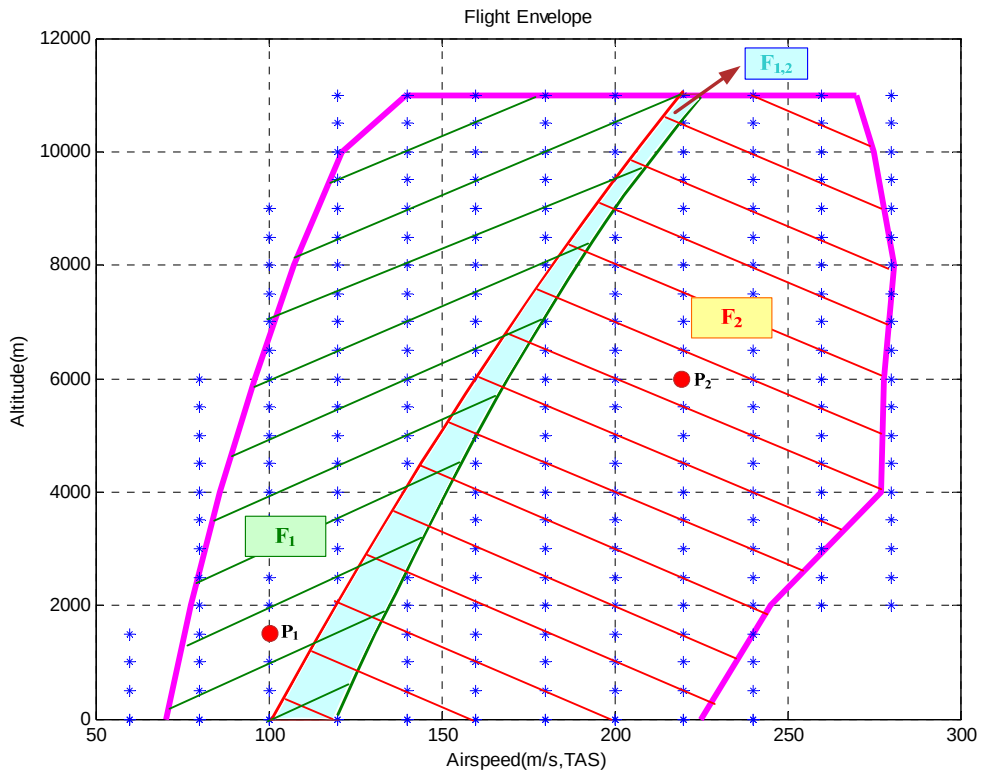

Figure 4-12 Damping Assessment for the Whole Envelope of C_1 and C_2

5 GAIN SCHEDULING

In the previous chapters, the SAS control laws have been designed at two operating design points which can provide satisfactory flying and handing qualities in both regions $F_1(C_1)$ and $F_2(C_2)$. Consequently, in this chapter, a gain scheduling technique is used to vary the gains according to suitable variables, which aims to obtain the satisfactory flying and handing qualities at each operation condition in F .

Initially, the scheduling variables selection is a significant aspect to be accomplished which determines the change of gains and performance of aircraft. In the first section, the selection of the variable dynamic pressure (Q) will be discussed. On the basis of this variable being determined, the gain schedule could be developed according to the variation of Q. Finally, three operating points are chosen to be validated in the interpolation area and the satisfactory results will be obtained in the last section.

5.1 Scheduling Variables Selection

In terms of the gain scheduling design process, the first step is to select the scheduling variable parameters. On one hand, these variables can determine the operating area which the system is currently in; on the other hand, they are able to determine the appropriate linear controller. A simply qualitative principle was proved that the scheduling variables should be slowly changing and governing the nonlinearities of system [37]. To apply gain scheduling method into flight control system, there are several common scheduling variables that could be chosen, such as airspeed, Mach number, dynamic pressure, altitude, angle of attack or their various combinations.

In aerospace engineering, it is well-known that many airplanes, like the F-16 fighting Falcon, are nonlinear dynamical systems, but they could be well approximated as a LTI system at a constant altitude. Hence, by viewing the aircraft as a collection of LTI behaviours corresponding to different altitude

levels and using the altitude variable as a scheduling, an approximation of the global controller can be obtained [38].

In many situations, it is known how the aircraft dynamics change with its operating point. It might be possible to model the system in such a way that the operating point is parameterized by one or more scheduling variables [39].

In this study, it is found that the damping ratios in whole flight envelope, the significant dynamic response parameter of the SPO mode, are approximated as equal at a constant dynamic pressure Q ($Q = \frac{1}{2}\rho v^2$, N/m^2 , represents the altitude and airspeed) and CG position over the whole flight envelope. Moreover, the damping varies monotonously with Q variation as well. Thus, gain coefficients of controllers would be programmed as a function of dynamic pressure and performed using Q as the sole scheduling input for the SAS design [26].

5.2 SAS Gain Scheduling Scheme

In order to smooth controller gains from one controller to the other, a strategy of gain scheduling is needed to be designed. The gains of linear controllers in each condition in F could be described as follows:

$$K_i = [K_{\alpha i} \quad K_{q_i}] \tag{5-1}$$

For controller C_1 and C_2, the gains are as shown in Table 5-1.

Table 5-1 Condition of C_1 and C_2

	K_i	**Altitude (m)**	**Airspeed (m/s, TAS)**	**Dynamic pressure (10^3 N/m^2)**
C_1	$K_{C1} = [-0.55 \ -1.41]$	1500	100	5.30
C_2	$K_{C2} = [-0.03 \ -0.50]$	6000	220	1.60

Initially, the satisfactory region of the controllers in the flight envelope should be divided by the variable of Q at P_1 and P_2 in Figure 5-1.

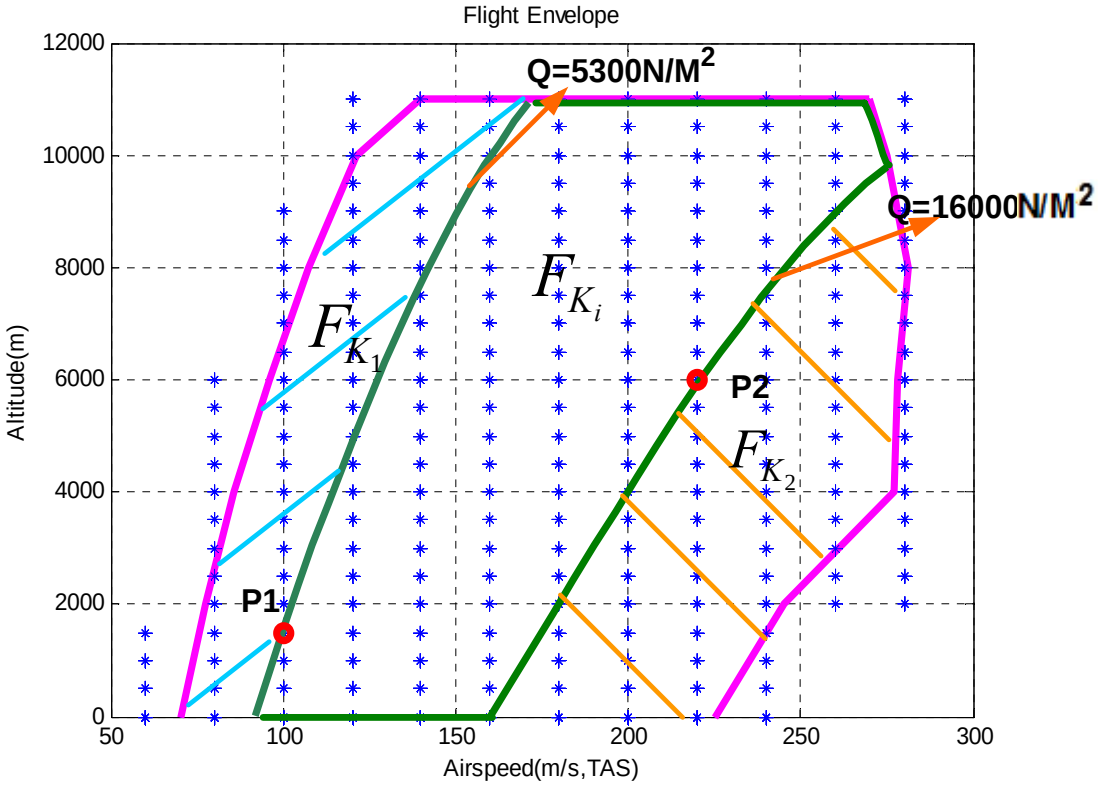

Figure 5-1 Definition of F_{k1}, F_{k2} and F_{ki}

The relationship between the new regions of F_{k1}, F_{k2}, F_{ki} and previous regions of F_1, F_2, $F_{1,2}$ could be described as follows:

$$Q(F_{k1}) \le Q(K_{c1}) \quad , \quad F_{k1} \subset F_1 \tag{5-2}$$

$$Q(F_{K1}) \le Q(F_{ki}) \le Q(K_{c2}) \quad , \quad F_{1,2} \subset F_{Ki} \tag{5-3}$$

$$Q(F_{k2}) \ge Q(K_{c2}) \quad , \quad F_{k2} \subset F_2 \tag{5-4}$$

Thus, the gain schedule could be developed by the linear fitted curve in F_{ki} and kept constant at F_{k1} and F_{k2} respectively as equation (5-5) and (5-6). The scheduling scheme is shown in Figure 5-2.

$$K_{ai} = \begin{cases} K_{\alpha\_C1} & (Q_{aircarft} \le Q(K_{C1})) \\ b_\alpha * (Q_{aircraft} - Q(K_{C1})) - 0.55 & (Q(K_{C1}) < Q_{aircarft} \le Q(K_{C2})) \\ K_{\alpha\_C2} & (Q_{aircarft} > Q(K_{C2})) \end{cases} \quad (5\text{-}5)$$

$$K_{qi} = \begin{cases} K_{q\_C1} & (Q_{aircraft} \le Q(K_{C1})) \\ b_q * (Q_{aircraft} - \mathrm{Q}(K_{C1})) - 1.41 & (Q(K_{C1}) < Q_{aircraft} \le Q(K_{C2})) \\ K_{q\_C2} & (Q_{aircraft} > Q(K_{C1})) \end{cases} \quad (5\text{-}6)$$

where: $b_\alpha = 4.86\times10^{-5}, b_q = 8.50\times10^{-5}, Q_{k1} = 0.53\times10^4, Q_{k2} = 1.6\times10^4$.

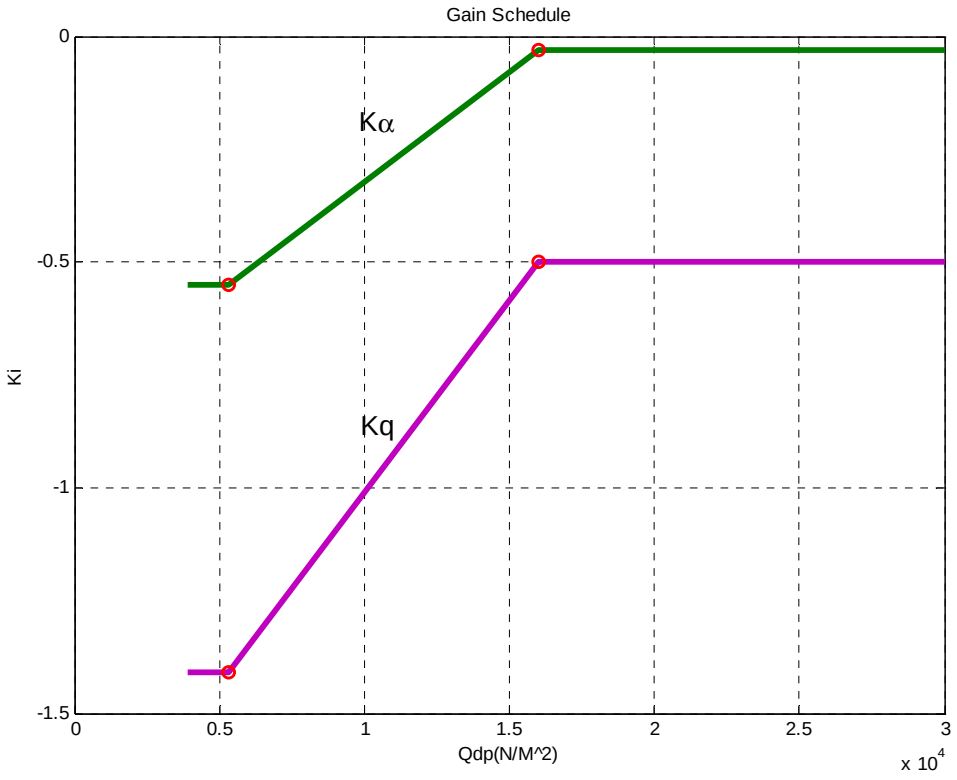

Figure 5-2 SAS Gain Scheduling Scheme

5.3 Flying and Handing Qualities Assessment in F_{ki}

It is necessary to evaluate the scheduled gains influence on the flying and handing qualities in interpolation region F_{ki}. Three operation points in F_{ki} are selected at different dynamic pressure in Figure 5-3 and described in Table 5-2.

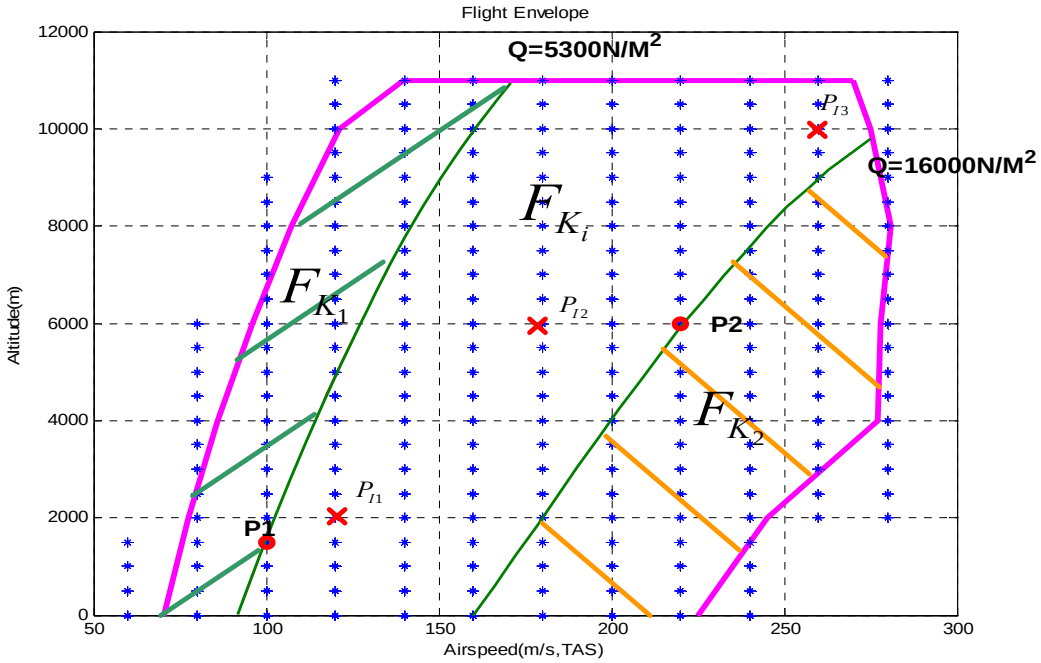

Figure 5-3 Assessment points in F_{ki}

Table 5-2 Description of Assessment points in F_{ki}

	Altitude(m)	Airspeed (m/s, TAS)	Dynamic Pressure (10^4, N/M^2)	$K_\alpha(P_I)$	$K_q(P_I)$
P_{I1}	2000	120	0.73	-0.45	-1.24
P_{I2}	6000	180	1.07	-0.29	-0.95
P_{I3}	10000	260	1.40	-0.13	-0.67

Consequently, the aircraft augmented by $K_\alpha(P_I)$ and $K_q(P_I)$ will be assessed with flying and handing quality constraints in Section 3.2. In addition, the comparison of damping and CAP between open loop and closed loop for each point are illustrated in Table 5-3. It is clear that both damping and CAP have been increased to the ideal value at each assessment point. More specific process and results are shown in Appendix C.

Table 5-3 Comparison of Damping and CAP

CAP / ζ_s / P_{Ii}	Open loop without feedback			Closed loop with feedback		
	ζ_s	ω_n	CAP	ζ_s	ω_n	CAP
P_{I1}	0.37	1.30	0.19	0.90	2.12	0.51
P_{I2}	0.30	1.57	0.18	0.91	2.36	0.42
P_{I3}	0.24	1.82	0.18	0.85	2.4	0.32

5.4 Summary

In order to transfer gains smoothly between trim points of P_1 and P_2, a global gain schedule has been designed with the scheduling variable of dynamic pressure. With the flying and handing qualities assessment at three points in the interpolation area, it is valid that this gain scheduling scheme could provide suitable gains to the SAS controller with the variation of the flight operating condition. Therefore, the inner loop SAS control laws design is completed with satisfactory flying and handing qualities.

6 EFFECT OF CG POSITION VARIATION

6.1 Introduction

In previous chapters, the SAS controller with automatic gain adjustment in terms of dynamic pressure has been developed over the whole envelope. Practically, not only does the aircraft dynamics change according to the altitude and airspeed (dynamic pressure), but also varies according to the CG variation.

A CG position more aft than in usual concepts is much sought-after by industry as it could improve the manoeuvrability, reduce trim drag in cruise and give a greater flexibility with regard to load charge. It also allows for the installation of a smaller elevator and a smaller horizontal trim plane [40]. But the natural aircraft with this reduced stability does not necessarily meet the flying and handing qualities for certification. Hence, the control system has to be developed which not only satisfies the handing qualities requirements over the flight envelope, but also is robust to mass and CG position variation.

Taking the F-16 for example, high manoeuvrability is provided by allowing the CG to move from the stable CG region to the unstable but relaxed static stable CG region. However, this aircraft can not fly unless the control augmentation system is used. The control system could improve the dynamic characteristics of the F-16. Therefore, it would remain stable, even though CG lies on the unstable region [41].

For the present civil aircraft, due to the variable weight of aircraft such as fuel, luggage, passengers, CG position will not stay the same all the time. In order to grantee the aircraft safety, the static margin is designed stable enough with the minimum static margin as 10% [42]. Therefore, for the natural static stable aircrafts, the controller could be designed compromising the forward with backwards CG position.

However, for the tailless configuration aircraft, it is hard to arrange a static margin to be the same as a conventional aircraft. The reference BWB aircraft is very sensitive to CG displacement. It affects trimming the aircraft as well as controlling it. Its static margin changes from $18.1\%\overline{\overline{c}}$ to $-22.5\%\overline{\overline{c}}$ (Table 6-1) with

the CG moving back. During the cruise phase, the margin is only $1.9\%\bar{\bar{c}}$ (Table 6-2). Thus, the influence of CG position variation must be considered for flight control system design to prevent or at least minimize unstable motions [4].

Table 6-1 Static Margin with CG Variation

CG Position(m)	**29.4**	**30.4**	**31.4**	**32.4**	**33.4**	**34.4**
$C_{z\alpha}$	5.4868	5.4868	5.4868	5.4868	5.4868	5.4868
$C_{m\alpha}$	-0.9950	-0.5493	-0.1036	0.3422	0.7879	1.2336
$K_n \approx -\frac{C_{m\alpha}}{C_{z\alpha}}$	$18.1\%\bar{\bar{c}}$	$10\%\bar{\bar{c}}$	$1.9\%\bar{\bar{c}}$	$-6.2\%\bar{\bar{c}}$	$-14.4\%\bar{\bar{c}}$	$-22.5\%\bar{\bar{c}}$

Table 6-2 Control Fixed Static Margin

	$h_0 = \frac{X_0}{\bar{\bar{C}}}$	$h_{CG} = \frac{X_{CG}}{\bar{\bar{C}}}$	$K_n = h_0 - h_{CG}$
Cruise Phase	1.188	1.169	1.9%
Approach Phase	1.1598	1.1448	1.5%

6.2 Poles of SPO with CG Position Variation

The developed SAS in the previous chapters aims to provide satisfactory damping and natural frequency for the SPO mode. The phugoid mode is largely unaffected by SAS feedbacks, hence, in this section, only the short period mode poles are discussed as a function of CG position.

The open loop poles of SPO with the CG position variation from 29.4m to 34.4m are displayed in Figure 6-1 and 6-2 for equilibrium points P_1 (100m/s, 1500m)

and P_2 (220m/s, 6000m) respectively. Both figures illustrate that for CG position between 29.4m and 31.4m, the SPO poles are complex-conjugate with damping ration $\zeta > 0.3$ without the SAS controller engaged in. The SPO then becomes aperiodic and include unstable poles when the CG positions more aft than 31.4m.

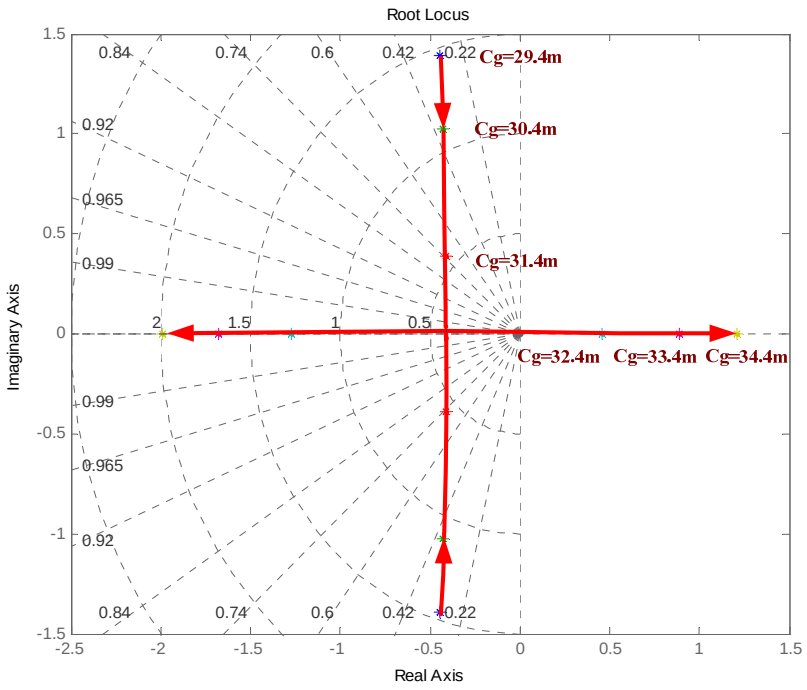

Figure 6-1 Open Loop Poles of SPO with CG Variation at P_1

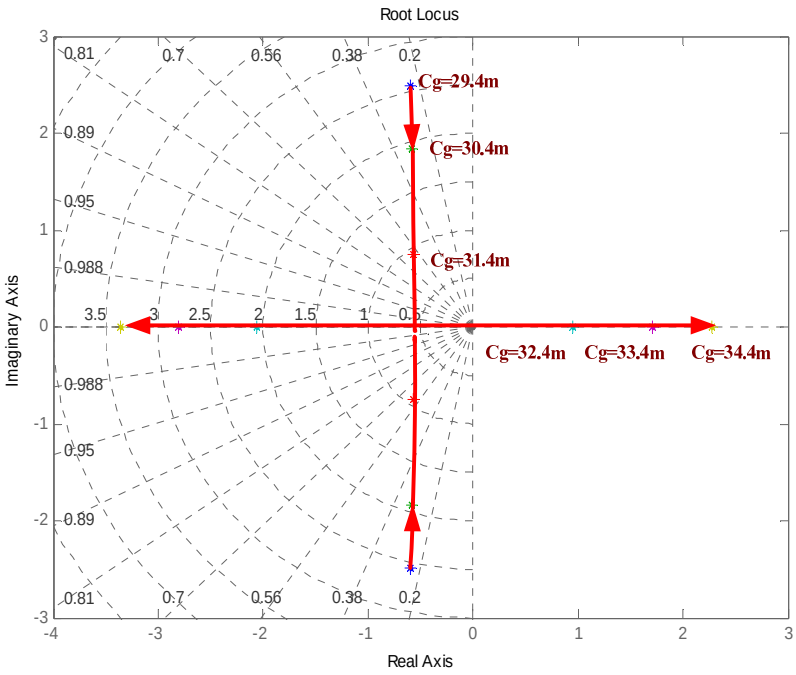

Figure 6-2 Open Loop Poles of SPO with CG Variation at P_2

Compared with the open loop poles of SPO, Figure 6-3 and Figure 6-4 presents the movement trend of the closed loop poles.

In terms of the SAS controller C_1 at operating point P_1 (taking-off and landing phase), the damping ratio has been increased from 0.85 to 0.95 before the CG position at 31.4m, whereas the unstable poles exist at the CG more aft 33.4m. At the stable CG range, it complies with the FAR requirement that the SPO of the aircraft during take-off and landing has to be “heavily damped” [43].

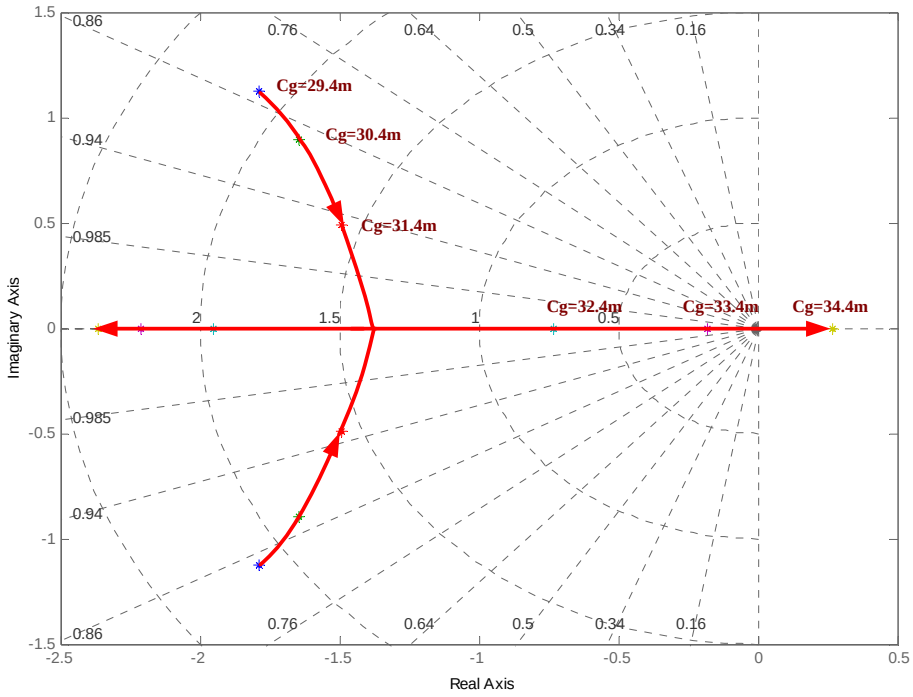

Figure 6-3 Closed Loop Poles of SPO with CG Variation at P_1

Meanwhile, the SAS controller C_2 at operating point P_2 (cruise phase), damping ration is also improved from 0.7 to 0.95 as CG moves before 31.4m. When the CG lies more aft 32.4m, the SPO enters to the unstable motion.

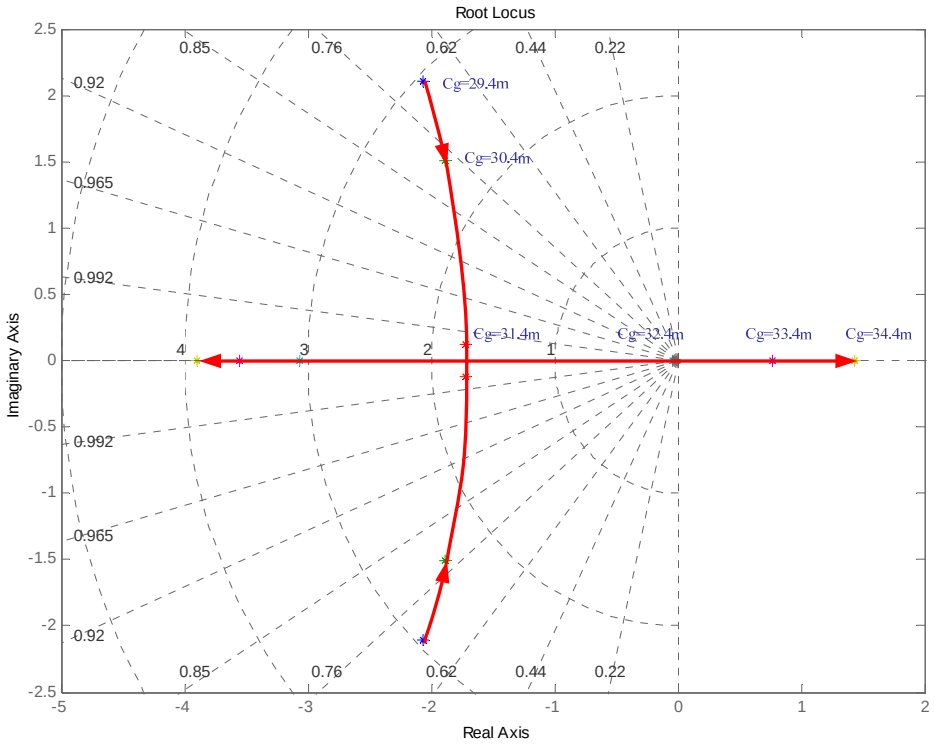

Figure 6-4 Closed Loop Poles of SPO with CG Variation at P_2

Even though the SAS controllers can not cover the whole range of CG position, according to the display in Table 6-2, the static margin at approach and cruise are all positive value. It means that the CG position lies in front of the ac at the normal flight condition. Hence, the designed SAS is regarded as the reasonable and satisfactory control system as a function of CG position variation.

6.3 Approaches of Control System Design with CG Variation

The location of CG position affects the stability and control of the aircraft. In control system design, some approaches could be used to take the influence of CG position variation into account.

The view of the robust control laws design is to provide a satisfactory performance on a large range of CG position including the aft positions without the CG measurement.

Such as a polytopic design technique [40][44] which has been used by Feuersanger in these papers for both longitudinal and lateral control laws design of the future aircraft concept VELA over a wide range of CG positions. The polytopic technique they used is to synthesize a state feedback controller satisfying simultaneously for different models modal and I/O specification (pole placement in a region of the complex plane, H_∞ and positivity constrains on transfer functions). The controller is valid for a large range of CG position and the results is a multi-objective synthesis with guaranteed minimal flying and handing qualities, minimization of actuator activity and quasi-global-stability in the presence of saturation on the actuator rate output.

In addition, as well as the study [45] of David, the H_∞ synthesis is performed to get a robust controller which satisfies the handing qualities in spite of mass and CG variation. Moreover, the high order controller will be reduced without losing performance and then be put in a classical form. This method keeps the simplicity of classical architectures while using modern technique advantages of analysis.

Besides, the control system also could be designed utilizing the CG position in-flight measurement. The reference 46 presents that an attitude control system is developed to guarantee the consistent performance with varying CG locations by the in-flight estimation of CG position. A synthesis method based on in-flight CG position estimation could be used effectively and directly in the attitude controller design. It could reduce the design complexity and make the process easy and clear in implementation.

6.4 Summary

The poles movement of SPO induced by varying CG position are analysed. It could be seen that the stability is reduced with the CG moving back. However, the most of poles of SPO have been moved to the left of s-plane with the SAS controller engaged. Actually, it is hard to apply this conventional design approach for the good performance over the wide CG variation range. Thus,

some advanced methods to eliminate this CG variation influence for control system are discussed as well.

7 OUTER LOOP CONTROLLER DESIGN

7.1 Introduction

From Chapter 3 to Chapter 5, the inner loop SAS design which is to improve the short period mode dynamics has been accomplished with the automatic adjustment of inner loop feedback gains. Consequently, outer feedback control loop will be closed around the pitch SAS to provide autopilot function. The SAS are conventionally designed separately for the longitudinal and lateral dynamics. Thus, autopilots design would be separated into these two for the SAS design.

For longitudinal autopilots, it can be stabilized and controlled including the pitch attitude, height, Mach number, etc. of an aircraft. In this thesis, both pitch attitude hold and altitude hold will be implemented on the basis of the reference BWB aircraft with the designed SAS at the operating point of P_2.

Most of the flying quality specifications do not apply directly to autopilot design. In the case of autopilot modes, the autopilot control system must be designed to satisfy specifications on steady-state error, with less emphasis on dynamic response [30]. Hence, both the pitch attitude and height response are analyzed in time domain with the settling time and steady-state error.

7.2 Pitch Attitude Hold Autopilot

Automatic longitudinal control of an aircraft is implemented by means of pitch attitude commands. Due to the control of pitch attitude alone is of limited usefulness, this autopilot is not often required as a stand alone controller [47]. However, other longitudinal autopilots formulate their output in terms of pitch attitude demand. This autopilot is used in the inner loop of other autopilots, such as altitude hold and automatic landing. Therefore, the pitch attitude control will be designed initially in this section.

The basic architecture of a pitch attitude hold control system is shown in Figure 7-1 [47] as the proportional gain K_θ acting on pitch attitude error. The shaded area is the SAS control law which has been accomplished above.

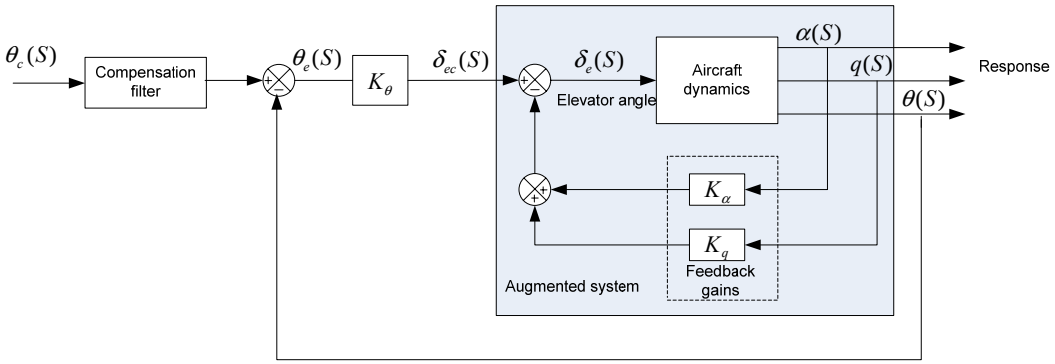

Figure 7-1 Pitch Attitude Hold Autopilot Architecture

The pitch feedback gain is designed using the model defined in Chapter 4.3, which the inner feedback loop is closed. The transfer function, equation (7-1), for pitch attitude with respect to elevator deflection at P_2 is obtained as the same as equation (4-9). Thus, the root locus plot is constructed and given in Figure 7-2.

$$\frac{\theta(s)}{\delta_e(s)} = \frac{-5.4877(s+0.7617)(s+0.0009963)}{(s^2+0.005647s+0.002254)(s^2+3.918s+6.109)} \quad \text{(deg/deg)} \qquad (7\text{-}1)$$

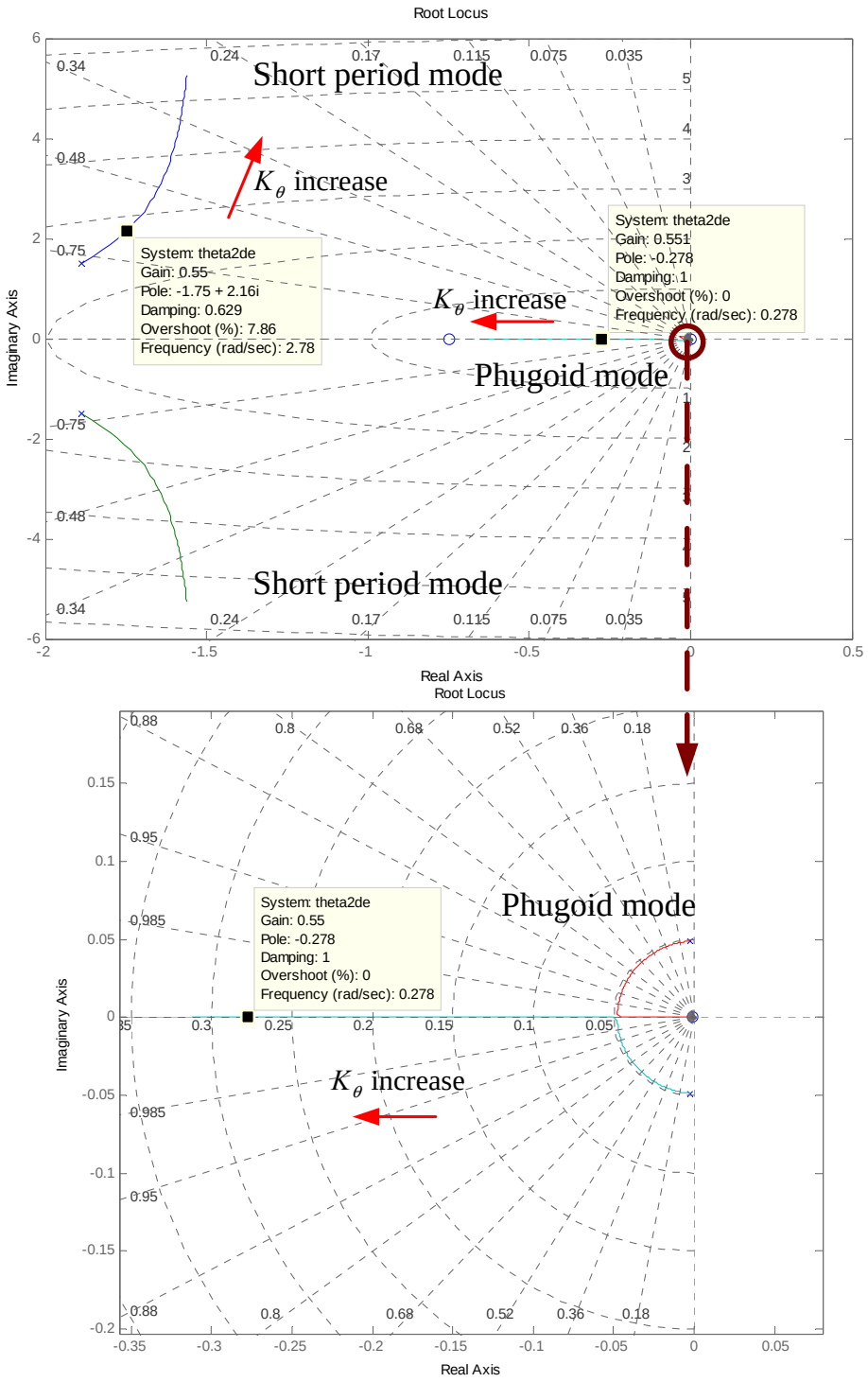

Figure 7-2 Root Locus Plot Pitch Attitude to Elevator

The effect of the K_θ increase improves the frequency and decreases the damping of short period, whilst the two real poles of phugoid give rise to two legs. One of them moves to the origin with increasing gain and will introduce an increasingly sluggish response. Considering the above restrictions, the result K_θ with the compromise and iteration is chosen as

$$K_\theta = -0.55 \tag{7-2}$$

The relation between input variables of elevator and pitch attitude control command is shown in equation (7-3), Thus, the equations of motion of equation (4-5) and transfer function with respect to pitch attitude control command become equation (7-4) and (7-5) respectively with SAS and K_θ engaged [6].

$$\delta_e = -\begin{bmatrix} 0 & 0 & 0 & K_\theta \end{bmatrix} \begin{bmatrix} v \\ \alpha \\ q \\ \theta \end{bmatrix} + K_\theta \theta_c \tag{7-3}$$

$$\begin{bmatrix} \dot{v} \\ \dot{\alpha} \\ \dot{q} \\ \dot{\theta} \end{bmatrix} = \begin{bmatrix} -0.001767 & -9.1162 & -17.872 & -10.846 \\ -0.00010079 & -0.87916 & 0.89602 & -0.10832 \\ 0.0012112 & -3.6272 & -2.8985 & -2.883 \\ 0 & 0 & 1 & 0 \end{bmatrix} \begin{bmatrix} v \\ \alpha \\ q \\ \theta \end{bmatrix} + \begin{bmatrix} 1.0864 \\ 0.10491 \\ 2.883 \\ 0 \end{bmatrix} \theta_c \tag{7-4}$$

$$\frac{\theta(s)}{\theta_c(s)} = \frac{-2.883(s+0.7488)(s+0.0007195)}{(s+0.2775)(s+0.00722)(s^2+3.495s+7.712)} \quad \text{(deg/deg)} \tag{7-5}$$

The uncompensated pitch attitude response to 1^o step attitude demand is shown in Figure 7-3.

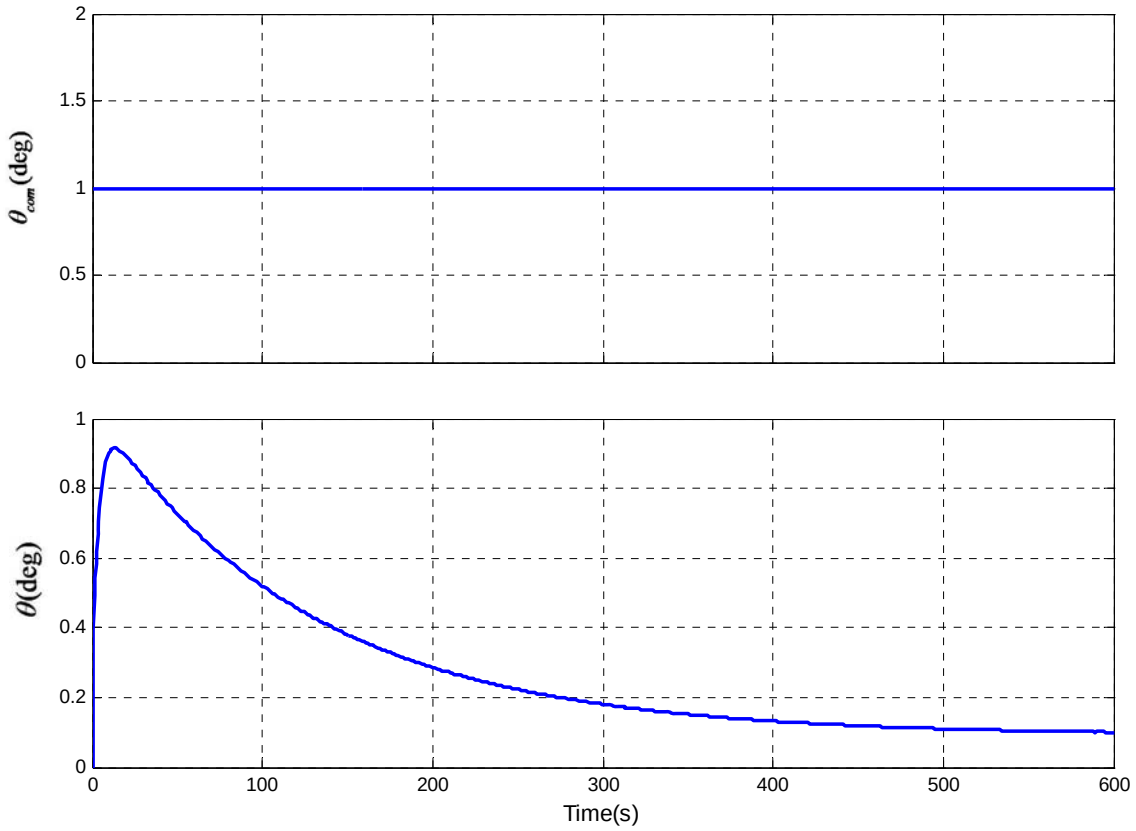

Figure 7-3 Pitch Attitude Response to 1^{o} Step Attitude Demand

The obvious response is the slow fall back to the steady condition of about 10% of the demand which is caused by the phugoid related terms marked by $^{\#}$ in equation (7-6). The numerator zero (s+0.007195) is the phase advance term with a very long time constant (an approximate differentiator) which produces the initial peak. The denominator pole (s+0.0072) is the phase lag term which produces the long decay. It is clear that the response is unsatisfactory for pitch attitude hold. Hence, a compensation filter is needed to design in this case.

$$\frac{\theta(s)}{\theta_c(s)} = \frac{-2.883(s+0.7488)(s+0.0007195)^{\#}}{(s+0.2775)(s+0.00722)^{\#}(s^2+3.495s+7.712)} \text{ (deg/deg)} \qquad (7\text{-}6)$$

In order to eliminate the unsatisfactory response, the command path filter is chosen as the lag-lead transfer function in equation (7-7).

$$F(s) = \frac{(s + 0.7488)}{(s + 0.00722)} \tag{7-7}$$

The compensated response to a 1^o step attitude command is shown in Figure 7-4. The settling time is 16s with almost zero steady-state error.

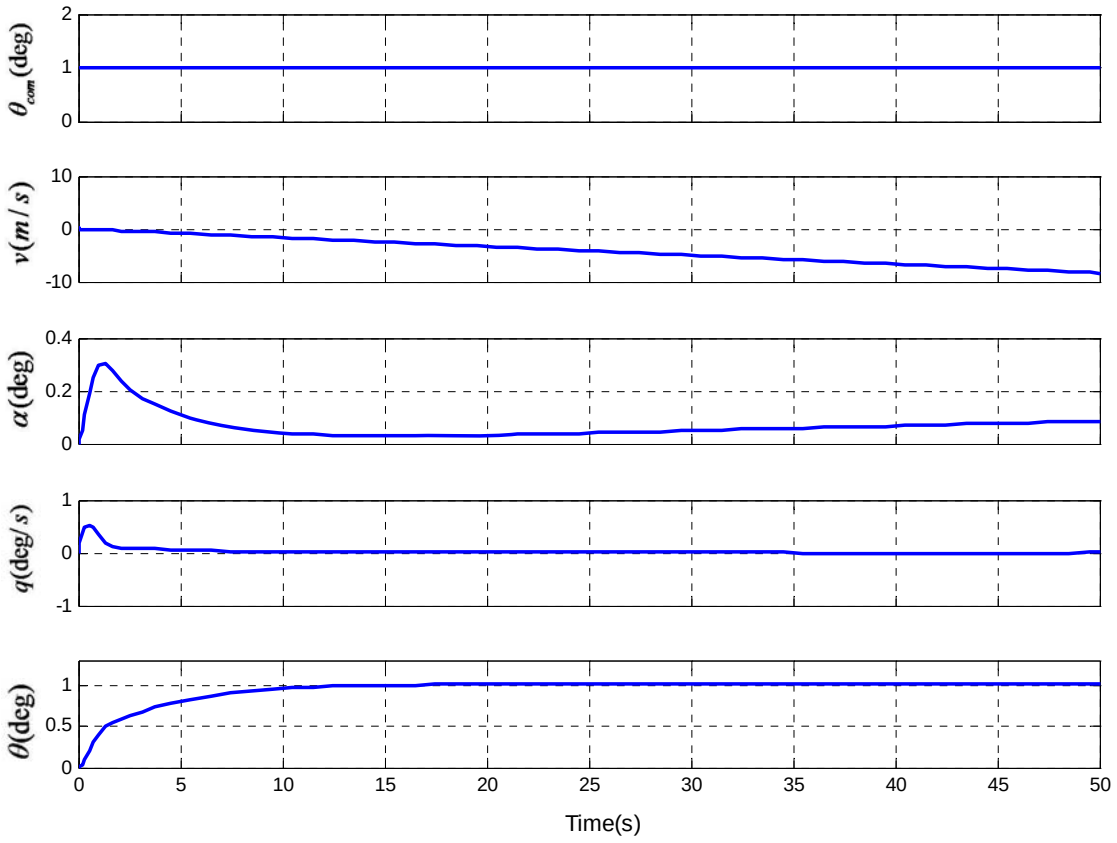

Figure 7-4 Compensated Response to 1^o Step Attitude Command

7.3 Altitude Hold Controller Design

Altitude hold is a significant pilot-relief mode which allows an aircraft to be held at a certain altitude in order to meet aircraft-traffic control requirements [30]. In this section, the pitch attitude hold pilot and augmented aircraft is used as the basic block on which the altitude hold auto pilot is designed. The classical height hold autopilot architecture is shown in Figure 7-5 [47].

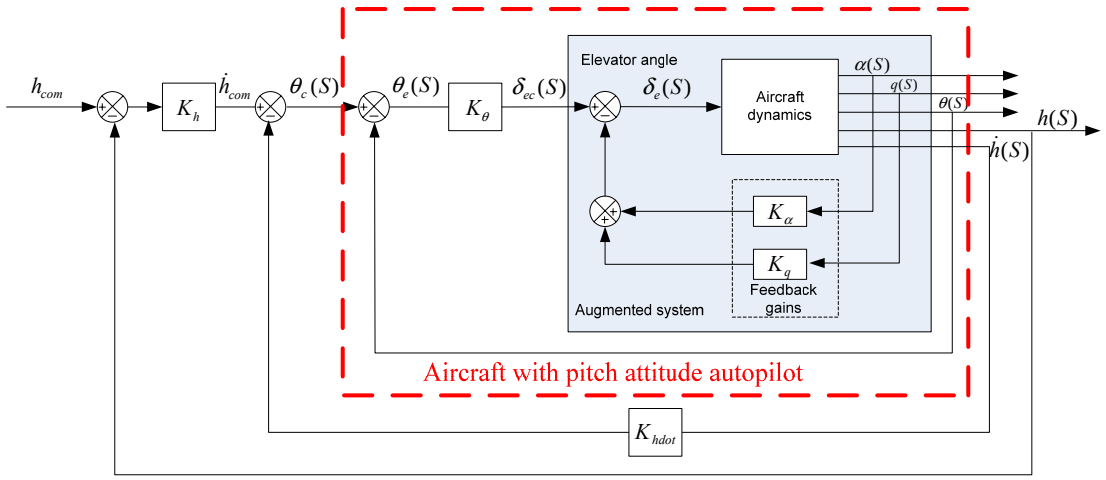

Figure 7-5 Altitude Hold Autopilot Architecture

The control law could be written:

$$\theta_c = (h_c - h)K_h - \dot{h}K_{h\,dot} \tag{7-8}$$

where:

$$\dot{h} = -w + V_0\theta = -V_0\alpha + V_0\theta \tag{7-9}$$

Taking the variables h into account by equation (7-9), the equation (7-4) could be augmented as the state equation (7-10) shows [6].

$$\begin{bmatrix} \dot{v} \\ \dot{\alpha} \\ \dot{q} \\ \dot{\theta} \\ \dot{h} \end{bmatrix} = \begin{bmatrix} -0.001767 & -9.1162 & -17.872 & -10.846 & 0 \\ -0.00010079 & -0.87916 & 0.89602 & -0.10832 & 0 \\ 0.0012112 & -3.6272 & -2.8985 & -2.883 & 0 \\ 0 & 0 & 1 & 0 & 0 \\ 0 & -220 & 0 & 220 & 0 \end{bmatrix} \begin{bmatrix} v \\ \alpha \\ q \\ \theta \\ h \end{bmatrix} + \begin{bmatrix} 1.0864 \\ 0.10491 \\ 2.883 \\ 0 \\ 0 \end{bmatrix} \theta_c \tag{7-10}$$

7.3.1 Design of the Height Rate Loop Feedback Gain

Solution of equation 7-10 that provides the response transfer function of height rate response to pitch attitude command:

$$\frac{\dot{h}(s)}{\theta_c(s)} = \frac{-23(s+4.557)(s-4.514)(s-0.00116)}{(s+0.2775)(s+0.007219)(s^2+3.494s+7.712)} \quad \text{(m/s/deg)} \tag{7-11}$$

A root locus plot of the transfer function (7-11) is constructed in Figure 7-6. With the increase of the $K_{h\,dot}$, the damping of the SPO mode is decreased and this mode becomes unstable at gain $K_{h\,dot} = 0.045$. The phugoid heave mode pole moves to the right to become much slower whilst the surge mode becomes faster. Considering the SPO mode stability, the gain is needed to smaller than 0.045. For phugoid, it is significant to avoid the excessive lag to prevent long settling times after a disturbance. Hence the suitable gain is chosen as:

$$K_{hdot} = 0.01 \tag{7-12}$$

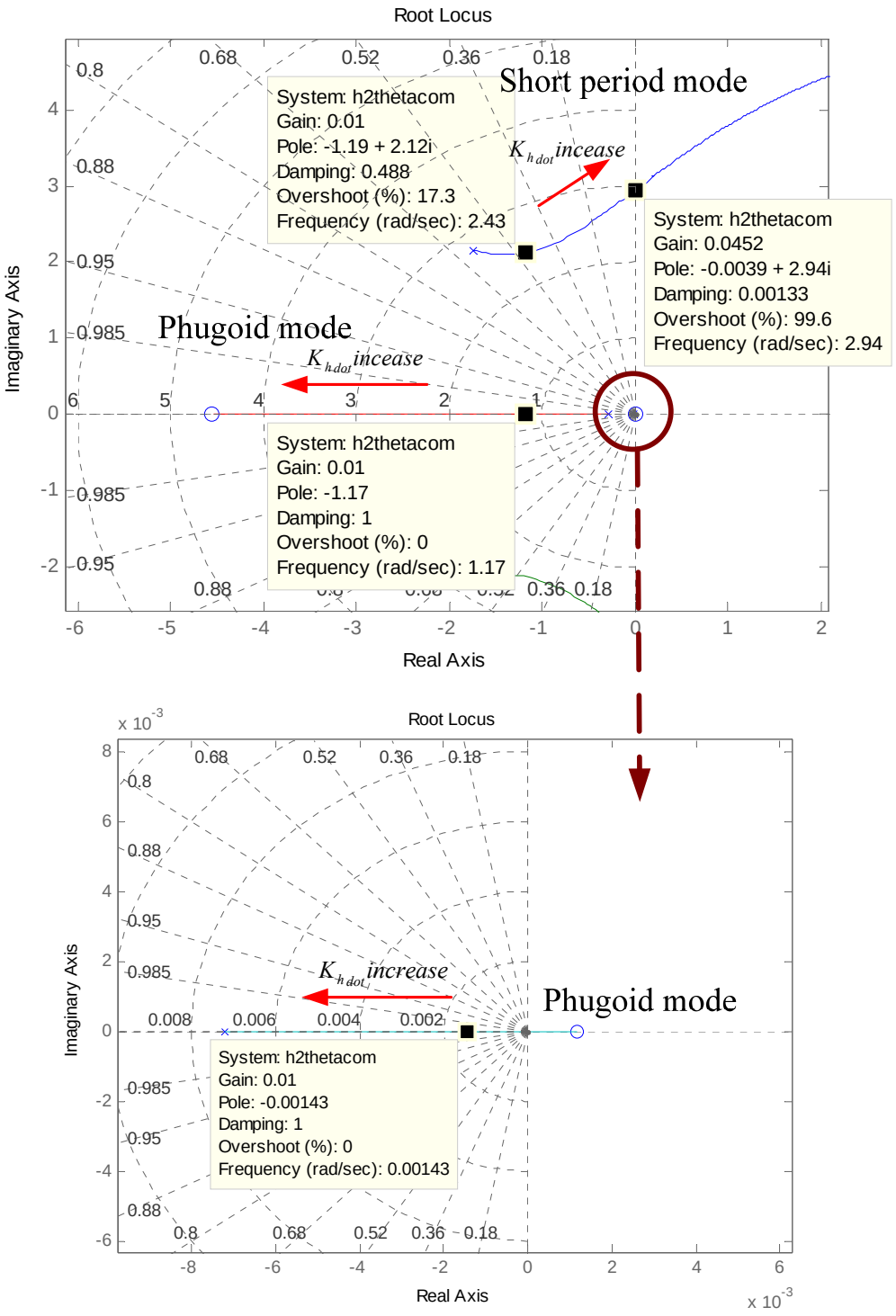

Figure 7-6 Root Locus Altitude to Pitch Attitude Command

7.3.2 Design of the Height Loop Feedback Gain

With the height rate feedback loop closed, the height loop gain could be designed. According to Figure 7-5 and equation (7-3), the inner loop control law could be given in equation (7-13). Thus, the equations of motion of equation (7-10) may be rewritten in equation (7-14) with respect to height rate command [6].

$$\theta_c = -[\,0 \quad -K_{\dot{h}} \quad 0 \quad V_0 K_{\dot{h}} \quad 0] \begin{bmatrix} v \\ \alpha \\ q \\ \theta \\ h \end{bmatrix} + \dot{h}_c \tag{7-13}$$

$$\begin{bmatrix} \dot{v} \\ \dot{\alpha} \\ \dot{q} \\ \dot{\theta} \\ \dot{h} \end{bmatrix} = \begin{bmatrix} -0.001767 & -9.1063 & -17.872 & -13.013 & 0 \\ -0.00010079 & -0.8782 & 0.89602 & -0.31753 & 0 \\ 0.0012112 & -3.601 & -2.8985 & -8.6321 & 0 \\ 0 & 0 & 1 & 0 & 0 \\ 0 & -220 & 0 & 219.36 & 0 \end{bmatrix} \begin{bmatrix} v \\ \alpha \\ q \\ \theta \\ h \end{bmatrix} + \begin{bmatrix} 1.0864 \\ 0.10491 \\ 2.883 \\ 0 \\ 0 \end{bmatrix} \dot{h}_c \tag{7-14}$$

Solution of equation (7-14) provides the response transfer function of height response to height rate command as:

$$\frac{h(s)}{\dot{h}_c(s)} = \frac{-23\,(s+4.557)\,(s-4.514)\,(s-0.00116)}{s\,(s+0.506)\,(s+0.002864)\,(s^2+3.27s+12.76)} \quad \text{(m/m/s)} \tag{7-15}$$

A root locus plot of this transfer function (7-15) is illustrated in Figure 7-7.

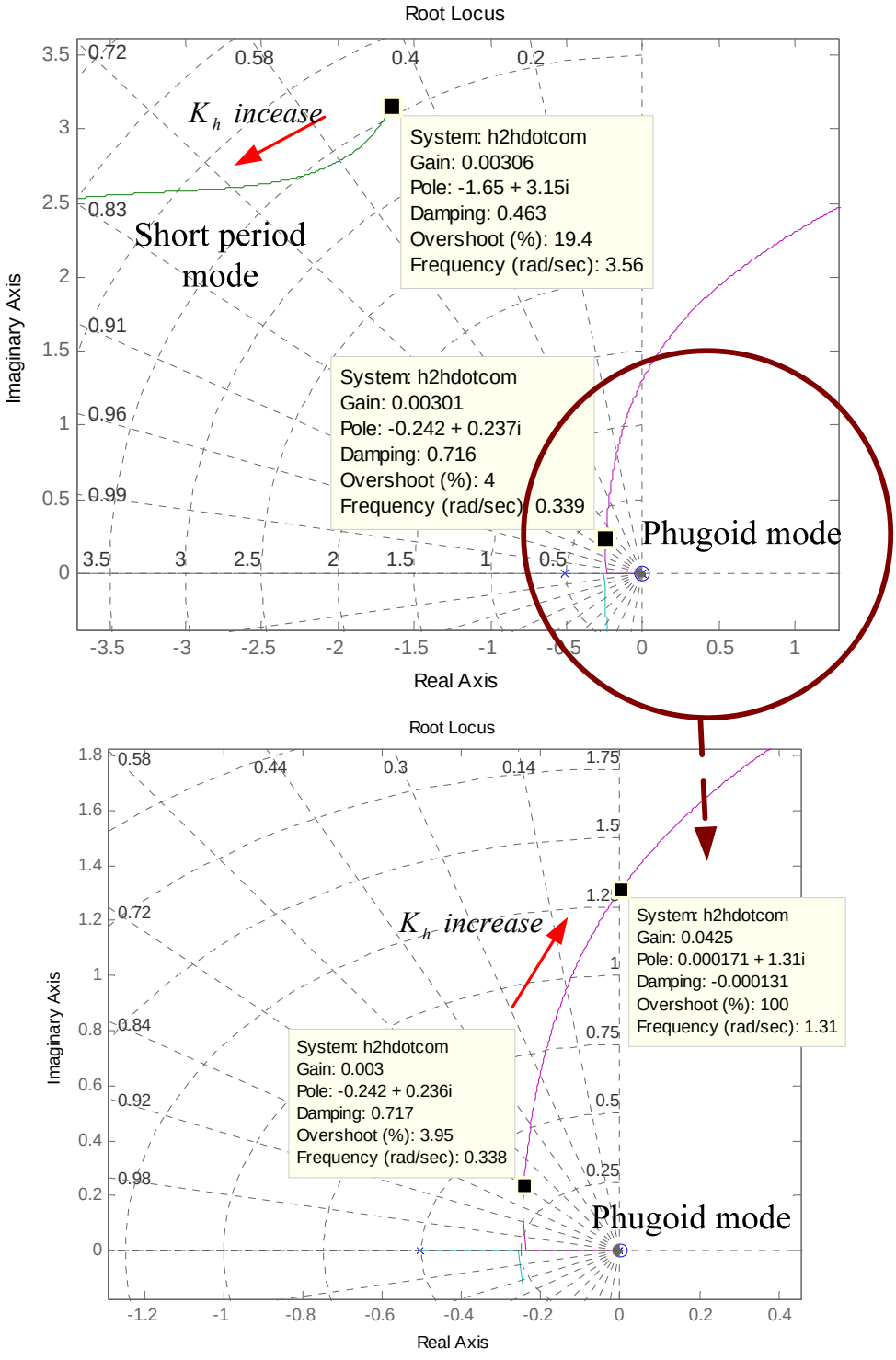

Figure 7-7 Root Locus Altitude to Altitude Rate Command

From Figure 7-7 it is demonstrated that as height feedback gain is increased the phugoid becomes unstable at $K_h = 0.0425$. By the adjustment of gain, K_h is selected below, whilst the SPO mode has an adequate margin of stability.

$$K_h = 0.003 \tag{7-16}$$

The system response to 200m height command shows in Figure 7-8. It is clear that the settling time is 17s with almost zero steady-state error.

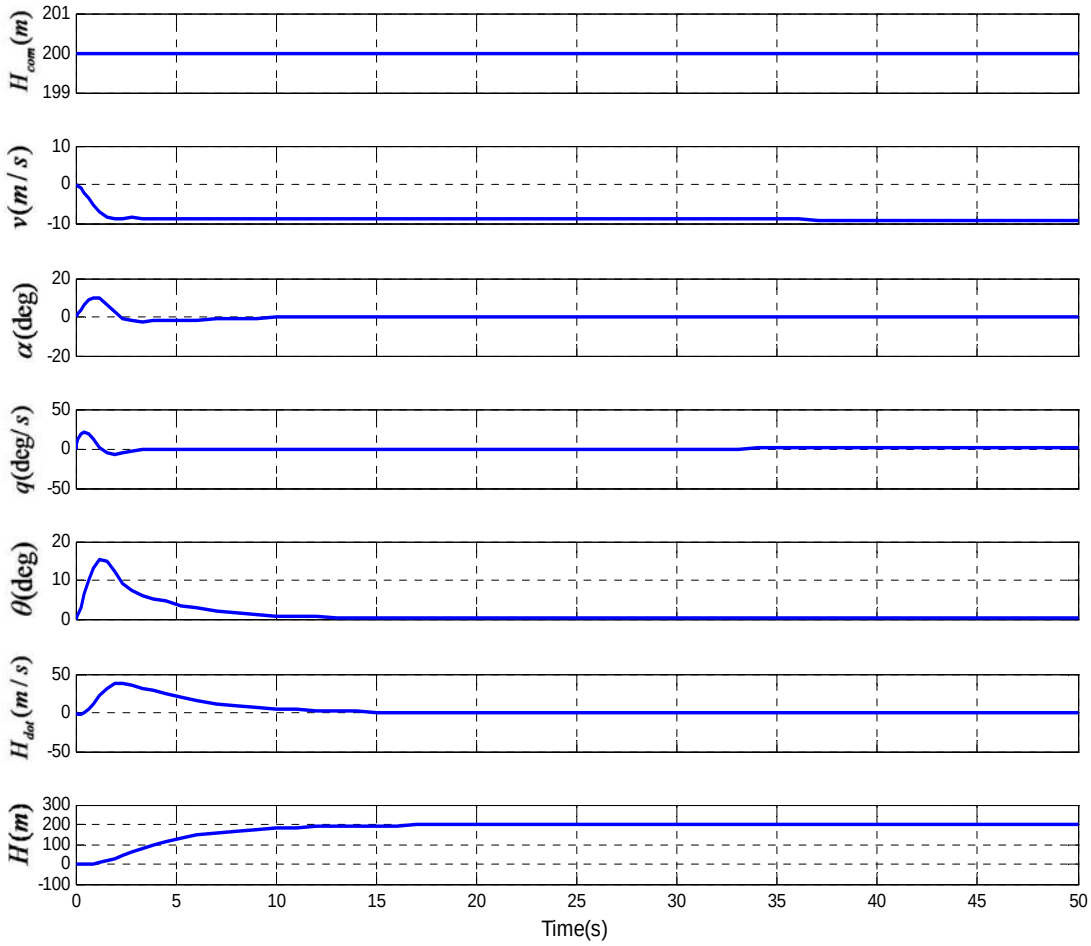

Figure 7-8 Aircraft Response to 200m Height Command

7.4 Summary

In order to achieve the command control for the aircraft, outer loop autopilot both pitch attitude hold and altitude hold are implemented by the root locus

method. It is found that the designed autopilot control laws could provide a satisfactory pitch attitude and altitude tracking performance.

8 CONCLUSION

On the basis of the above chapters, the study methods and results has been presented. This chapter will summarize this research work and conclude the main findings. Moreover, it recommends some guidelines for the further study on this subject.

8.1 Conclusions

This thesis presents the longitudinal control laws design for the reference BWB aircraft. Not only was the inner SAS controller developed for the whole envelope, but also the outer autopilot control laws have been implemented. More specifically, two sets of linear SAS feedback controllers was designed by means of pole placement method at equilibrium points, and then the resulting family of linear controllers were implemented as a single controller whose parameters are changed by monitoring the scheduling variables of dynamic pressure Q. Based on the existing SAS, both pitch attitude and altitude hold auto pilot control functions were achieved in order to realize command control characteristics. The overall conclusions are detailed as follows:

8.1.1 Inner Loop Control Laws Design

The most critical aspect of longitudinal flight control laws design is concerned with the inner loops which govern the control of essential aircraft stability characteristics. In this thesis, following procedures have been implemented to develop the inner loop control laws.

- **SAS controller design**

The SAS is to endow the aircraft with stability characteristics conductive to satisfactory flying and handing qualities. According to the damping ratio and CAP criteria in MIL-F-8785C specifications which restrict the system stability characteristics, the AOA and pitch rate feedback are engaged in the two sets of linear SAS feedback controllers by pole placement approach based on the reduced order linear model. It is valid that the AOA feedback could improve the frequency of system while the pitch rate feedback is considerably useful for

increasing damping. Since it is essential to check the system with full order system, aircraft responses of the long period mode and further the wind disturbance are verified for the designed controllers.

- **Assessment over the whole envelope**

In order to make the controller satisfy the flying and handing qualities over the whole envelop, two controller gains are fixed and assessed in the entire envelope with the damping ratio and CAP criteria. With the restriction of damping ration for two controllers, the flight envelope is divided into regions F_1 and F_2. In both of two areas, the damping and CAP can satisfy the requirements in MIL-F-8785C specifications as the corresponding controllers C_1 and C_2 engaged in. Therefore, F_1 and F_2 could cover the whole flight envelope together with the satisfactory flying and handing qualities.

- **Gain scheduling**

The designed gain schedule is a segmented but continuous function of dynamic pressure which is selected to schedule these two sets of controller gains. By the assessment of three trim points in the interpolation region, it is found that this scheduling scheme provides continuous and automatic gains change with respect to the scheduling variable. Moreover, the desired flying and handing qualities and performance are achieved by the augmented aircraft in the flight envelope assuming certain values of scheduling parameter Q.

- **Influence induced by the varying CG position**

The varying CG position generates a significant influence to the aircraft stability characteristics for the reference BWB aircraft. With the CG movement towards the back, the damping ratio increases (static stable condition) and the poles of SPO are going to exist in the right part of s-plane gradually. For the SAS controller in this study, it is difficult to cover the whole CG range by the traditional design approach. However, it is still satisfactory at the cruise and approach phase.

8.1.2 Outer Loop Control Laws Design

Since the flight control law is designed for a specific aircraft application, the control architecture tends to be unique. However, most of these control systems have some functional similarity and differ only in detail, which includes command path, forward path and feedback path. Through the completion of pitch attitude hole and altitude hold autopilot design, it is found that the effect of these could be valid and summarised as follows:

- The command path: shape the response with respect to control command without influencing the closed loop stability.
- The forward path: effect both closed loop stability and provide some control response shaping simultaneously.
- The feedback path: improve the required closed loop stability characteristics.

Moreover, it is also found that the root locus is helpful and convenient for the selection of controller gains. The suitable gains could be seen obviously as the pole and zero of system movement with the varying gains, so that the time of adjustment of gains will be reduced.

8.1.3 Application to the FW-11

Although the GDP work was concerned with the FW-11 flying wing aircraft, the work in this thesis has significant relevance to that aircraft. Due to the similarities discussed in subsection 1.2.2 between two aircraft, the methodology proposed here should be directly applicable to the design of the longitudinal SAS and autopilot control of pitch attitude and altitude hold for the FW-11.

8.2 Further Research

The completed work allowed the aims and objectives to be realised. But the control laws design for the reference BWB aircraft is a multidisciplinary design problem, which includes aerodynamics, flight dynamics, control theory (linear and nonlinear), flying and handing qualities assessment, etc. Hence, it is hard for a researcher to copy with all fields with equal efficacy. In spite of a humble effort has been made in a limited time frame, following suggestions are presented with regards to future work on this subject.

- **Aircraft model**

In this thesis, it is convenient to simplify the longitudinal movement of aircraft by the small perturbation equation of motion without actuators and nonlinearities. But these aspects exist in practical application which would induce the system lag and nonlinear influence to the response of aircraft. Hence, in order to make the control system applicable to the realistic aircraft, it is necessary to consider these effects at least by simulation testing. Nonlinear and high order controllers design will make the system more complex than before.

- **Flying and handing qualities**

The damping ratio and CAP criteria are selected as SAS design constraints. It is suggested to restrict an ideal range of them for the certain aircraft on the basis of MIL-F-8785C specifications which offer a general range for all the aircrafts. This research restricts the damping ratio only which represents the dynamic stability of aircraft. It is deserved to take the CAP value restriction or other criteria which are suitable for the BWB aircraft control laws design.

- **Control allocation**

In order to enhance the productivity of control surfaces for the tailless aircraft, redundant suits of control surfaces would become more common. In this study, all of the flaps for pitch control are simplified as an elevator. For further work, some sort of control allocation scheme needs to be developed to decide how to utilize these control effectors.

- **Gain scheduling**

Classical gain-scheduling approaches employed to handle the nonlinear property of the aircraft has been successfully used in this thesis and other engineering applications. Nevertheless, it may result in some problems, one of which is that it can not guarantee global robustness and stability in transitions of different flight conditions. Hence, advanced method of gain scheduling such as LPV control is a significant field to research for designers.

- **Control law design**

Generally, lateral control laws and other autopilot function (speed/mach hold, heading hold, roll attitude hold, etc.) would be developed in future work. Furthermore, designing the robust controller is also an interesting aspect to be researched, which could satisfy the flying and handing qualities over the entire envelope and whole range of CG variation without gain scheduling. Thus the flying and qualities degradation induced by the sensor failures of scheduling variables and influence by CG variation could be avoided.

REFERENCES

1. Dmitriev, V. G. (2003), "*The Flying-Wing Concept-Chances and Risks*", AIAA 2003-2887, International Air and Space Symposium and Exposition, 14-17 July 2003, Dayton, Ohio.
2. Bolsunovsky, A. L. and Boverya, N. P. (2001), "*Flying Wing -- Problems and Decisions*", Aircraft Design, vol. 4, pp. 193-219, 2001.
3. McKeand, R. G., "*Flight Dynamics of a Blended Wing Body Commercial Transport Aircraft*", MSc Thesis, Cranfield University, 2005.
4. Smith, H., Howe, D and Fielding, J.P., "*Blend-Wing-Body High Capacity Airliner BW-98 Project Specification*", Cranfield University, 1998.
5. Castro, H. V. de., "*Flying and Handling Qualities of a Fly-By-Wire Blended-Wing-Body Civil Transport Aircraft*", PhD Thesis, Cranfield University, 2003.
6. Rahman, N. U., "*Propulsion and Flight Controls Integration for the Blend Wing Body Aircraft*", PhD Thesis, Cranfield University, 2009.
7. Nickel, K. and Wohlfahrt, M., "*Tailless Aircraft in Theory and Practice*", Translated by Capt.Eric Brown RN, Edward Arnold, London, 1994.
8. Wood, R. and Bauer, S. "*Flying Wings/Fuselages*", 39th AIAA Aerospace Sciences Meeting and Exhibit, Reno, 8-11 January 2001.
9. www.en.wikipedia.org/wiki/Northrop_Grumman_B-2_Spirit
10. Casey, B., "*Flying Qualities and Control of a Blend Wing Body Transport Aircraft* ", MSc Thesis, Cranfield University, 2005.
11. www.boeing.com/news/frontiers/archive/2003/february/cover
12. Abzug, M. J., "*Airplane Static Stability and Control*", 2nd ed., Cambridge University, 2005.
13. www.tpub.com/content/aviation2/P-1231/P-12310030
14. Esteban, S., "*Static and Dynamic Analysis of an Unconventional Plane: Flying Wing*", AIAA 2011-4010, Atmospheric Flight Mechanics Conference

and Exhibit August, 2001.

15. Cook, M. V., “Flight Dynamics Principles”, Arnold publishers, 1997.
16. Cotting, C. M., “*Evolution of Flying Qualities Analysis: Problems for a New Generation of Aircraft*”, PhD Thesis, 2010.
17. Hodgkinson, J., “*Aircraft Handling Qualities*”, AIAA Education Series, *1999.*
18. Guo, W., “*Gain Scheduling for a Passenger Aircraft Control System to Satisfy Handling Qualities*”, MSc Thesis, Cranfield University, 2010.
19. Mitchell, David G., Doman, David B., Key, David L. and Klyde, David H., “*The Evolution, Revolution, and Challenges of Handing Qualities*”, AIAA 2003-5465, Atmospheric Flight Mechanics Conference and Exhibit, August 2003.
20. Holmberg, J. A. and Cotting, C. M. "*Flying Qualities Specifications and Design Standards for Unmanned Air Vehicles*", AIAA 2008-6555, Atmospheric Flight Mechanics Conference and Exhibit, Honolulu, Hawaii, 2008.
21. Kivioja, D. A., “*Comparison of the Control Anticipation Parameter and the Bandwidth Criterion during the Landing Task*”, Department of the Air Force Air University, 1996.
22. Cook. M. V, “*Flight Qualities and Flight Control Lecture Notes*”, Cranfiled University, February 2011.
23. Hendarko, H. "*Development of a Handing Qualities Evaluation Toolbox on the Basis of Gibson Criteria*", 23rd Congress of International Council of the Aeronautical Sciences, Toronto, Canada, 8-13 September, 2002.
24. www.dtic.mil/dticasd/edc/EDCSec07/e07-0707f1.html
25. Richardson, T. S. and Davison, P. M. "*Control of Nonlinear Aircraft Models Using Dynamic State-Feedback Gain Scheduling*", AIAA 2003-5503,

Guidance, Navigation, and Control Conference and Exhibit, Austin, Texas, 11-14 August 2003.

26. Rademakers, N. G. M. "*Control of a Tailless Fighter Using Gain-Scheduling*", Traineeship report, Eindhoven University of Technology Department Mechanical Engineering, 2004.
27. Sinha, N. K., Jangid, M. and Ananthkrishnan, N. "*Automated Gain Scheduling Using Continuation Techniques*", The Nonlinear Control Systems Conference, Stuttgart, September 2004.
28. Rugh, W. J. and Shamma, J. S., "*Research on Gain Scheduling*", Automatica, pp. 1401-1425, December 1999.
29. Marcos, A. and Balas, G. J., "*Development of Linear-Parameter-Varying Models for Aircraft* ", Journal of Guidance, Control, and Dynamics. Vol.27, pp. 218-228, 2004.
30. Stevens, B. L. and Lewis, F. L., "*Aircraft Control and Simulation*", 2nd ed., A Wiley-Interscience Publication, United States of America, 2003.
31. Anon, "*Military Specification-Flying Qualities of Piloted Airplanes*", MIL-F-8785C, Department of Defense, USA, 1980.
32. Przemienieck, J. S., "*Introduction to Aircraft Flight Dynamics*", AIAA Education Series, 1998.
33. Nelson, R. C., "*Flight Stability and Automatic Control*", 2nd ed., Aerospace Science & Technology Series, 1998.
34. Denis, H., "*Aircraft Loading and Structural Layout*", AIAA Education Series, 2004.
35. El-Dirani, T., "*Fidelity of Flight Control System in a Real-Time Optimal Trajectory Planner*", MSc Thesis, Massachusetts Institute of Technology, 1990.

36. Stenge, R. F., “Flight Dynamics”, Princeton University Press, 2004.
37. Akmeliawati, R., “Nonlinear Control for Automatic Flight Control Systems”, PhD Thesis, University of Melbourne, 2001.
38. Tóth, R., “*Modelling and Identification of Linear-Parameter-Varying Systems*”, Lecture Notes in Control and Information Sciences, 1st ed., Springer, 2010.
39. Leith, D. J. and Leithead, W. E., "*Gain-Scheduled Control: Relaxing Slow Variation Requirements by Velocity-Based Design*", Journal of Guidance Control and Dynamics, vol. 23, pp. 988-1000, 2010.
40. Feuersänger, A. and Ferreres, G., “*Design of a Robust Back- Up Controller for an Aircraft with Reduced Stability*”, AIAA-2006-6237, Guidance, Navigation and Control Conference, Colorado ,Keystone, 21-Aug-2006.
41. Rachman, E., Jaam, J. M. and Hasnah, A., “*Non-linear simulation of controller for longitudinal control augmentation system of F-16 using numerical approach*”, Information Sciences, vol.164, pp. 47-60, 2004.
42. Anon, “*Report on the Serious Incident at Oslo Airport Gardermoen on 21 September 2004 Involving Flight KAL520 Boeing 747-400F Registered HL 7467 Operated by Korean Air*”, Accident Investigation Board Norway, 2007.
43. Anon, ‘*Federal Aviation Regulations - Part 25 Airworthiness Standards: Transport Category Airplanes*”, Federal Aviation Administration, United states of department of Transportation.
44. Feuersanger, A. P. and Ferreres, G., "*Robust Aircraft Control Design with Reduced Stability and Saturated Actuators*", 17th IFAC Symposium on Automatic Control in Aerospace, Vol. 17, 2007.
45. Bérard, C. and Saussié, D. "*Robust Control of Longitudinal Flight with Handing Qualities Constraints*", Conference on Systems and Control, Marrakech, Morocco, 16-18 May 2007.

46. Zhang, J., Yang, L. and Shen, G. "*Modeling and attitude control of aircraft with center of gravity variations*", Aerospace conference 2009 IEEE, pp. 1-11, 7-14 March 2009.
47. Cook. M. V., "*Lecture Notes on Introduction of Applied Flight Control"*, Cranfield University, September 2011.
48. Roskam, J., "*Airplane Design Part 6 - Preliminary Calculations of Aerodynamics, Thrust and Power Characteristics, Design Analysis & Research*", June 1989.
49. Anon, "*Lift-Curve Slope and Aerodynamic Centre Position of Wings in* Inviscid Subsonic Flow", ESDU 70011.
50. Anon, "*Aerodynamic Centre of Wing-Fuselage Combinations*", ESDU 76015.
51. Anon, "*Aerodynamic Centre of Wing-Fuselage-Nacelle Combinations: Effect of Wing-Pylon Mounted Nacelles*", ESDU 77012.
52. Fang, Z., "*Aircraft Flight Dynamics*", Beijing University of Aeronautics and Astronautics Press, 2005.
53. Smith, H., "*Group Design Project Lecture Notes on Aircraft Drag Estimation*", Cranfield University, 2011.

APPENDICES

Appendix A GDP work

A.1 Introduction

From April to September, the flying wing civil aircraft (FW-11, 248 seats for all economic) was designed, which could achieve the range of 7772nm and 16-hours whole flight time. The layout and geometry data of the FW-11 are as Figure A-1 and Table A-1 illustrated.

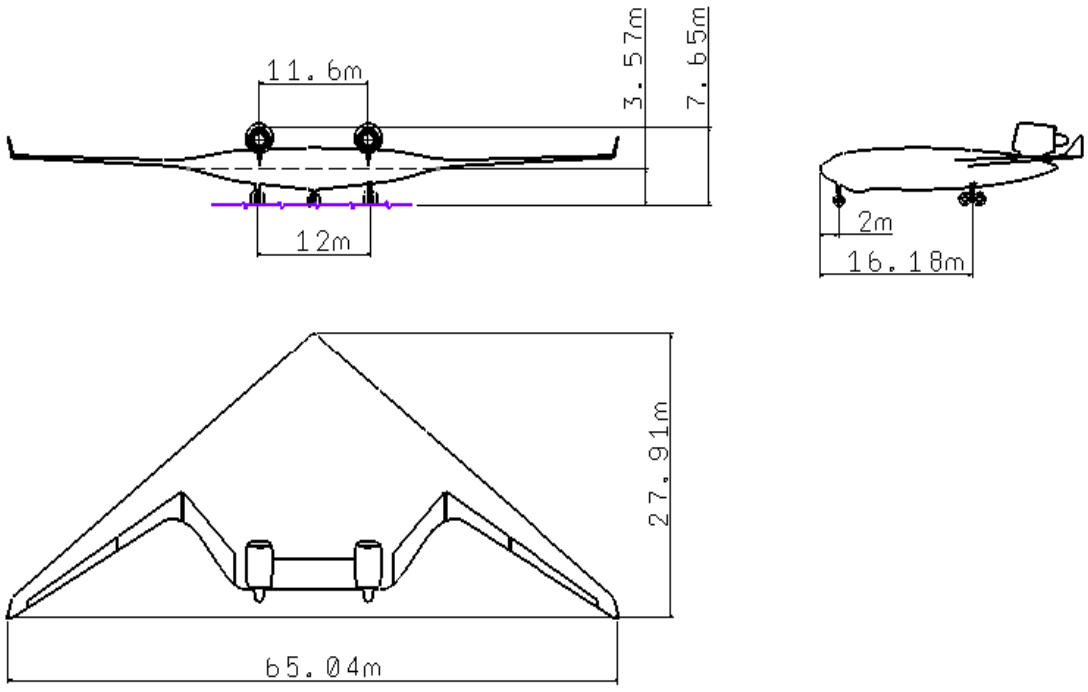

Figure A-1 Three-View Drawing of FW-11

Table A-1 Geometry Data of FW-11

Gross area (m^2)	647	**Taper ratio**	0.11
Wing loading (kg/m^2)	272	**Leading edge sweep angle (deg)**	39
Aspect ratio	6.33	**Quarter chord sweep angle (deg)**	34.3
Root chord (m)	25.2	**Mean aerodynamic chord (m)**	12.28
Tip chord (m)	2.0	**Dihedral angle (deg)**	2.0

In terms of design processes, in order to check the validation of the collected aircraft data, some estimation methods were used initially. Then the requirement, namely the design diver, was determined according to the market and strategy analysis. Consequently, a baseline aircraft which is a conventional configuration for design approaches study and comparison with the fly wing was obtained. Finally, it was developed that the flying-wing configuration aircraft of Blue Bird (FW-11). It is not only a quiet, comfortable and eco-friendly airliner, but also could save 29% fuel consumption than the A330-200 due to the higher lift drag ratio.

A.2 Specific Work

A.2.1 Stability and Control

Referring to the reference [48], ESDU 70011[49], 76015 [50] and 77012 [51], the aerodynamic Centre Estimation of the A330, baseline and FW-11 aircraft are shown as Table A-2.

.

Table A-2 Aerodynamic Centre Estimation Results

	AC	CG range
A330	61%(ma=0.82)	37%(aft)
Baseline	47.8%$\bar{\bar{c}}$	23.1%$\bar{\bar{c}}$ ~ 34.3%$\bar{\bar{c}}$
FW-11	38.2%$\bar{\bar{c}}$	30.68%$\bar{\bar{c}}$ ~ 37.09%$\bar{\bar{c}}$

As Table A-3 shows, the FW-11 is static stable but the static margin is not as large as the conventional configuration aircraft.

Table A-3 Three Axes Static Stability

Stability / Aircraft	Static Margin	Roll (Cl_β)	Yaw (Cn_β)
A330	24%		
Baseline	13.5%$\bar{\bar{c}}$ ~24.7%$\bar{\bar{c}}$	-0.5853	2.029
FW-11	1.11%$\bar{\bar{c}}$ ~7.52%$\bar{\bar{c}}$	-0.072	0.0378

A.2.2 Trim for Control Surfaces Productivity Evaluation

a) Longitudinal Moment Trim

The approach which is used for pitch trimming is presented by Figure A-2 and equation A-1 [15]. Due to the landing phase and CG forward cases are more

serious than others, only the condition of CG forward during cruise and landing phase is taken into account.

$$M_0 + L_w(h_{CG} - h_0)\bar{\bar{c}} - L_T l_T + \tau_e z_\tau = 0 \qquad \text{(A-1)}$$

where:

M_0 — Zero-lift moment

L_w — Lift of wing-body

L_T — Lift of tailplane

l_T — Tail arm

τ_e — Engine thrust

z_τ — Normal coordinate of engine thrust line

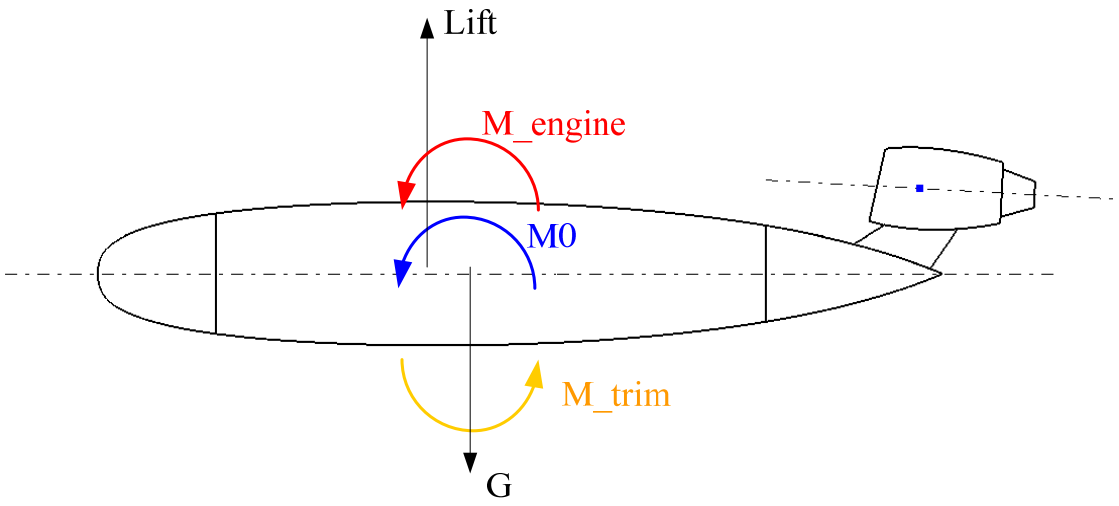

Figure A-2 Trim Moment of FW-11

The trimming results are illustrated by Figure A-3 and Figure A-4 for the baseline and FW-11 aircraft respectively.

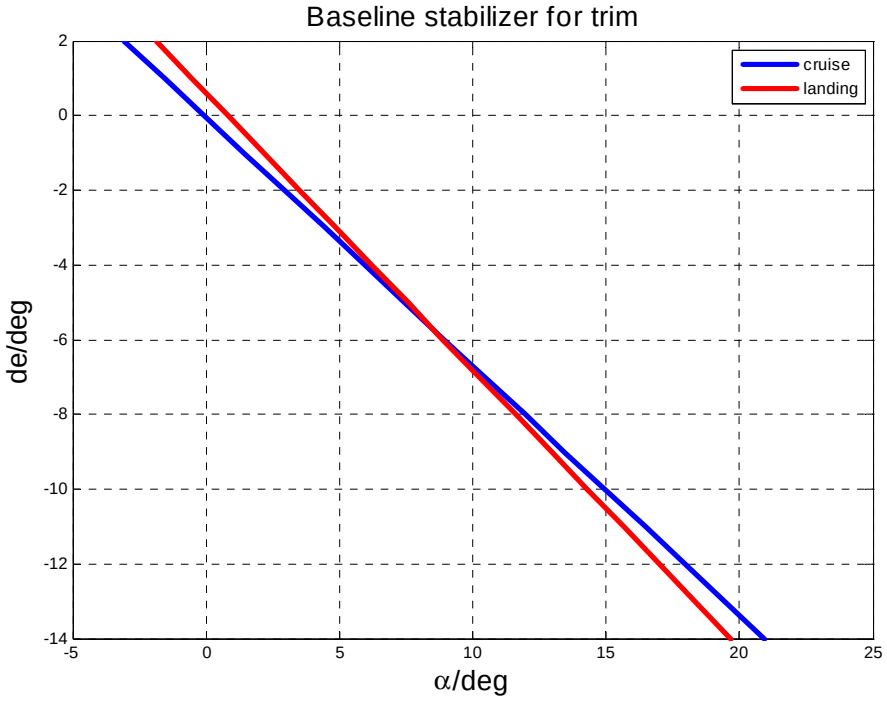

Figure A-3 Longitudinal Trim (CG forward) for Baseline

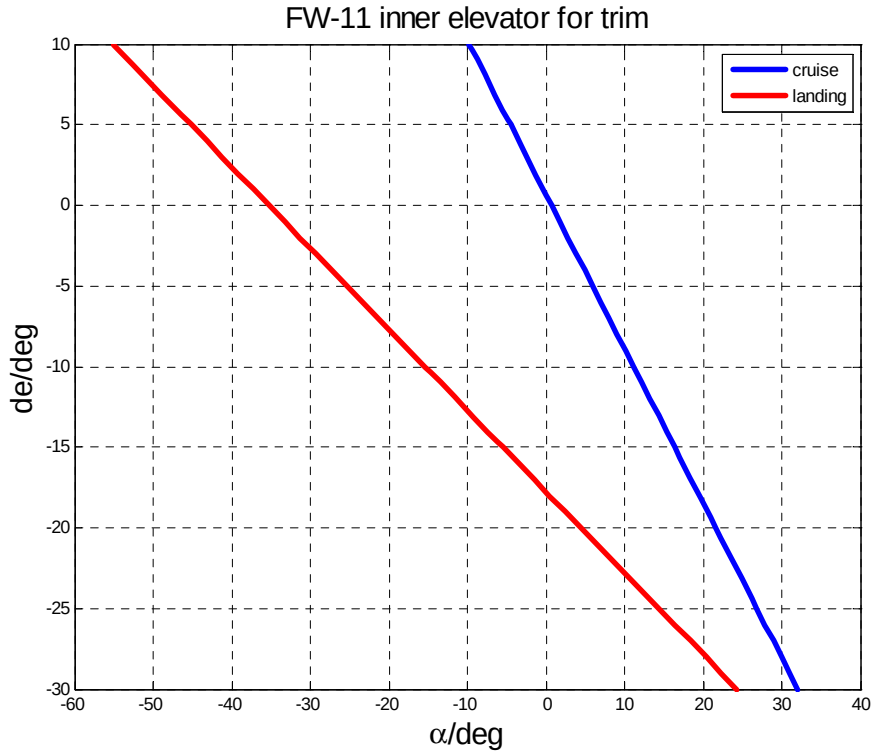

Figure A-4 Longitudinal Trim (CG forward) for FW-11

It is found that the conventional aircraft of baseline is capable for trim by stabilizers. In term of the FW-11, it also has the enough trim capability at cruise phase, but in landing phase, the elevator trim deflection is needed more due to the flap extension and downwash influence.

b) Directional Trim [52]

Because of the tailless configuration, the directional trim is necessarily considered as well.

The split drag rudder productivity is as Figure A-5 shows. In addition, both the one engine failure and cross-wing landing case are calculated for control surfaces effectiveness evaluation.

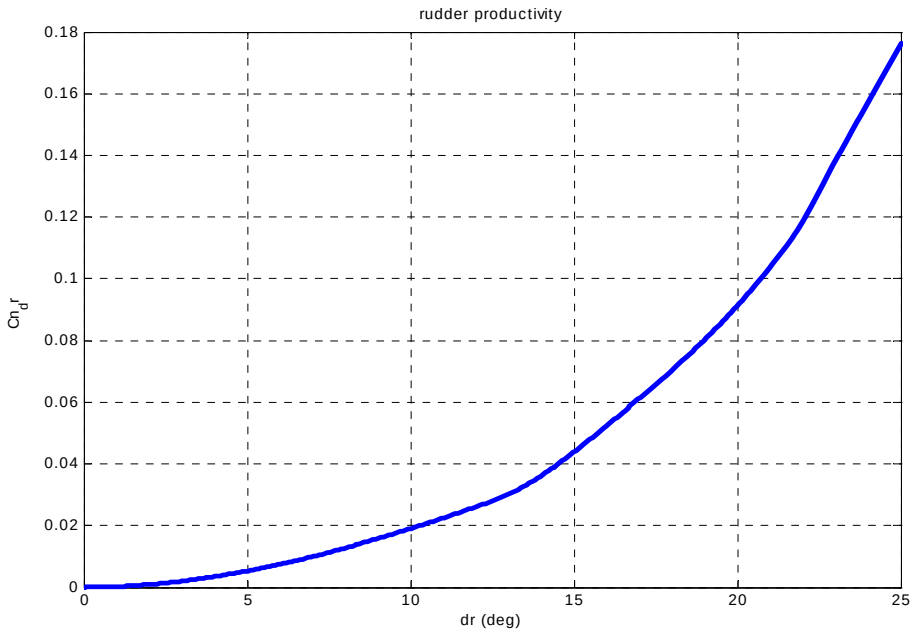

Figure A-5 Split Drag Rudder Productivity

- One engine failure taking-off

The directional moment balance at one engine failure is obtained by equation (A-2).

$$(T + D_w) \cdot L_y = C_n^{\delta_r} \cdot \delta_r \cdot qbs \qquad \text{(A-2)}$$

where: T —One engine thrust

D_w —Drag of wind milling

L_y —Distance between fuselage axes and engine position

The split drag rudder deflection at one engine failure is demonstrated in Table A-4.

Table A-4 Rudder Deflection at One Engine Failure Taking Off

Condition1: one engine failure taking off		
T (N)	C_{D_engin}	δ_r (deg)
173000	0.0007	7.85

where: C_{D_engin} —Drag coefficient of wind milling

δ_r —Split drag rudder deflection

- **Cross-wind landing**

The directional moment balance at cross-wind landing case is presented in equation (A-3) and (A-3).

$$\beta = \sin^{-1}\frac{Vw}{V} \tag{A-3}$$

$$\delta_r = -\frac{C_{n\beta}}{C_{n\delta_r}}\beta \tag{A-4}$$

where: V —Velocity of aircraft

V_W —Velocity of Cross-wind

$C_{n\beta}$ —Yaw moment due to side slide angle

$C_{n\delta_r}$ —Yaw moment due to rudder

The split drag rudder deflection at crosswind landing case demonstrates in Table A-5.

Table A-5 Rudder Deflection at Cross-Wind Landing

Condition 2:cross wind landing		
V (m/s)	V_W (m/s)	δ_r (deg)
68.54	10.3	10.8

Moreover, according to the different sideslip angle, the directional trim curve by split drag rudder is obtained as Figure A-6 shows.

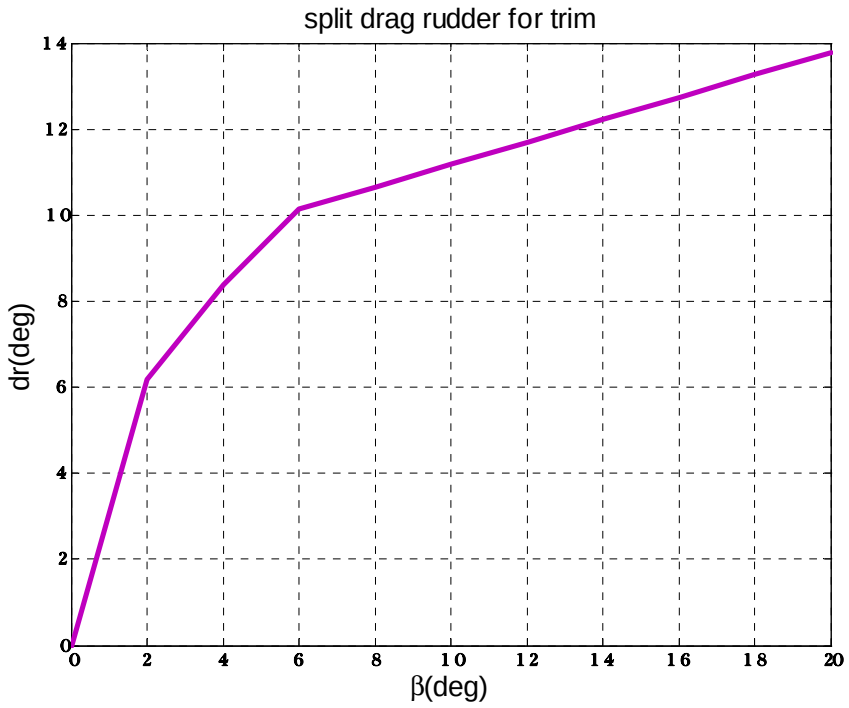

Figure A-6 Split Drag Rudder Deflection to Sideslip Angle

A.2.3 Drag Estimation

The drag feature of the baseline and FW-11 aircraft have been estimated in cruise for payload range calculation and aerodynamic optimization according to reference [53].

$$C_D = C_{DZ} + KC_L^2 \tag{A-5}$$

$$C_D = C_{Df} + C_{DW} + C_{DLW} + C_{DLV} \tag{A-6}$$

where: C_D — Coefficient of drag

C_{DZ} — Coefficient of zero-lift drag

K —Drag factor due to lift

C_{Df} —Zero lift incompressible drag coefficient

C_{DW} —Wave drag duo to the volume of the aircraft

C_{DLW} —Wave drag due to lift coefficient

C_{DLV} —Vortex drag due to lift

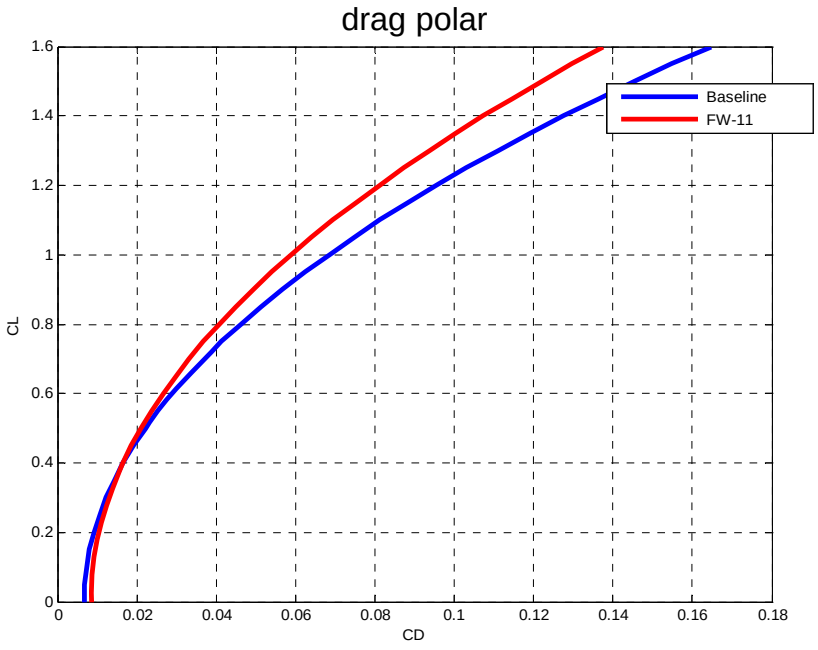

Figure A-7 Drag Polar (Baseline and FW-11)

Table A-6 Aerodynamic Performance Parameters (Baseline and FW-11)

	Baseline	**FW-11**
C_{DZ}	0.0167	0.00848
K	0.0487	0.0535
$K_{\max}$ (Maximum lift drag ratio)	17.5	23.471

According to the drag polar in Figure A-7 and aerodynamic performance parameters in Table A-6, it is found that the flying wing configuration is a more aerodynamic efficient (higher lift and lower drag) concept compared with the conventional aircraft.

Appendix B Flight Envelope Exploration and Calculation

Table B-1 Thrust of Three RR TRENT 500 (N)

Mach / Altitude （m）	0.1	0.2	0.3	0.4	0.5	0.6	0.7	0.8	0.9
0	738735.5	654620.1	585686.4	530123.3	483306.9	446046.4	418727.2		
2000	727715.4	653772.4	591581.8	541104.9	499760	469396.8	445121.7	424969.4	407437.4
4000	690108.1	625913.8	580869.9	542915.9	509585.7	484000.5	463154.6	445661.1	428707
6000	561532.2	527128.6	497948.9	469616.9	448699.5	432554.6	418603.3	408439.1	405268.5
8000	446216.7	420103.1	397936.2	381472.1	369133.6	358919.8	351290.5	343820.8	341162.1
10000	319622.5	306604.2	298413.4	292738.2	290396.1	288777.7	287142.9	287118.1	288172.2
12000				250719.2	249822	247658.2	250230.4	250787.5	257897.2

Table B-2 Required Thrust

Airspeed（m/s） / Altitude（m）	55.6	111	166.7	222.2	281
0	27735.46	110543.1	249320	442969.6	707424.4
2000	22777.04	90780.74	204747.7	363777.5	580954.3
4000	18545.4	73915.01	166708.6	296193	473021.5
6000	14936.4	59530.87	134266.4	249520.7	416001.4
8000	11891.16	47393.68	106892.1	211745.9	373020.9
10000	9344.021	37241.76	83995.39	171535.1	320512.6
12000	7036.883	28046.37	63256.04	144683	282635.2

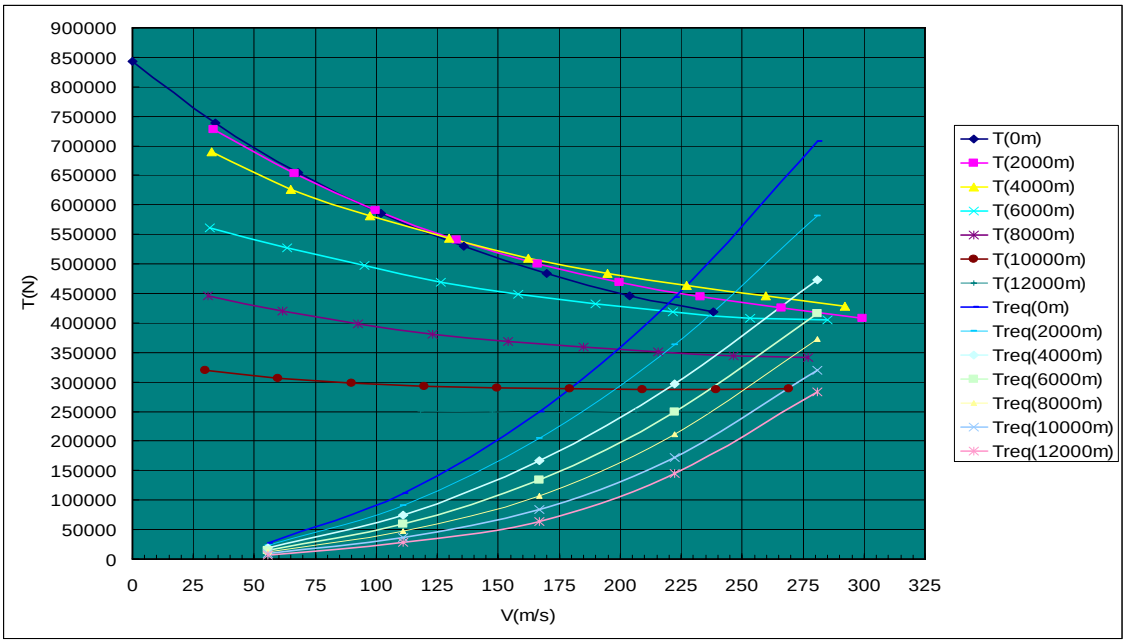

Figure B-1 Graphing of Maximum Airspeed Seeking

Appendix C Assessment Results at Three Points in F_{ki}

The previous assessment methods are used continuously so that only results are presented in following section.

C.1.1 Assessment Results at P_{I1}

Assess P_{I1}(120m/s, 2000m) with controller gains $K(P_{I1}) = [-0.45 \; -1.24]$ and the augmented state equation and transfer functions of each variable (u, α, q, θ) with respect to elevator deflection as equation (C-1) to (C-5) show [6].

$$\begin{bmatrix} \dot{u} \\ \dot{\alpha} \\ \dot{q} \\ \dot{\theta} \end{bmatrix} = \begin{bmatrix} 0.0020671 & -12.13 & -21.333 & -9.688 \\ -0.0004539 & -0.78631 & 0.79499 & -0.01248 \\ 0.0019306 & -2.5351 & -3.0797 & 0 \\ 0 & 0 & 1 & 0 \end{bmatrix} \begin{bmatrix} u \\ \alpha \\ q \\ \theta \end{bmatrix} + \begin{bmatrix} -2.4238 \\ -0.15499 \\ -2.3033 \\ 0 \end{bmatrix} \delta_e \qquad \text{(C-1)}$$

$$\frac{q(s)}{\delta_e(s)} = \frac{-2.3033s\,(s+0.6246)(s-0.00888)}{(s^2+0.003201s+0.005764)(s^2+3.861s+4.447)} \quad \text{(deg/s/deg)} \qquad \text{(C-2)}$$

$$\frac{\alpha(s)}{\delta_e(s)} = \frac{-0.15499\,(s+14.89)\,(s^2-0.002329s+0.005646)}{(s^2+0.003201s+0.005764)\,(s^2+3.861s+4.447)} \quad \text{(deg/deg)} \qquad \text{(C-3)}$$

$$\frac{u(s)}{\delta_e(s)} = \frac{-0.042301\,(s-18.73)\,(s+1.33)\,(s+0.2229)}{(s^2+0.003201s+0.005764)\,(s^2+3.861s+4.447)} \quad \text{(m/s/deg)} \qquad \text{(C-4)}$$

$$\frac{\theta(s)}{\delta_e(s)} = \frac{-2.3033(s+0.6246)(s-0.00888)}{(s^2+0.003201s+0.005764)(s^2+3.861s+4.447)} \quad \text{(deg/deg)} \qquad \text{(C-5)}$$

An improvement of the damping and CAP are demonstrated in Table C-1.

Table C-1 Damping and CAP Comparison with Open Loop and Close Loop

Open loop without feedback			Closed loop with feedback		
ζ_s	ω_n	CAP	ζ_s	ω_n	CAP
0.37	1.30	0.19	0.90	2.12	0.51

The damping and CAP in Phugoid mode are $\delta_p = 0.02$ and $\omega_{np} = 0.07$ rad/s. From the Figure C-1 to C-5, the short period response, full order system response, CAP and wind disturbance response will be illustrated.

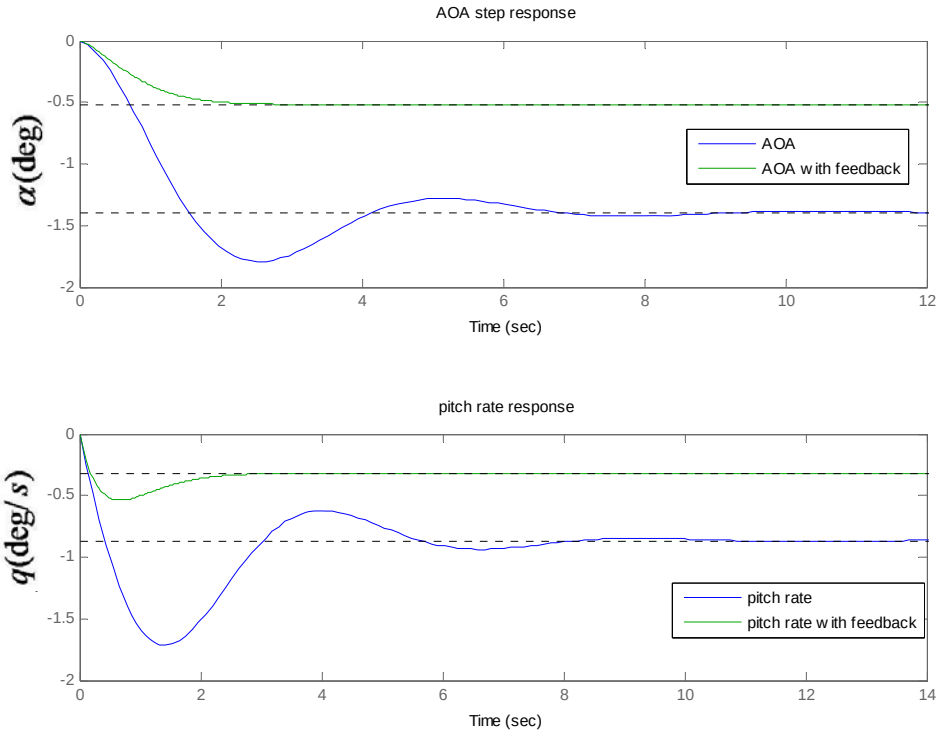

Figure C-1 Short Period Response on Reduced Second Order System

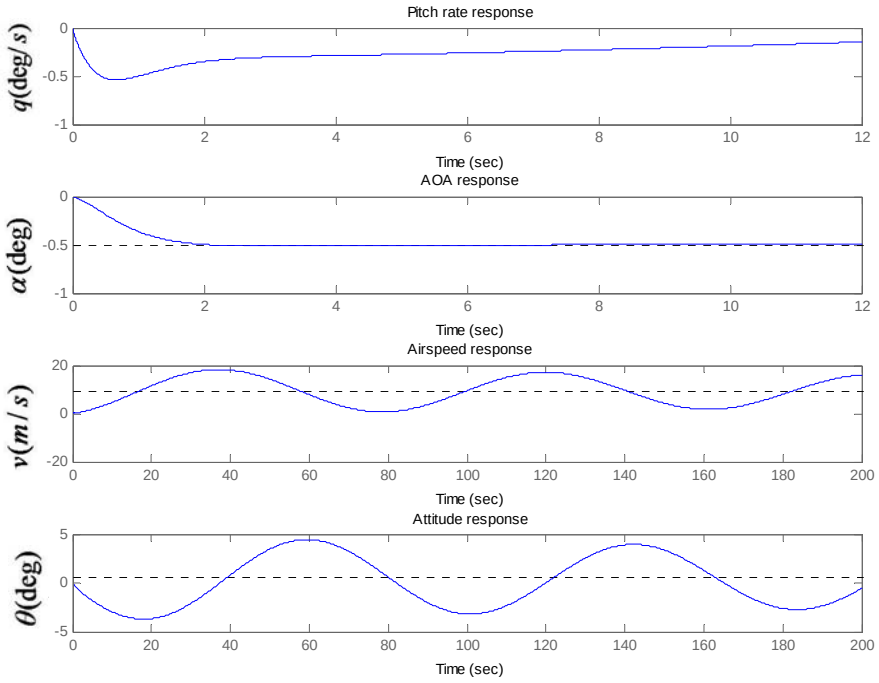

Figure C-2 Output Variables Response for 1° Step Elevator Command

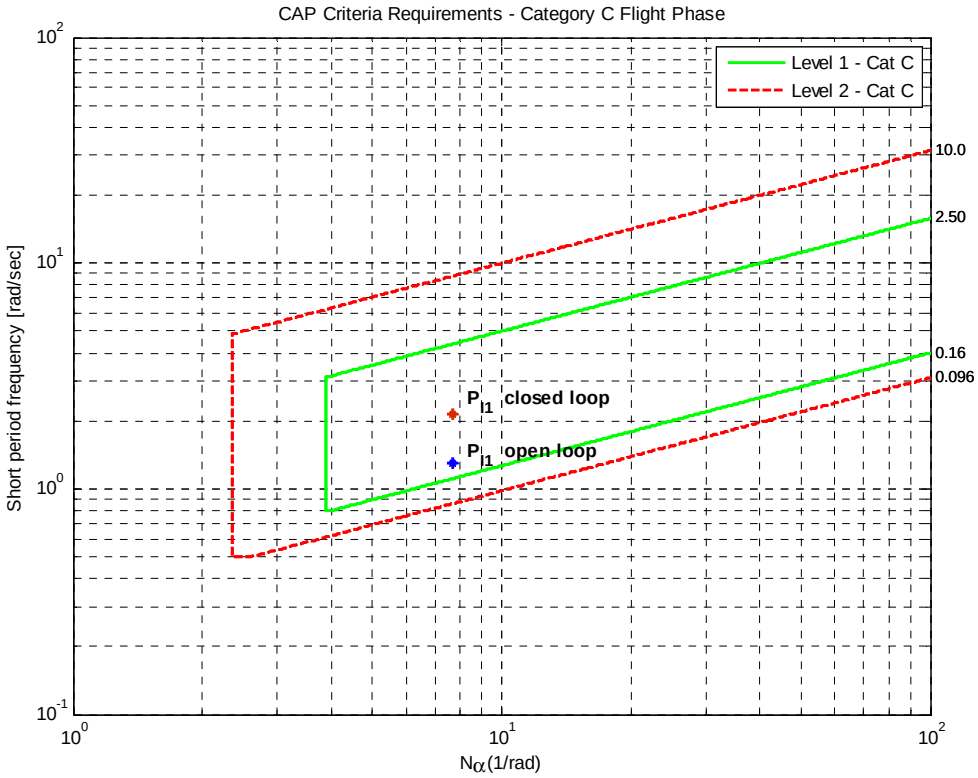

Figure C-3 CAP of P_{I1} in Category C

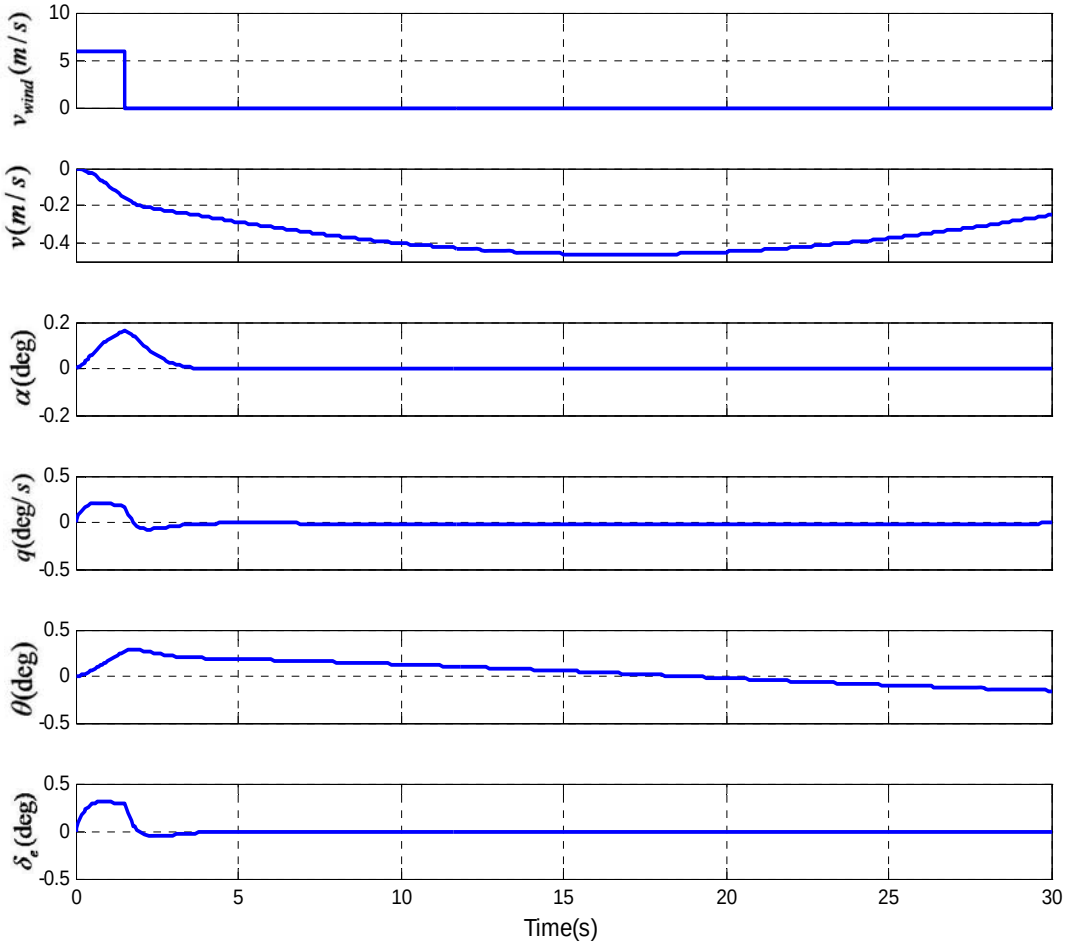

Figure C-4 Response of Up-wind Gust

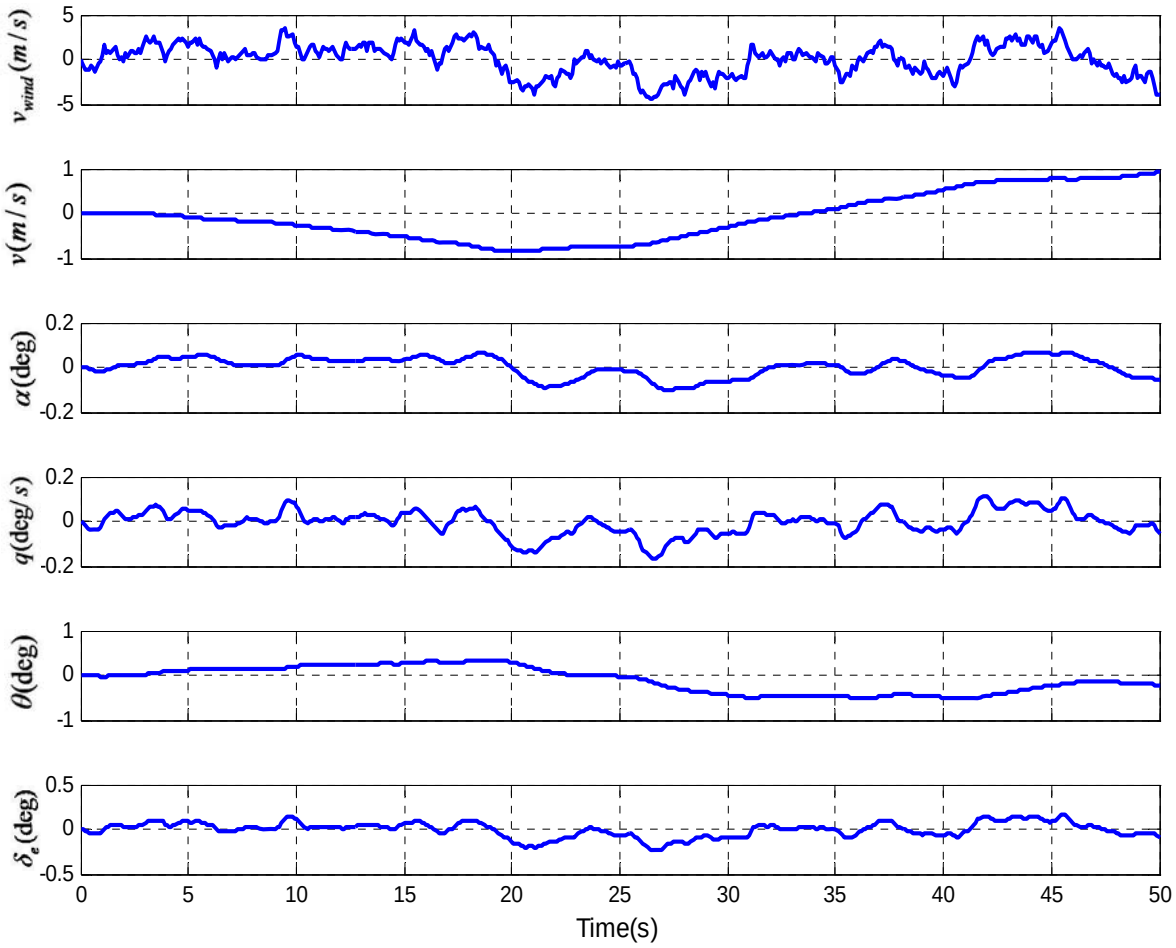

Figure C-5 Response of Wind Turbulence

C.1.2 Assessment Results at P_{I2}

Assess P_{I2} (180m/s, 6000m) with controller gains $K(P_{I2}) = [-0.29 \; -0.95]$ and the augmented state equation and transfer functions of each variable (u, α, q, θ) with respect to elevator deflection as equation (C-6) to (C-10) show [6].

$$\begin{bmatrix} \dot{u} \\ \dot{\alpha} \\ \dot{q} \\ \dot{\theta} \end{bmatrix} = \begin{bmatrix} -0.00023841 & -10.913 & -21.243 & -9.7336 \\ -0.00018174 & -0.76398 & 0.84271 & -0.0057683 \\ 0.0013692 & -3.3281 & -3.5607 & 0 \\ 0 & 0 & 1 & 0 \end{bmatrix} \begin{bmatrix} u \\ \alpha \\ q \\ \theta \end{bmatrix} + \begin{bmatrix} -2.2445 \\ -0.15649 \\ -3.509 \\ 0 \end{bmatrix} \delta_e \qquad \text{(C-6)}$$

$$\frac{q(s)}{\delta_e(s)} = \frac{-3.509\,s\,(s+0.619)(s-0.002337)}{(s^2+0.00426s+0.002889)(s^2+4.321s+5.532)} \quad \text{(deg/s/deg)} \qquad \text{(C-7)}$$

$$\frac{\alpha(s)}{\delta_e(s)} = \frac{-0.15649\,(s+22.45)\,(s^2-0.0001522s+0.002354)}{(s^2+0.00426s+0.002889)\,(s^2+4.321s+5.532)} \quad \text{(deg/deg)} \qquad \text{(C-8)}$$

$$\frac{u(s)}{\delta_e(s)} = \frac{-0.03917\,(s-31.17)\,(s+1.294)\,(s+0.2302)}{(s^2+0.00426s+0.002889)\,(s^2+4.321s+5.532)} \quad \text{(m/s/deg)} \qquad \text{(C-9)}$$

$$\frac{\theta(s)}{\delta_e(s)} = \frac{-3.509\,(s+0.619)(s-0.002337)}{(s^2+0.00426s+0.002889)(s^2+4.321s+5.532)} \quad \text{(deg/deg)} \qquad \text{(C-10)}$$

An improvement of the damping and CAP are demonstrated in Table C-2.

Table C-2 Damping and CAP Comparison with Open Loop and Close Loop

Open loop without feedback			**Closed loop with feedback**		
ζ_s	ω_n	CAP	ζ_s	ω_n	CAP
0.30	1.57	0.18	0.91	2.36	0.42

The damping and CAP in Phugoid mode are $\delta_p = 0.04$ and $\omega_{np} = 0.054$ rad/s.

From the Figure C-6 to C-10, the short period response, full order system response, CAP and wind disturbance response will be illustrated.

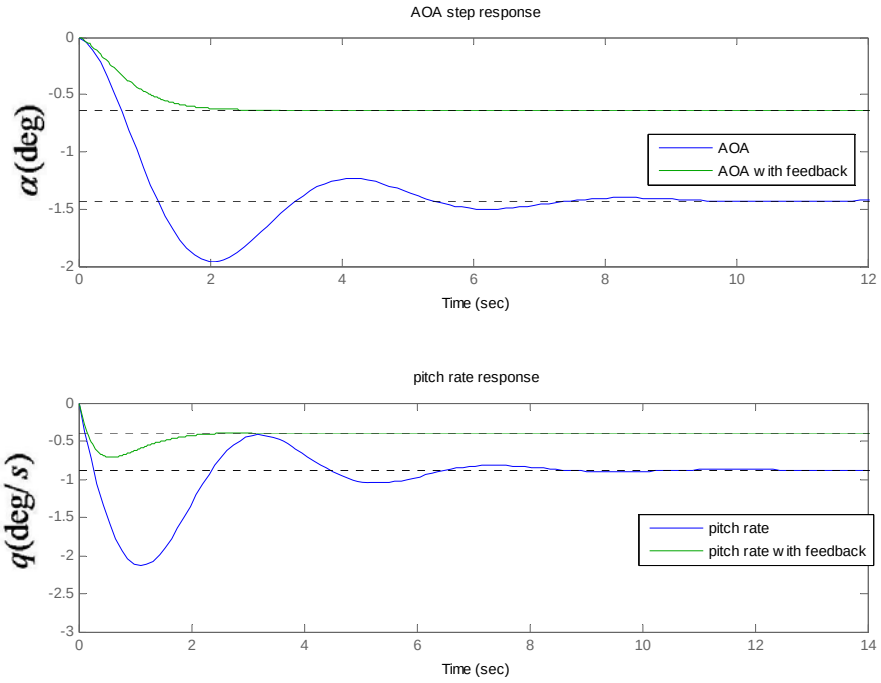

Figure C-6 Short Period Response on Reduced Second Order System

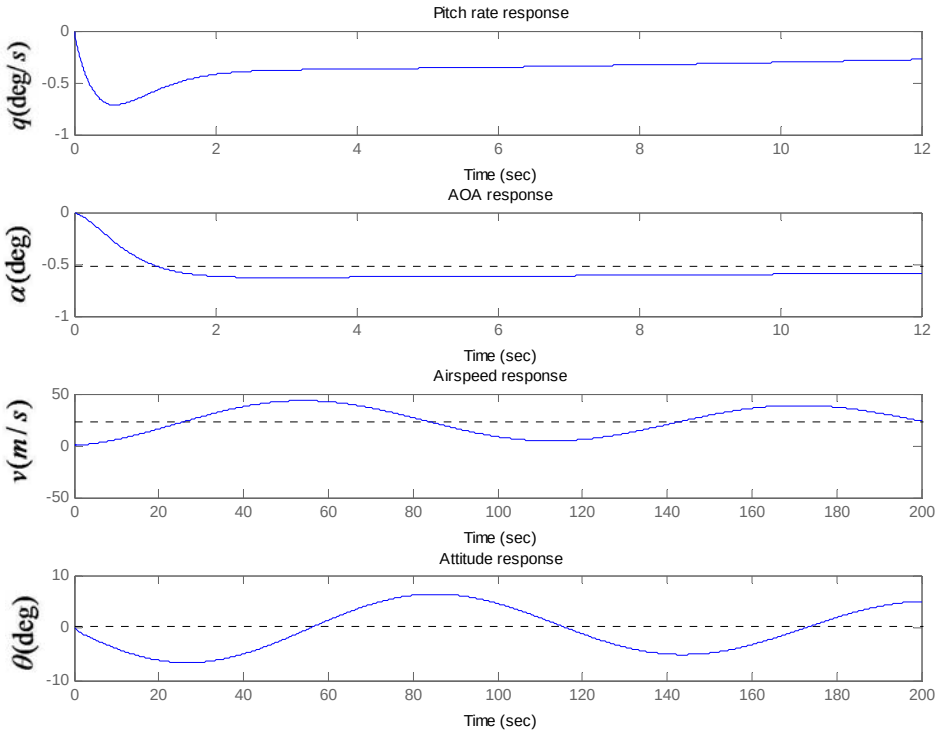

Figure C-7 Output Variables Response for 1° Step Elevator Command

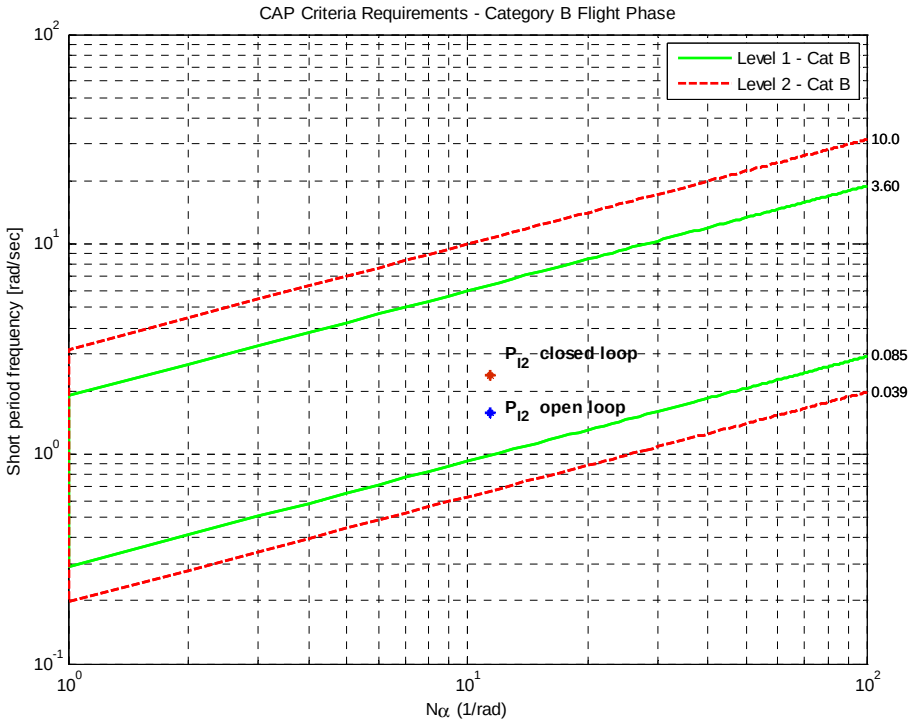

Figure C-8 CAP of P_{I2} in Category B

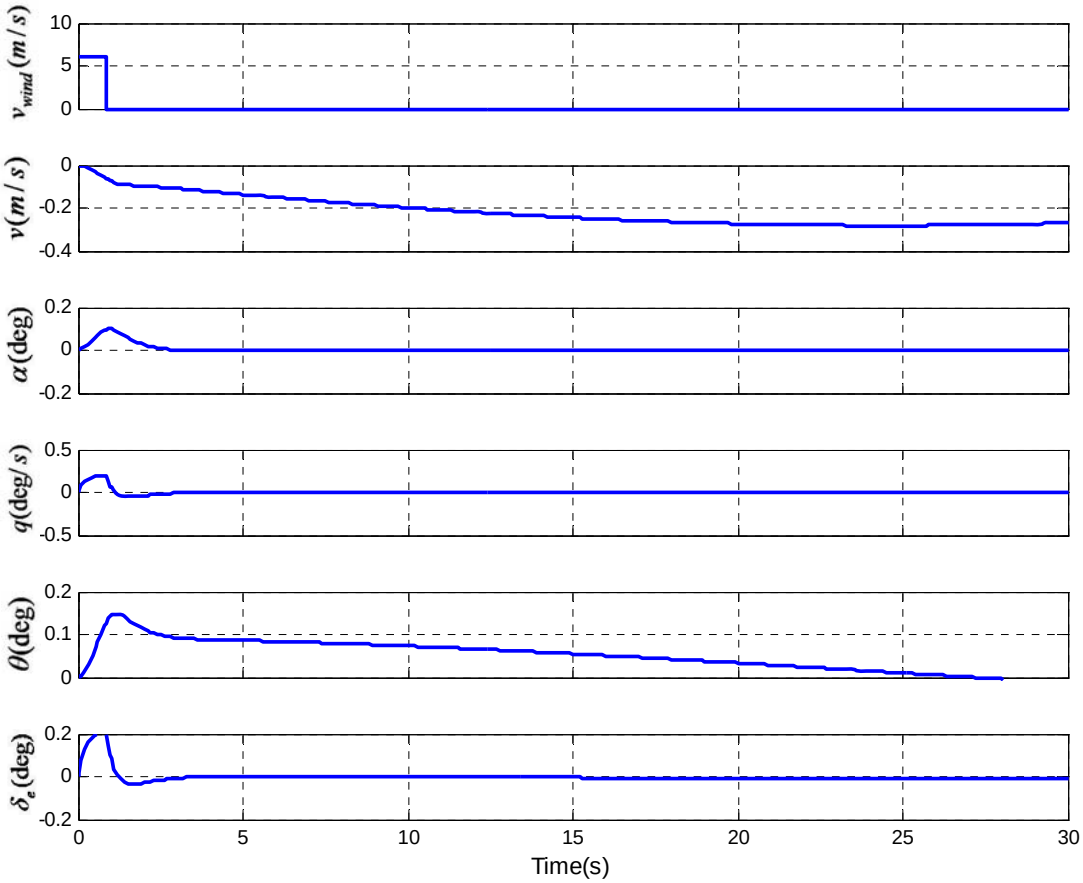

Figure C-9 Response of Up-wind Gust

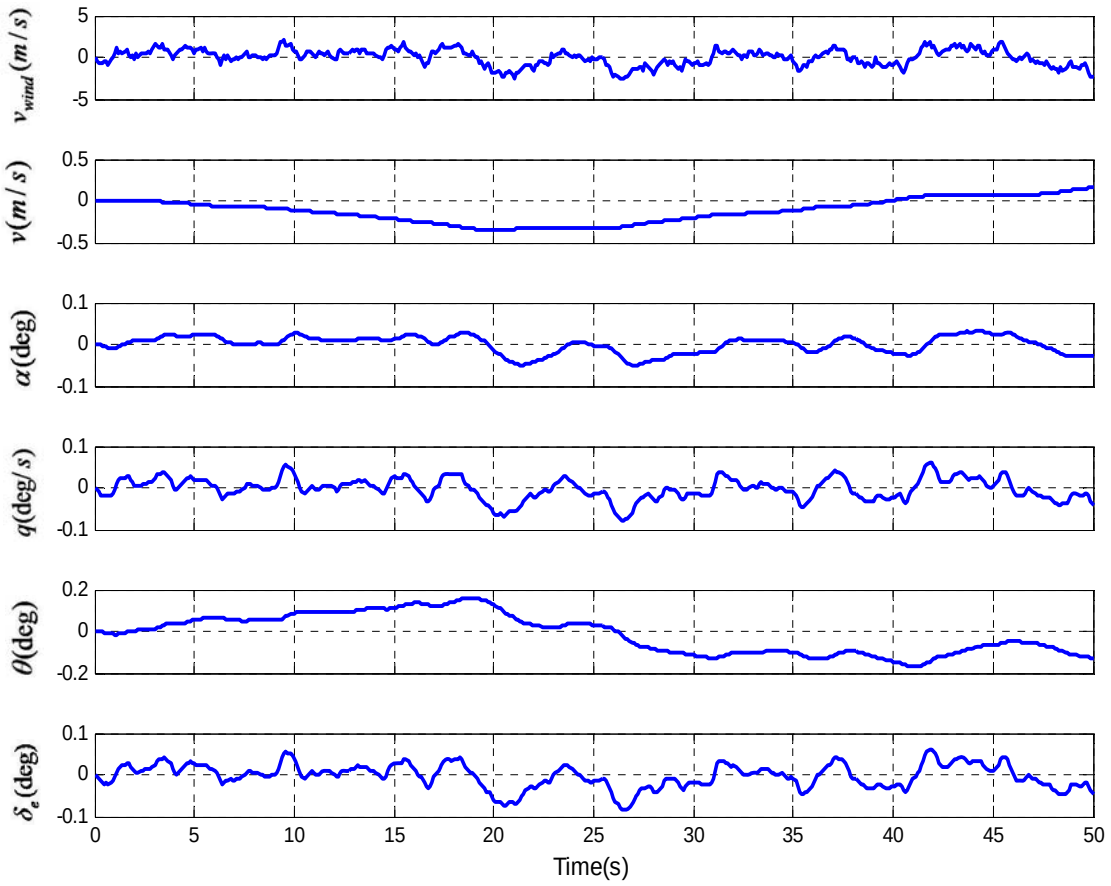

Figure C-10 Response of Wind Turbulence

C.1.3 Assessment Results at P_{I3}

Assess P_{I3} (260m/s, 10000m) with $K(P_{I3}) = [-0.13 - 0.67]$ and the augmented state equation and transfer functions with respect to u, α, q, θ as equation (C-11) to (C-15) show [6].

$$\begin{bmatrix} \dot{u} \\ \dot{\alpha} \\ \dot{q} \\ \dot{\theta} \end{bmatrix} = \begin{bmatrix} -0.00023841 & -10.913 & -21.243 & -9.7336 \\ -0.00018174 & -0.76398 & 0.84271 & -0.0057683 \\ 0.0013692 & -3.3281 & -3.5607 & 0 \\ 0 & 0 & 1 & 0 \end{bmatrix} \begin{bmatrix} u \\ \alpha \\ q \\ \theta \end{bmatrix} + \begin{bmatrix} -2.2445 \\ -0.15649 \\ -3.509 \\ 0 \end{bmatrix} \delta_e \quad \text{(C-11)}$$

$$\frac{q(s)}{\delta_e(s)} = \frac{-4.7871s\,(s+0.5795)(s+0.0001104)}{(s^2+0.004596s+0.001654)(s^2+4.113s+5.777)} \quad \text{(deg/s/deg)} \qquad \text{(C-12)}$$

$$\frac{\alpha(s)}{\delta_e(s)} = \frac{-0.14747\,(s+32.49)\,(s^2+0.0007471s+0.001036)}{(s^2+0.004596s+0.001654)\,(s^2+4.113s+5.777)} \quad \text{(deg/deg)} \qquad \text{(C-13)}$$

$$\frac{u(s)}{\delta_e(s)} = \frac{-0.035657\,(s-51.23)\,(s+1.158)\,(s+0.2214)}{(s^2+0.004596s+0.001654)\,(s^2+4.113s+5.777)} \quad \text{(m/s/deg)} \qquad \text{(C-14)}$$

$$\frac{\theta(s)}{\delta_e(s)} = \frac{-4.7871(s+0.5795)(s+0.0001104)}{(s^2+0.004596s+0.001654)(s^2+4.113s+5.777)} \quad \text{(deg/deg)} \qquad \text{(C-15)}$$

An improvement of the damping and CAP are demonstrated in Table C-3.

Table C-3 Damping and CAP Comparison with Open Loop and Close Loop

Open loop without feedback			**Closed loop with feedback**		
ζ_s	ω_n	CAP	ζ_s	ω_n	CAP
0.24	1.82	0.18	0.85	2.4	0.32

The damping and CAP in Phugoid mode are $\delta_p = 0.057$ and $\omega_{np} = 0.04$ rad/s.

From the Figure C-11 to C-15, the short period response, full order system response, CAP and wind disturbance response will be illustrated.

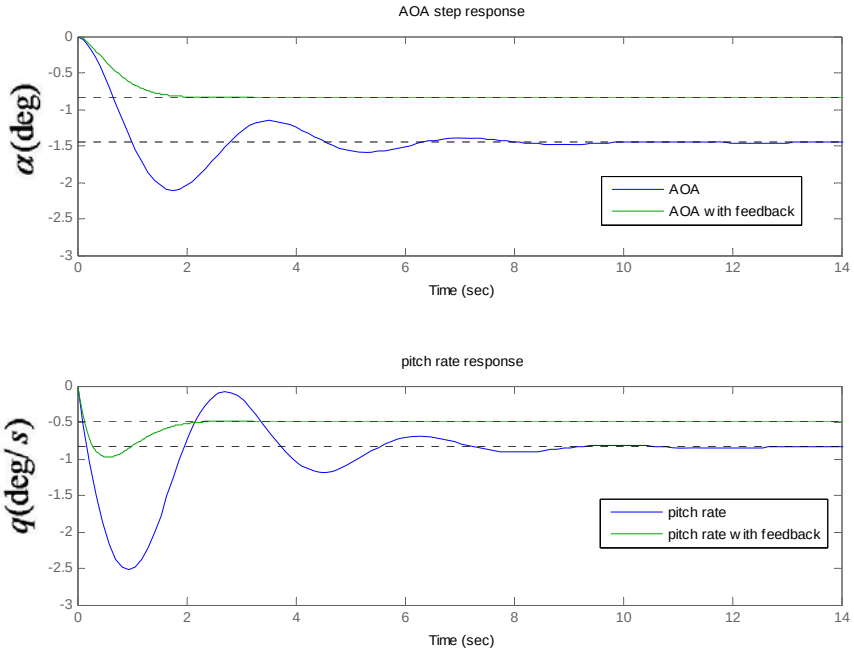

Figure C-11 Short Period Response on Reduced Second Order System

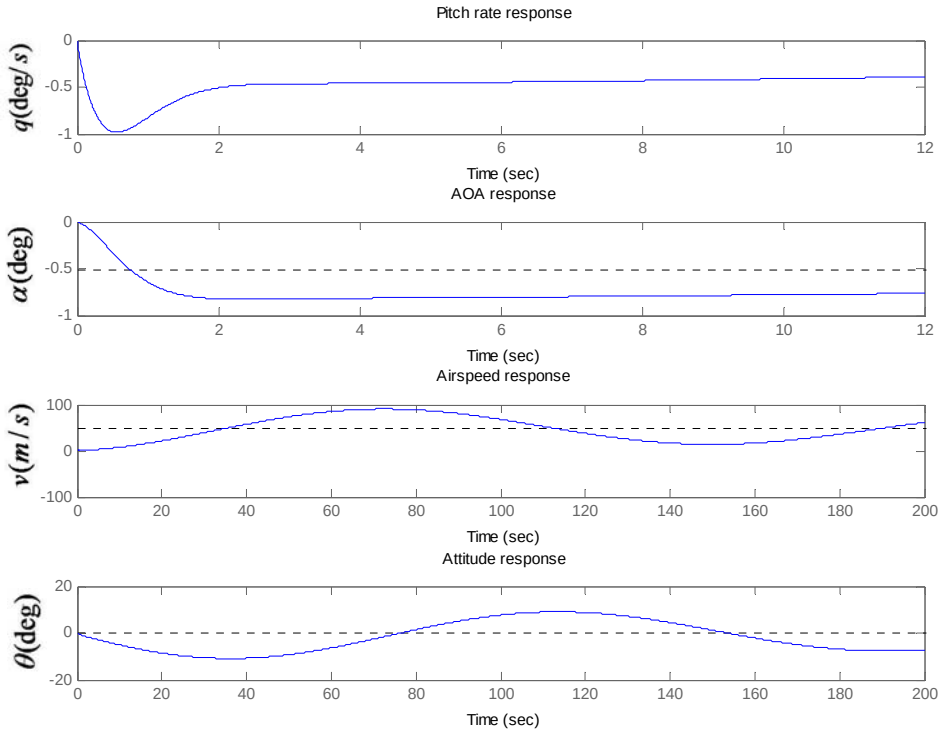

Figure C-12 Output Variables Response for 1^{o} Step Elevator Command

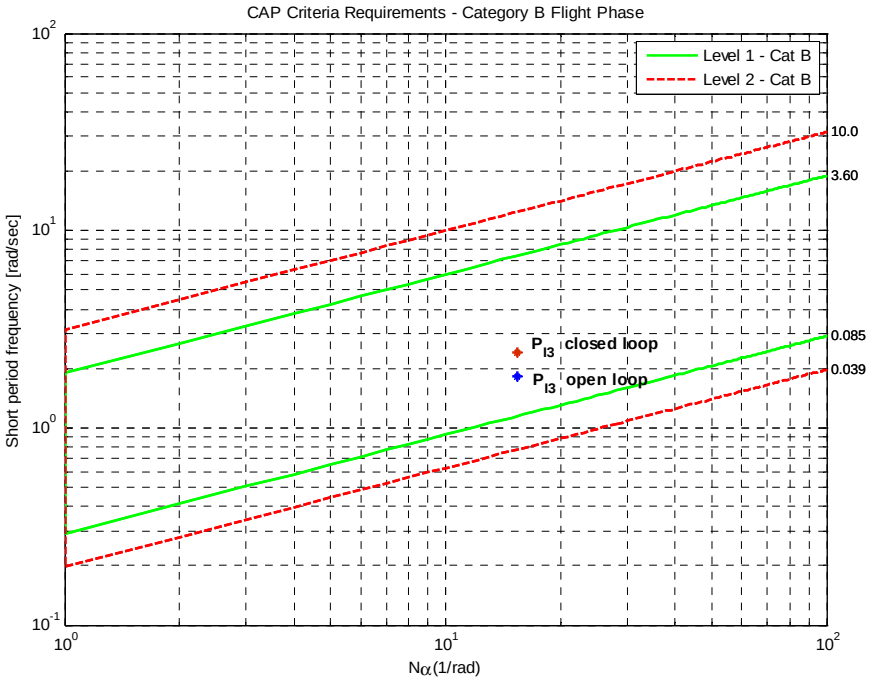

Figure C-13 CAP of P_{I3} in Category B

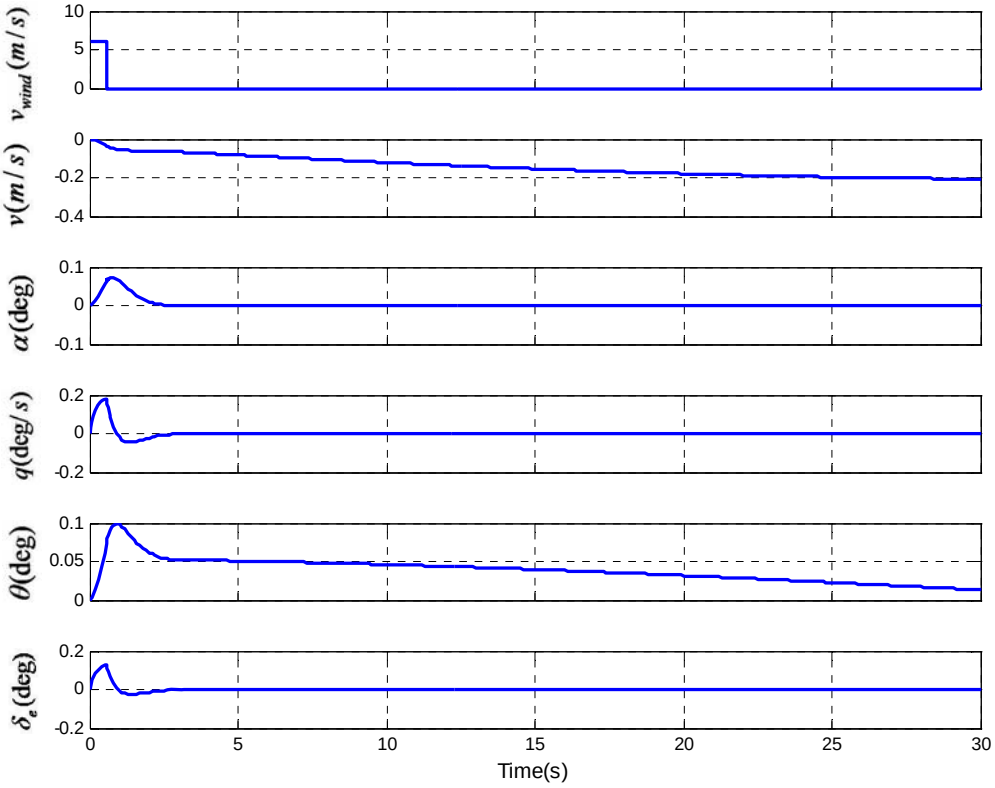

Figure C-14 Response of Up-wind Gust

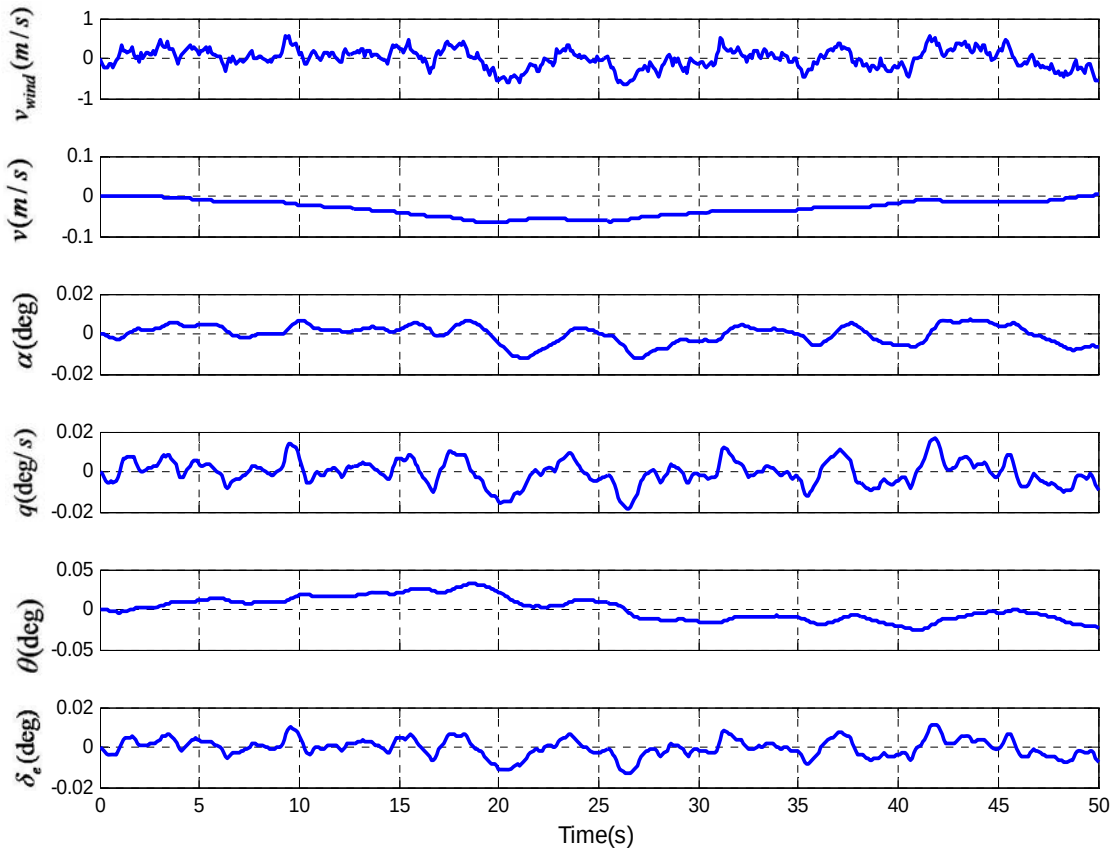

Figure C-15 Response of Wind Turbulence

Appendix D MATLAB Program

```
%%---------------------------------------
%1.Augmented system of second order model with design feedback gains
%---------------------------------------
A1=[Zw 1; Mw * (Zq+U1) Mq];
B1=[Zde/U1 ; Mde];
C1=eye(2);
D1=[0 ;0];
[b,a]=ss2tf(A1,B1,C1,D1);
h1=tf(b(1,:),a);
zpk(h1);
h2=tf(b(2,:),a);
zpk(h2);
% calculate the new matrix after increasing the alpha and pitch rate feedback
K_alf=-0.55;
K_q=-1.41;
A_new=A1-B1*[K_alf K_q];
a11=A_new(1,1);
a12=A_new(1,2);
a21=A_new(2,1);
a22=A_new(2,2);
[b1,a1]=ss2tf(A_new,B1,C1,D1);
h1_new=tf(b1(1,:),a1);%alpha to elevator
zpk(h1_new);
h2_new=tf(b1(2,:),a1);%pitch rate to elevator
zpk(h2_new);
%calculate the frequency , damping and CAP
Wn=(a11*a22-a12*a21)^0.5
Dsp=-(a11+a22)/2/Wn
CAP2    = Wn^2/Nalf
%---------------------------------------
%%---------------------------------------
```

```
%%%-------------------------------------------------------------
%%---------------------------------------
%2.Augmented system of full order model with design feedback gains
%---------------------------------------
Az =[A_lon(1,1),    A_lon(1,2)*U1, A_lon(1,3),    A_lon(1,4);
    A_lon(2,1)/U1, A_lon(2,2),    A_lon(2,3)/U1, A_lon(2,4)/U1;
    A_lon(3,1),    A_lon(3,2)*U1, A_lon(3,3),    A_lon(3,4);
    A_lon(4,1:4)];
Bz=[B_lon(1,1);B_lon(2,1)/U1;B_lon(3,1);B_lon(4,1)];
Cz=[1 0 0 0;0 1 0 0;0 0 1 0;0 0 0 1];
Dz=[0 ;0 ;0 ;0];
K_alfz=-0.13; % gain of alpha feedback
K_qz=-0.67; % gain of pitch feedback
Kz=[0 K_alfz K_qz 0];
Az_new=Az-Bz*Kz;
[numz_new,denz_new]=ss2tf(Az_new,Bz,Cz,Dz);
%pitch rate to elevator
q2dez_new=tf(numz_new(3,:),denz_new);
zpk(q2dez_new)
figure(1)
subplot(4,1,1)
step(q2dez_new,[0:0.01:12])
title('Pitch rate response')
%alpha to elevator
alpha2dez_new=tf(numz_new(2,:),denz_new);
zpk(alpha2dez_new)
figure(1)
subplot(4,1,2)
step(alpha2dez_new,[0:0.01:12])
title('AOA response')
% v to elevator
v2dez_new=tf(numz_new(1,:),denz_new);
zpk(v2dez_new)
```

```
figure(1)
subplot(4,1,3)
step(v2dez_new,[0:0.01:200])
title('Airspeed response')
%theta to elevator
theta2dez_new=tf(numz_new(4,:),denz_new);
zpk(theta2dez_new)
figure(1)
subplot(4,1,4)
step(theta2dez_new,[0:0.01:200])
title('Attitude response')
%----------------------------------------
%%----------------------------------------
 %%%-------------------------------------------------------------
 %%----------------------------------------
%3.Modification of aircraft model with the wind disturbance input
%----------------------------------------
A =[A_lon(1,1),    A_lon(1,2), A_lon(1,3),    A_lon(1,4);
    A_lon(2,1),   A_lon(2,2), A_lon(2,3),    A_lon(2,4);
    A_lon(3,1),   A_lon(3,2), A_lon(3,3),    A_lon(3,4);
    A_lon(4,1:4)];
Cl_alpha=5.382;
B=[B_lon(1,1);B_lon(2,1);B_lon(3,1);B_lon(4,1)];
B_wind=[0    ;Cl_alpha*U1*rho*S/2/m;Cl_alpha*(31.6-30.4)*rho*U1*S*c/2/Iyyb;
0] ;
B1=[0 B_lon(1,1);
   Cl_alpha*U1*rho*S/2/m  B_lon(2,1);
   Cl_alpha*(31.6-30.4)*rho*U1*S*c/2/Iyyb B_lon(3,1);
   0  B_lon(4,1)];
C=[1 0 0 0;0 1 0 0;0 0 1 0;0 0 0 1];
D1=[0 0;0  0 ;0 0 ;0 0 ];
D=[0 ;0 ;0 ;0];
%----------------------------------------
```

```
%%----------------------------------------
 %%%-------------------------------------------------------------
 %%----------------------------------------
%4.Pole placement method
%----------------------------------------
% Get out the coefficient with variables from the polynomial
function coef=ssym2poly(f,var)
%Get the f coefficient of var, the result is evaluated to coef
%f can be the polynomial with multi-variable
%var is the fixed variable, X
%Use function poly_degree() to acquire the highest power
if nargin==1, var=sym('x'); end
degree=poly_degree(f,var); temp_f=f;
coef(degree+1)=subs(temp_f,var,0);
for n=1:degree
   temp_f=simple((temp_f-coef(degree+2-n))/var);
   coef(degree+1-n)=subs(temp_f,var,0);
end
%=====================================================
 function degree=poly_degree(f,var)
%feedback the highest power of var in f,evaluate it to degree
if nargin==1
var=sym('x');
end
temp=f;
n=0;
while 1
if diff(temp,var)==0
break
end
n=n+1;
temp=diff(temp,var);
end
```

```
degree=n;
%=====================================================
 syms K K1 K2 S ds ws d1 d2 Kalf Kq
%input the equivalent second modal
A=input('system equivalent second modal A metrix');
B=input('system equivalent second modal B metrix');
% feedback gains
K=[K1 K2];
I=[1 0;0 1];
%characteristic equation after feedback
E=S*I-A-B*K;
%acquire the eigenvalue
h=det(E);
delta_s_aug=vpa(ssym2poly(h,S))
%input the expect damping ratio and frequency
ds =input('expect damping ratio =');
ws =input('expect nature frequency =');
%construct the equation of K1 and K2
d1=vpa(delta_s_aug(1,2)-2*ds*ws)
d2=vpa(delta_s_aug(1,3)- ws^2)
%solve the K1 and K2
k=solve('0.17658*K1 + 3.9966*K2 - 2.15525','4.037284032*K1 + 3.1548405546*K2 - 3.24724376','K1','K2');
Kalf=k.K1
Kq=k.K2
%=====================================================
```